10th INTERNATIONAL WORKSHOP ON TEACHING IN PHOTOVOLTAICS

IWTPV'22

PROCEEDINGS

16 – 17 June 2022

Czech Technical University in Prague

CZECH REPUBLIC

ORGANISER: The IET Czech Network, Technická 2, 166 27 Praha 6
In cooperation with: Czech Technical University in Prague, Faculty of Electrical Engineering

ORGANISING COMMITTEE:

Prof. Vitezslav Benda, PhD (chairman)
Dr. Ladislava Černá
Dr. Tomáš Finsterle
Dr. Pavel Hrzina

INTERNATIONAL PROGRAMME COMMITTEE:

Prof. Vítězslav Benda, Czech Technical University in Prague (chairman)
Prof. Thomas Hannapel, Helmholtz Centrum Berlin, Germany
Prof. Socrates Kaplanis, Technological Educational Inst. of Western Greece
Prof. Tom Markvart, University of Southampton, U.K.
Prof. Jean-Michel Nunzi, Queen's University, Kingston, Ontario, Canada
Dr. Jatindra Kumar Rath, Utrecht University, Netherland
Prof. João Manuel de Almeida Serra, University of Lisboa, Portugal
Prof. Mitko Stoev, University of Blagoevgrad, Bulgaria
Prof. Vladimír Šály, Technical University Bratislava, Slovakia
Prof. Santiago Silvestre, Universidad Politécnica de Cataluña, Barcelona, Spain
Prof. Marko Topic, University of Ljubljana, Slovenia
Prof. Miro Zeman, Technical University Delft, Netherland

EDITOR: V. Benda and L. Černá

ISBN 978-80-01-07013-0 (print)
ISBN 978-80-01-07014-7 (on-line)

CONTENTS

ORAL PRESENTATIONS

Education in Photovoltaics as a part of the REPowerEU

V. Benda
Department of Electrotechnology
Czech Technical University in Prague, Faculty of Electrical Engineering
Technicka 2, Praha 6, Czech Republic

Abstract

Photovoltaics has been recognised as a renewable energy technology having the potential to contribute significantly to future energy supply. The European Green Deal has added to the importance of photovoltaics as one of the most important component in the future energy mix, and the new REPowerEU programme further emphasizes its importance. To establish an infrastructure and to meet the requirements of the market, education and training are needed for specialists in this field. Different aspects of education in photovoltaics are discussed.

Keywords: photovoltaics, photovoltaic cells, photovoltaic modules, photovoltaic systems, education.

INTRODUCTION

Atmospheric pollutions and climate changes represent a serious problem for present civilization. There is very important to decrease pollutions at energy generation. This year, incoming European Commission proposed as one of its most important political priorities the 'European Green Deal'[1].

The European Green Deal has been at once conceived of as a climate project, aimed at making Europe a climate neutral continent; as a social project, to support a just transition; as an economic project, seeking to rejuvenate EU investment and competitiveness; as a European project, to give new purpose and unity to the EU; and as an international project which will take a more geopolitical approach to global climate security [2]. One of the most important targets is the transition from using energy sources based on fossil fuel combustion to using Renewable Energy sources (RES). The 2018 energy mix [3] is shown in Fig.1a.

Problems connected with the energy mix transition were in details studied at LUT University [4]. The result of this study is shown in Fig.1b. This study shows that 69% of electricity needs to be generated by photovoltaics in order to meet the needs of electricity by renewable energy only. Some other studies assume a lower share of photovoltaics in the energy mix in 2050 (e.g. [5]), as demonstrated in Fig.1c.

From that can be expected that in 2050 the share of photovoltaics could exceed 30% of total energy production [6]. Therefore, photovoltaics is a strategically important part of the coming sustainable energy system.

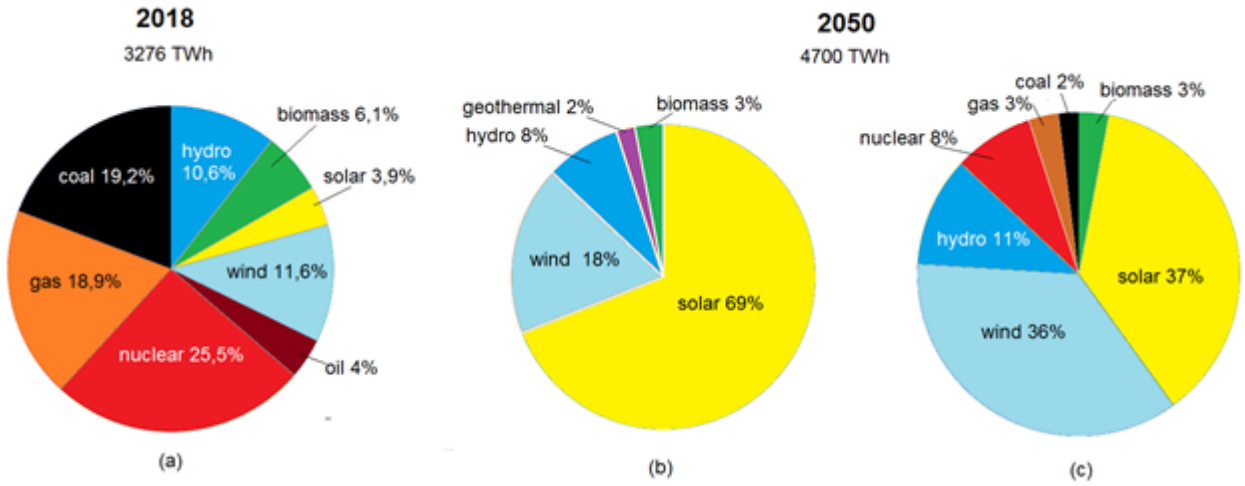

Fig.1. Shares of primary European energy supply in 2015 (a) and 2050 (b),(c).

Thanks to the abundant availability of sunlight, the technology's modularity, and continuous cost reductions and photovoltaics can become the largest source of energy worldwide.

PHOTOVOLTAICS IN ELECTRICAL ENERGY PRODUCTION

The photovoltaic industry has recently shown an unprecedented rate of growth with the installed global PV power increasing by more than forty fold over the past twelve years: from 20 GW_p in 2009 to nearly 1 TW_p in 2021 of cumulative installed power (about 165 GW_p in EU). The global annually installed photovoltaic system power grew from 8 GW_p in 2009 to about 175 GW_p in 2021 [7], as demonstrated in Fig.2.

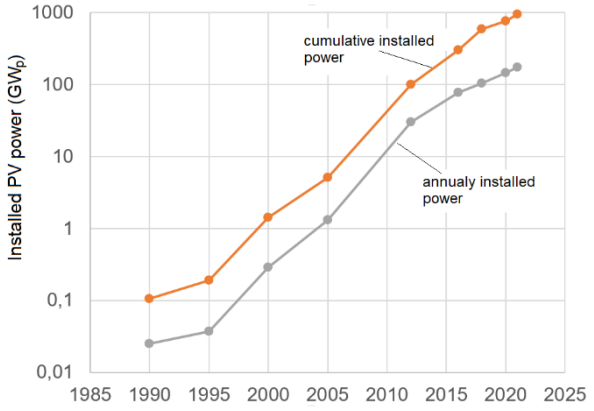

Fig.2. The developments of the PV cumulative installed capacity and annual production

It results in a considerable decrease of the costs of electrical energy produced by photovoltaic systems close to the long-term costs of receiving traditionally produced and supplied power over the grid. Already today photovoltaics provides a power generation solution, which is more efficient and cheaper than conventional energy sources in a large part of the world, as demonstrated in Fig.3.

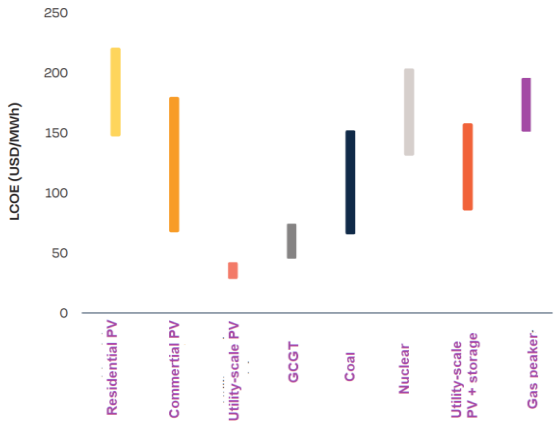

Fig.3. PV elektricity generation cost in comparison with conventional power sources in 2021 [8]

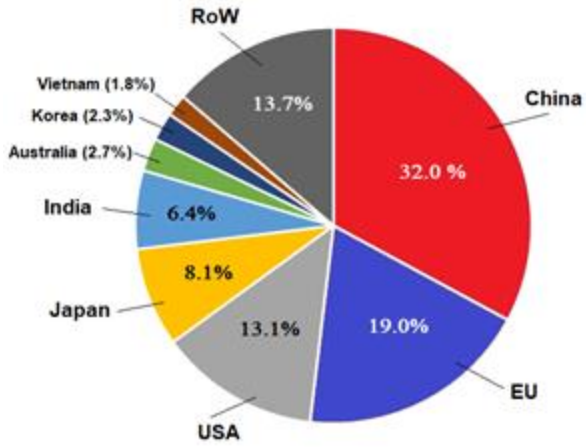

Fig.4. Distribution of cumulative installed PV power in 2021 by country

The most of PV installations is in China, followed with EU and USA [7], as demonstrated in Fig.4. In Europe, a very high increase in annual photovoltaic installations in the period 2005-2011 was followed by a decrease in the period 2012 – 2016. Since 2019, annually installed power has started grow again, as shown in Fig.5.

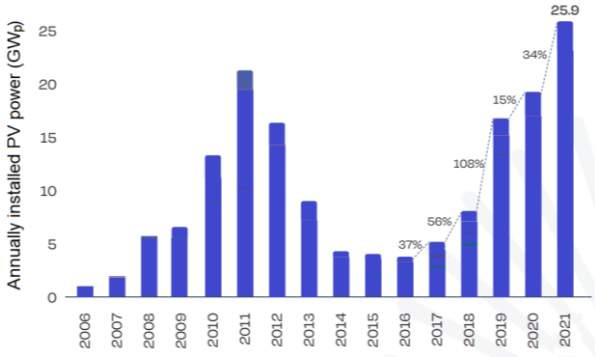

Fig.5. The development of the annually installed PV capacity in EU [9]

China plays a key role in the entire field of photovoltaics. 95% of PV modules is currently realized from crystalline silicon. China produces 64% of the world's polycrystalline silicon, more than 95% of silicon wafers, 80% of photovoltaic cells and 75% of modules. The EU's share of this production is very low. From a strategic point of view, therefore, at least the majority of production of all key parts of the production chain needs to be realized in the EU.

In response to the hardships and global energy market disruption caused by Russia's invasion of Ukraine, the European Commission presented the REPowerEU Plan [10] for

- saving energy
- producing clean energy
- diversifying EU energy supplies

Renewables are the cheapest and cleanest energy available, and can be generated domestically, reducing the need for energy imports. The European Commission is proposing to increase the EU's 2030 target for renewables from the 40% to 45%**.** This EU Solar Energy Strategy will boost the roll-out of photovoltaic energy. Under the REPowerEU plan, this strategy aims to increase the cumulative capacity of solar photovoltaic power plants to at least 320 GW_p (nearly double today's level) by 2025 and to 740 GW_p by 2030.

PRIORITIES IN THE FIELD OF PHOTOVOLTAICS

Priorities for the field of photovoltaics have been set for the implementation of this ambitious project [11]:

- Delivering solar industrial leadership
- #Solar4Buildings
- Transitioning former coal regions to solar
- Providing skills and training programmes to support the energy transition
- Unlocking the potential of flexible large-scale solar installations
- Accelerating solar-powered mobility
- Prioritising renewable-based electrification of the European economy and developing truly renewable hydrogen

All these priority areas are multidisciplinary and require the cooperation of many specialists. The training of experts and executives is the task of specialist workplaces, especially universities.

Very important part of projects above are problems connected with distribution and transmission of hard-to dispatch control PV power generation become more and more important. Dispatching tools such as peak power curtailment or reactive load connections significantly reduce converse efficiency. Therefore, the introduction of new tools such as energy storage, cogeneration, and consumption of produced electricity as close as possible to their place of production and at the time of production is necessary. It is also useful optimizing grid codes and other tools for the electricity transition [12]. Digitization and new market patterns are essential for a new efficient integration solution energy production built into local distribution networks, interactions and sharing additional services between distribution and transmission system [13].

EDUCATION ASPECTS IN PHOTOVOLTAICS

The expected growth of photovoltaics is connected with an increased demand for new specialists. In past SET Plan [14] sets a target of 12% electricity generation by PV by 2020. This target would require a cumulative total capacity of some 308 GW_p, producing 400TWh of electricity per annum. Till the end of 2020, only 139 GW_p have been installed and the SET target will not be reached. Next increase of PV power demand on the level over 700 GW_p is expected in period 2020-2030 under REPowerEU plan. And to realize European Green Deal, it will be necessary to increase the installed photovoltaic power in Europe to more than 1 TW_p by 2050. Tens of thousands of new jobs in the photovoltaic sector are likely to be created to implement these plans during the next few years in Europe.

Given the decline in installed capacity annually from more than 20 GW_p in 2011 to about 8 GW_p in period 2014 – 2017, the demand for specialists in photovoltaics was not as high as expected by EPUE [15]. However, the area of photovoltaic installations has been growing since 2017 and reached the level of 28 GWp in 2021, and due to future ambitious plans, increased demand for installations as well as for specialists in the field of photovoltaics is expected in the future [1].

The education and training of professionals in the field of photovoltaics is essential for the establishment and maintenance of the market and its infrastructure. It will also be necessary to raise public awareness of the nature and use of photovoltaic systems. In addition to training new professionals, it will also be necessary to retrain employees from existing professions, particularly those related to energy production and transmission and the construction of buildings.

A broad-based education system needs to be put in place to increase knowledge about photovoltaics. The education system should combine relevant information with the relationship between this knowledge and everyday life. In addition to universities, many studies can contribute to the study of photovoltaics at different levels. In order to improve the general knowledge of the public, it is necessary to present basic information to children in primary and secondary schools. The implementation of the curriculum requires teachers with extended knowledge and therefore education of teachers should be an important aspect of the program.

The temporary shortage of experts can be solved by organizing short retraining courses for engineers from various fields of technology (electrical, civil, mechanical, architecture, chemistry, economics), which often take place without practical exercises. Short courses can only

provide an incomplete set of information. Therefore, the training of future experts is an important task for universities (higher education).

One problem with teaching photovoltaics is that the field of photovoltaics is in fact relatively broad and interdisciplinary. On the one hand, knowledge of the physics of materials and interactions with incident light is required, cell structure optimization, anti-reflective coating to understand the physical design of various types of solar cells. Many different technological processes are used to produce solar cells and photovoltaic modules. The knowledge in this field enables better orientation in many types of modules offered on the market. On the application side, knowledge of characteristics, load-to-peak relationships as well as relatively deep knowledge of power and control electronics is important. Because the output power of photovoltaic systems depends on temporary solar radiation, some basic knowledge of solar physics and meteorology is very important for proper system design and implementation. Photovoltaic systems should be resistant to environmental degradation processes, so knowledge of material degradation and reliability issues is desirable. AI should be broadly used both in production and in PV system monitoring. And the economic analysis of projected systems is also very important. Last but not least, it is necessary to understand the basic problems associated with connecting photovoltaic systems to the grid, energy storage and the basics of smart grids.

The training of professionals in the field of photovoltaics can be implemented in many different ways, from short courses and vocational training to high-level university programs. The organization of international summer schools and intensive courses is very useful for the exchange of knowledge and for improving the level of teaching. However, the preparation of curricula and specific lectures requires well-developed links between universities and industry.

The general course "photovoltaics" covering the whole field could be introduced at the bachelor level in the electrical engineering curriculum. Courses that are more oriented on e.g. materials, physics and cell technology or system applications aimed at preparing new specialists for research, development and production of solar modules and other parts of photovoltaic technology could be introduced at master and doctoral level.

Application-oriented courses with an emphasis on optimum use of current photovoltaic technology will be very useful for architects, designers and installers of PV systems, utilities and some other professionals, e.g. in the energy or building authorities. These types of courses may highlight some areas with regard to specific orientation, but some basic knowledge of the whole area is desirable. But it is also very important to ensure that substantial knowledge is passed on to politicians and government officials who have a major impact on technological development.

With increasing installed PV power, system diagnostics and increased reliability are also very important. In addition to theoretical knowledge, practical laboratory or project work is highly desirable for the preparation of future specialists. There are various educational programs at universities around the world with an emphasis on different parts of photovoltaic technology using different tools, from computer simulation to experimental work on photovoltaic systems. A very important part of the education system is the doctoral study preparing new scientists for research activities to achieve innovation. In addition to traditional methods of university (or high school) teaching, new forms such as e-learning can be very effective and very promising for the dissemination of knowledge [16], [17]. Thousands of participants can take such courses. The disadvantage of e-learning courses is that the theoretical parts are supplemented only by virtual experiments.

The development of new teaching and learning methods at bachelor's, master's, and doctoral levels, including interdisciplinary and experimental approaches, research-based or digital media training, as well as ongoing training for professionals, is also an important part of the ambitious European Green Deal plan and its implementation. Vision 2050 Plan [18]. And the REPowerEU program further emphasizes the importance of skills training.

This specially oriented event – International Workshop on Teaching in Photovoltaics – could help us to exchange experiences that might be useful for optimising education and training in the field of photovoltaics and relative areas.

REFERENCES

[1] EC Communication „The European Green Deal“ https://ec.europa.eu/info/sites/info/files/european-green-deal-communication_en.pdf

[2] Gaventa, J.: How The European Green Deal will succseed or fail, December 2019, www.e3g.org

[3] https://www.agora-energiewende.de/fileadmin2/Projekte/2018/EU-Jahresauswertung_2019/Agora-Energiewende_European-Power-Sector-2018_WEB.pdf

[4] Ram M., et al,: Global Energy System based on 100% Renewable Energy – Energy Transition in Europe Across Power, Heat, Transport and Desalination Sectors, study by LUT University and Energy Watch Group, Lappeenranta, Berlin;2018

[5] http://taiyangnews.info/markets/bloomberg-expects-1400-gw-pv-for-europe-by-2050/

[6] Jäger-Waldau, A., *PV Status Report 2019*, EUR 29938 EN, Publications Office of the European Union, Luxembourg, 2019,

[7] 2022 Snapshot of Global PV Markets, Report IEA-PVPS T1-42:2022 April 2022

[8] Global Market Outlook For Solar Power 2022 – 2026, Solar Power Europe 2022

[9] EU Market Outlook For Solar Power 2021 - 2025 Solar Power Europe 2021

[10] https://ec.europa.eu/info/strategy/priorities-2019-2024/european-green-deal/repowereu-affordable-secure-and-sustainable-energy-europe_en

[11] https://www.solarpowereurope.org/advocacy/european-green-deal

[12] IRENA (2018), Power System Flexibility for the Energy Transition, Part 1: Overview for policy makers, International Renewable Energy Agency, Abu Dhabi

[13] G. Masson and I. Kaizuka: IEA PVPS TRENDS 2019 IN PHOTOVOLTAIC APPLICATIONS, www.iea-pvps.org

[14] EC Communication "Preparing for our future: Developing a common strategy for key enabling technologies in the EU", SEC (2009) 1257

[15] EPUE report, 2013

[16] https://online-learning.tudelft.nl/courses/solar-energy/

[17] http://pvinnovation.ca/pv-resources/pv-education/

[18] European technology and innovation platform for smart networks for the energy transition, Vision 2050, 2018, https://www.etip-snet.eu/etip-snet-vision-2050/.

Address of the author:
Czech Technical University in Prague,
Dept. Electrotechnology, Technicka 2, 166 27 Praha 6,
Czech Republic
E-mail: benda@fel.cvut.cz

BIPV planning process towards nearly zero energy districts

Nikolaos Skandalos
University Centre for Energy Efficient Buildings, Czech Technical University in Prague
Třinecká 1024, 273 43 Buštěhrad, Czech Republic

Abstract

Buildings can be classified among the leading energy consumers and CO_2 emitters contributing by 40% of the primary energy in EU. Consequently, the development and implementation of energy efficiency strategies in building sector becomes top priority. In this context, Building Integrated Photovoltaics (BIPV) is being considered as promising contributors for both on-site electricity generation and energy savings in buildings.

This paper presents a framework for the development and early-design guidance of a nearly-zero neighborhood in Prague using open-source simulations tools suitable for educational purposes. The approach starts with methods for urban solar analysis to identify the most radiated parts of buildings' surfaces, propose suitable PV systems and estimate the annual energy yield. Then, simulation model is presented for the assessment of the operational Energy Use Intensity (kWh/m^2) that feed the input for BIPV sizing. Calculated metrics, based on the design parameters selected by the user, will provide information on energy balance and potential for energy self-sufficiency leading to Zero-Energy Building target.

Keywords: photovoltaics, building energy simulation, early design, architecture

INTRODUCTION

The building sector is classified among the key energy consumers and CO_2 emitters in Europe [1]. Currently, there is a major transformation taking place through national building codes, roadmaps and building rating systems. The energy needs has to be reduced and supply the remaining low demand from renewables (EPBD recast) [2].

From this perspective, Building-Integrated Photovoltaics (BIPV) could be the main technology to generate on-site electricity, satisfying part of buildings' demand. Generated electricity cannot only be used instantly to cover building needs (e.g. lighting, appliances, cooling, etc.), but also exchanged between a cluster of buildings. Buildings with a positive energy balance can compensate those with negative balances increasing the PV self-consumption and achieve the zero energy target.

In the current study, BIPV technology is presented as an effective option for buildings to optimize the use of the solar energy source. The paper prsesents a design methodology aiming to provide effective guidance to building engineers, architects or students during the early-design phase. The method employs specific "integrated" software tools, able to address all issues related to the project (e.g. energy balance, life-cycle costs, economic issues, architectural appearance, etc.) into a single platform.

SOLAR CITY CONCEPT

In project CAP, we are focusing on the development of the "Solar City" – a self-sufficient zero energy neighbourhood. A residential district in Zizkov (Fig.1) with a total gross floor area of approx. 100 000 sqm, was selected as demo case for the implementation of the proposed methodology. Design and analysis are integrated within a single simulation environment, where a model is constructed and evaluated according to several targets, in order to allow the designer/student to provide quick and reliable predictions.

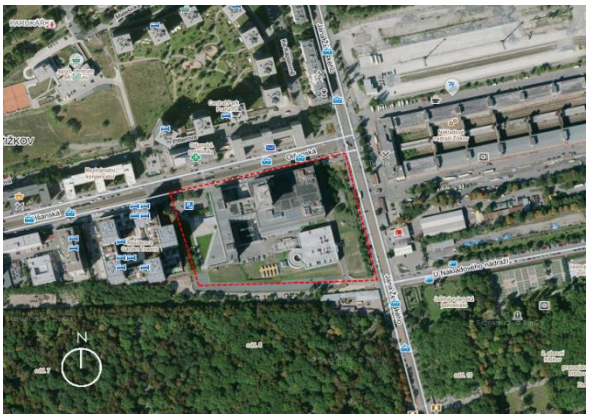

Fig.1: The selected site for the development of Solar City neighborhood (total site area of 39471 m^2).

DESIGN PROCESS

The process starts with a volumetric study (heights, views, construction details) considering all typologies of the building complex. The buildings are modelled in the Rhinoceros environment - a commercial CAD application software (student license around 195 EUR) – using Grasshopper, a visual programming language for parametric modelling.

Then, an urban solar analysis is needed to identify the suitable surfaces for PV integration and the estimation of the annual energy yield. Radiance-based plug-ins such as DIVA [3] and Ladybug [4] are suitable for this process. Basic information regarding the occupancy schedules, equipment and internal gains for each building typology are used for estimating the electricity demand and optimal sizing (installed capacity, orientation, etc.) the BIPV systems.

In parallel, building energy calculations are provided by Honeybee [5] or ClimateStudio. Both tools use the EnergyPlus engine [6] - a whole building energy simulation program - widely used both in research and industry. Users can experiment and explore different materilas and parameters and conclude to the design that minimizes the Energy Use Intensity (EUI) of the building complex. In addition, BIPV systems are proposed taking into account not only the generated electricity, but also their effect on the built environment (thermal, daylighting).

Calculated metrics for the final design will provide information on energy balance and potential for energy self-sufficiency leading to Zero-Energy Building target.

SOLAR ANALYSIS

Details about the shape, dimension and building materials as well as obstacles and construction in the perimeter of the building are collected and 3D model of the building complex is prepared in Rhino. With the Ladybug [4] tools, the students can import and analyse standard weather data, draw diagrams like Sun-path, run radiation analysis, and shadow study. For the design of BIPV this is particularly important, especially for environments where shadow paths can dramatically reduce the PV generation. In our case, Ladybug [4] tool is used to conduct grid-based solar irradiation analysis.

Building surfaces were divided according to the dimensions of the PV modules and the software calculates the hourly irradiation (in Wh/m^2) at every sensor of the analysis grid, during one year period. Each of these surfaces receive different amount of solar radiation, based on the orientation, tilt angle and shadows or reflections from nearby objects. Simulation results can be presented as colored irradiation maps (Fig.2) indicating all the suitable surfaces that PVs can be integrated. Based on the irradiation differences and shading patterns, different string matching scenarios can be proposed by the students.

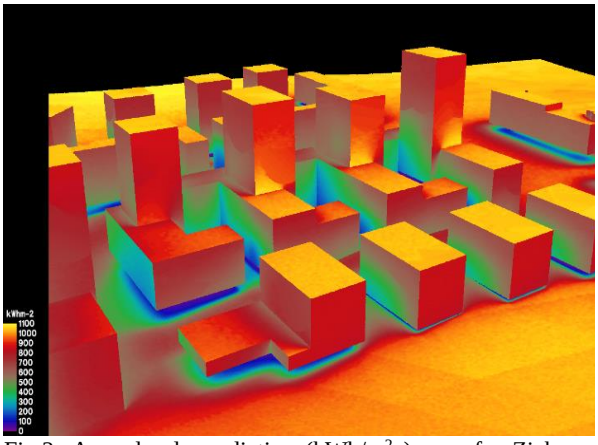

Fig.2: Annual solar radiation (kWh/m^{2}a) map for Zizkov building surfaces prepared in DIVA.

SURFACE SELECTION

Once the radiation values on each surface are available, they can be use to identify suitable surfaces for PV integration. For this purpose, an irradiation threshold is commonly used indicating the minimum amount of annual radiation required for an effective BIPV installation. Such thresholds are somewhat arbitrary; mainly based on financial aspects according to the following equation (Eq.1):

$$PBT = \frac{PV_{cost}\ [€/m^2]}{Threshold\ \left[\frac{kWh}{m^2\ year}\right] * \eta_{ref} * PR * E_{cost}\ [\frac{€}{kWh}]} \quad (1)$$

Where:
PBT = Payback time,
PV_{cost} = PV system cost,
η = PV conversion efficiency,
PR = performance ratio and
E_{cost} = grid selling price

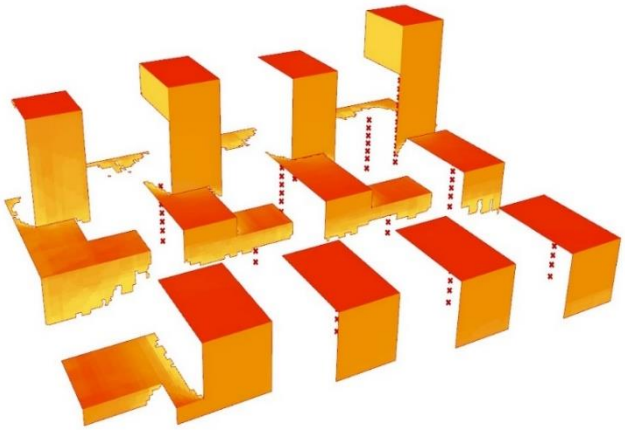
Fig.3: Illustration of the PV-suitable surfaces using irradiation thresholds (650kWh/m^2 annually) with Ladybug tool.

Here, the students can observe how the selected irradiation thresholds affect the relative fraction (percentage) of the surfaces and thus the PV capacity that

could be installed in each building. An example of the available surfaces considering an irradiation threshold of 650kWh/m^2 is presented in Fig.3. Commonly, a conservative value of 1000 kWh/m^2 per year is assumed for the roofs and 800 kWh/m^2 per year for facades [7]. Considering the technological progress and enormous decline of PV costs within last decade, lower values such as 650 kWh/m^2 are still reasonable. However, final desicions regarding the PV surface areas will be taken considering the results from the energy balance calculations in later stage.

PV POTENTIAL

Honeybee is a free plug-in that integrates EnergyPlus to Grasshopper and includes PV simulation components. With the PV component the students need to define the efficiency and effective area of these PV panels. Then they can connect the PV panels to a 'PV simulation' component to link them to EnergyPlus. Based on the area of the suitable surfaces a simple model can be applied to quantify the annual energy output (E_{PV}) of each building block according to Eq.2:

$$E_{PV} = \eta * PR * \sum_{i=1}^{n_{threshold}} (I_i * A_i) \qquad (2)$$

Where:
η = PV conversion efficiency,
PR = performance ratio
$n_{threshold}$ = number of surfaces exceeding threshold,
I_i = cumulative insolation (kWh/m2.year) and
A_i = relative area (m2) of surface i.

For more accurate PV modelling EnergyPlus offer two more options; a) the "Equivalent One-Diode" and b) "Sandia" models. Modules´ parameters can be extracted from Sandia and CEC module libraries. Based on the type of PV integration, EnergyPlus allows for different ways of integrating with heat transfer surfaces and models and calculating phtotovoltaic cell temperature. The students can select among different options offered throuth the 'integrationMode' parameter shown in Fig.4.

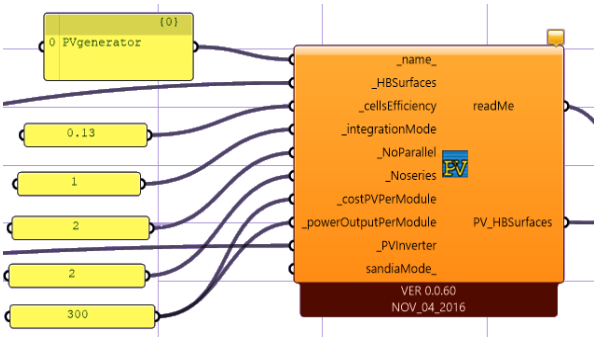

Fig.4: PV generator settings for Honeybee component.

Hourly solar radiation together with the modules´ parameters and inverter technical characteristics will be used to simulate the energy performance for each configuration considered earlier and obtain optimal solution. This could vary according to the objectives i.e. maximizing annual energy yield, load matching, etc.

ELECTRICITY DEMAND

Afterwards, a suitable procedure is used to derive the annual electricity load curves of the representative buildings on hourly basis. Only non-thermal use of electricity is considered here, i.e. the derived load curves include all means of households' electricity consumption except the use for space heating and hot water preparation.
Occupancy schedules are selected to define the presence of peoples in a zone and the use of electric equipment. Typical profiles (Fig.5) for various building typologies can be found in standard library and can be selected via drop-down menus.

In adittion, custom definitions can be prepared by students. This is done by providing an array of 24 values between 0 and 1 (Fraction schedule). The next step is to define a Week Schedule with a typical differentiation between working days and weekends. Ultimately, the Week Schedules are combined to define a Year Schedule. Figure 6 illustrates a complete setup and the relative components in the Grasshopper environment.

Subsequently, representative values for the equipment power density are selected for the estimation of the electricity demand (in kWh/m^2). Lighting energy can also be considered based on the selected values for lighting power density, dimming control and representative illuminance threshold for the interior spaces.

Based on the peak loads and selected objectives, PV systems can be sized properly, in order to enhance the PV self-consumption and reduce excess power during the summer period. In addition, a comparison between the electrical loads and PV generation for the whole building complex can be made through the calculation of load match index [8]. According to the Eq.3 it indicates the average hourly contribution of the PV systems on the building loads (in hourly time intervals).

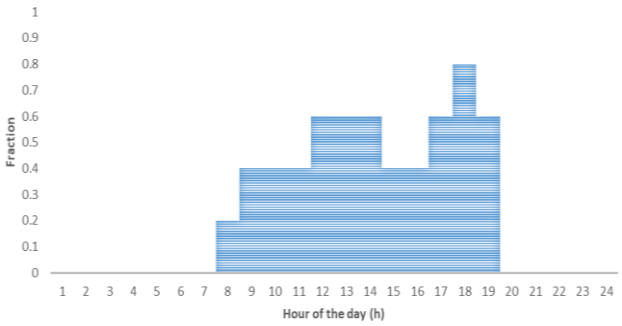

Fig.5: Normalized schedule for commercial building according to SIA2024 [9].

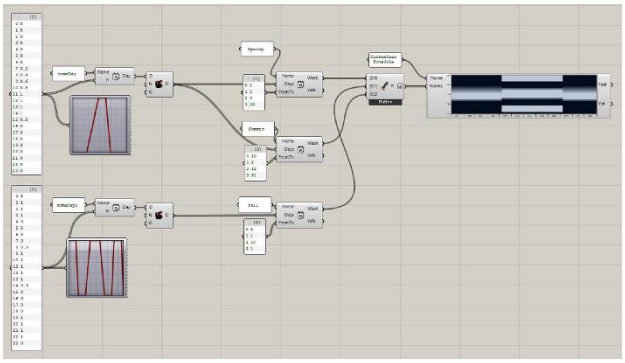

Fig.6: Complete setup for annual schedule definition in Grasshopper environment.

$$f_{load,i} = \frac{1}{n}\sum_{i=1}^{n} min\left[1, \frac{g_i}{l_i}\right] * 100\ [\%] \qquad (3)$$

Where:
i = time interval (hour, day, month),
g_i = instantaneous on-site electricity generation,
l_i = instantaneous electricity demand and
n = sum of time steps over a year period

THERMAL ENERGY DEMAND

EnergyPlus was used to simulate the energy consumption for heating, cooling, ventilation and lighting in buildings. This is done in Grasshopper environment through the use of ClimateStudio and/or Honeybee [5] tools. In this process, the model takes into account the envelope transmission losses, infiltration, ventilation and the solar gains, but also interal flows such as heat emitted from occupants and equipment (Fig.7). These flows are not always in balance and hence heating, cooling and ventilation systems are required to provide a comfortable indoor environment.

Here, students can calculate the energy balance of each building, considering heat gains and losses, an example of which is presented in Fig.8. The students can also investigate the effect of key design parameters on the Energy Use Intensity (EUI) and make an early assessment.

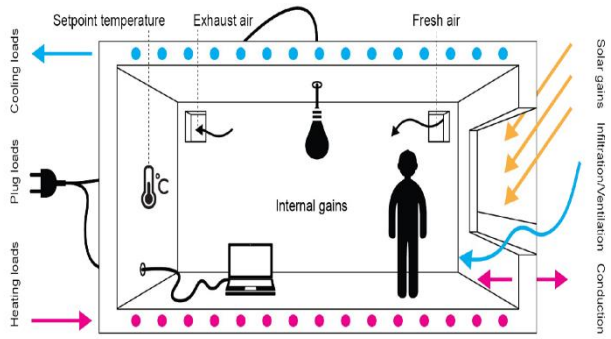

Fig.7: Main heat and mass transfer considered in a room [10].

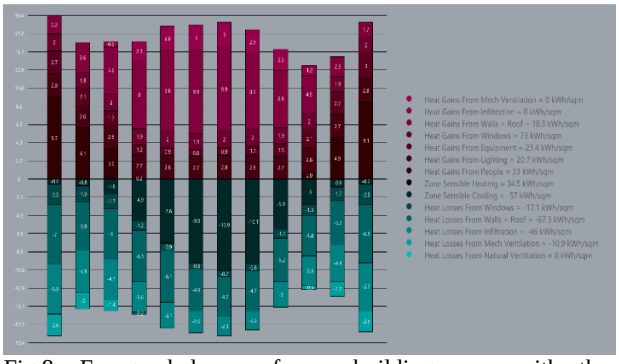

Fig.8: Energy balance of one building zone with the corresponding gains and losses.

Parameters for investigation include both a) envelope and b) system settings. The former corresponds to building envelope construction (insulation, thermal mass, etc.), window-to-wall ratio (WWR), insulating glazing units (U-value, SHGC, TVIS) and shading depth, while the latter include artificial lighting (density, dimming control), heating/cooling systems (gas-fired boiler, electric heating, heat pump) and ventilation strategies. Simulation inputs are fully parametric and can be coupled with optimization algorithms within Grasshopper. Results from selected strategies will be used together with the ones from previous stages to provide final recommendations regarding the design of the BIPV systems leading to Zero-Energy Building target.

CONCLUSION

The paper presented a methodology for the design of BIPV systems in the early design phase of near zero energy districts. Students can learn how to design, configure and optimize BIPV systems using open-source simulation tools. The process includes varyous methods from grid-based solar analysis and PV modelling up to whole building energy simulations and optimization process for BIPV systems.

ACKNOWLEDGEMENTS

This work has been supported by the Operational Programme Research, Development and Education of the European Structural and Investment Funds, project CZ.02.1.01/0.0/0.0/15_003/ 0000464 Centre for Advanced Photovoltaics.

REFERENCES

[1] UNEP, Building Design and Construction: Forging Resource Efficiency and Sustainable Development., (2012).
[2] Directive 2010/31/EU of the European Parliament and of the Council of 19 May 2010 on the energy performance of buildings (recast), Official Journal of the European Communities, (2010).
[3] R.C. Jakubiec JA, DIVA 2.0: Integrating daylight and thermal simulations using rhinoceros 3D, DAYSIM and EnergyPlus. , in: 12th International conference of Building Performance Simulation Association, 2011.

[4] M. Sadeghipour Roudsari, M. Pak, “Ladybug: A Parametric Environmental Plugin for Grasshopper to Help Designers Create an Environmentally-Conscious Design.”, in: 13th International conference of Building Performance Simulation Association. , Chambery, France, Aug 25-28 2013.
[5] Ladybug tools, in, https://www.ladybug.tools/honeybee.html.
[6] D.B. Crawley, L.K. Lawrie, F.C. Winkelmann, W.F. Buhl, Y.J. Huang, C.O. Pedersen, R.K. Strand, R.J. Liesen, D.E. Fisher, M.J. Witte, J. Glazer, EnergyPlus: creating a new-generation building energy simulation program, Energy and Buildings, 33 (4) (2001) 319-331.
[7] R. Compagnon, Solar and daylight availability in the urban fabric, Energy and Buildings, 36 (4) (2004) 321-328.
[8] Karsten Voss, Eike Musall, M. Lichtmeß, From Low-Energy to Net Zero-Energy Buildings: Status and Perspectives, Journal of Green Building, 6 (1) (2011) 46-57.
[9] SIA Merkblatt 2024. Raumnutzungsdaten für die Energie- und Gebäudetechnik (in German); Swiss Society of Engineers and Architects: Zürich, Switzerland, (2015).
[10] ArchSim Primer, in, https://legacy.gitbook.com/book/tkdogan/archsim-primer.

Addresses of the author:

Nikolaos Skandalos, CTU UCEEB, Trinecka 1024, Bustehrad, Czech Republic, nikolaos.skandalos@cvut.cz

PV-measurement system for remote laboratory sessions

R. Vági and B. Plesz,
Department of Electron Devices
Budapest University of Technology and Economics
Budapest, Hungary

Abstract

In recent years the advance of IoT technologies enabled the connection of a wide variety of devices into networks, enabling communication and remote access in an extent that was unseen before. Beside the various applications in consumer electronics, industry 4.0 or interlinking of vehicles the advantages can also be exploited for educational purposes. The possibility of providing remote access to laboratory equipment makes it possible for students to perform some lab practices without physical attendance, thus students in distant locations can be reached and equipment can also be shared among more institutions. This overall increases the range and the effective usage of lab equipment significantly. Also, last two years with COVID-restrictions showed us, how important it is, to be able to provide quality alternatives to the commonly used, attendance-based laboratory work sessions. In this paper we present a fully remote-controlled measurement setup for laboratory practices demonstrating the measurement and the behaviour of PV-cells. The system consists of two main components: a fully remote controllable solar simulator with an I-V curve measurement system and special demo solar module that is capable of simulating different environmental effects and simulating different faults. The functions of this module can also be activated remotely. With this the user is able to perform the measurements and change the measurement conditions remotely during the lab session and can study the behaviour of the PV-device either freely or guided by a tutorial.

Keywords: I-V characteristics, solar simulator, remote access, remote education

INTRODUCTION

To reduce the impact of the COVID-19 pandemic, online formats were introduced in several fields of higher education. The evolution of the Internet of Things (IoT) made it possible to hold not only theoretical lectures, but also practical sessions in the online space. During the online sessions the students - under guidance of an instructor - can handle the same devices and can perform the same tasks as on attendance-based lessons.

To give a deep understanding of the processes, tools and systems in the field of photovoltaics, it is especially important, to develop also practical abilities in addition to the theoretical knowledge. A PV-module for example is a device with a quite complex behavior under operating conditions. Its electric behavior is significantly influenced by the connection configuration of the cells, the cells' temperature dependence, inhomogeneous illumination, and possible inhomogeneous temperature distribution. To describe these phenomena based on a theoretical approach is possible, but much too complicated and the lesson's learned is not proportionate to the effort and mathematical apparatus needed. However, a single laboratory session is already enough to give the students a good insight into the basic behavioral patterns of a PV-device and the hand-on approach of a practical lab session is most often much more memorable than a theoretic lecture. Thus for a long time we included laboratory practices in our curricula where students can measure solar cells and modules under different environmental conditions, and evaluate them in different configurations and under different operational conditions.

For this evaluation of the module behavior the module's I-V curve is used, since this representation is used in applications in practice and it is able to visualize a wide variety of effects, including the dependence on operational behavior and specific defects. During the attendance-based practical session the students work in smaller groups in the lab where they are measuring the I-V curve of the solar cell or module the guidance of the instructor. Afterwards, they determine the device specific properties for example efficiency, operating point, short circuit current, open circuit voltage from the measurement results. They also explore the effects of inhomogeneous illumination and the module's temperature dependence. The knowledge gained in these lab session helps to develop the necessary professional perspective for the design, measurement, and servicing of multi-module PV systems.

Due COVID-19 restrictions, these practical lessons could not be hold in the usual attendance-based form. In order to make the practical knowledge transferable, we have created a complex solar cell measurement system that can be operated remotely (Fig. 1). With this system the students can perform the lab tasks during the online practice from home and can compose the documentation based on the results. The system performs measurement of each I-V curve measurement fully automated, the students only have to set the measurement parameters (representing the different environmental conditions) and start the acquisition of the I-V curve. The main components of the system are an illumination unit and a special PV-module. On the module every cell's temperature can be changed individually. In addition, there is the possibility to change the wiring of the cells within the module, and the users can add an error to a specific cell. This system is not only capable of remote control, but is also faster and thus allows more measurements and the examination of more operational scenarios than the previous manual setup used in the attendance-based lab sessions. With this system each student can perform the lab sessions individually instead of crating smaller groups. If the special demo module is replaced with a DUT (device under test), the system acts as a remote controlled solar simulator and I-V tester, and can be applied for testing different devices.

SYSTEM SETUP

The system consists of two main components: a fully remote controllable solar simulator with an I-V curve measurement system and a special demo solar module that is capable of simulating different environmental effects and simulating different faults. The functions of this module can also be activated remotely. With this the user is able to perform the measurements and change the measurement conditions remotely during the lab session and can study the behavior of the PV-device either freely or guided by a tutorial.

On the special solar module there are four solar cells which can be connected in series or in parallel or measured separately. In addition, single cells can be short circuited, to show the effects of cell failure. The temperature of each cell can be adjusted by heaters installed below the single cells.

During the measurements the module is illuminated by the solar simulator. The solar simulator is built up modularly from 110 x 110 mm LED-modules. In the current arrangement a 3 x 3 LED-module arrangement is used, ensuring class A homogeneity and time stability on an area of 20 x 20 cm in a light intensity range from 100 to 2000 W/m^2. Due to the modular arrangement various solar simulators sizes can be constructed, up to the size of commercial panels.

To use the system, the user logs into the control computer in remote access mode and uses the control software (written in LabVIEW) to set the module switching parameters, the light intensity and then start the measurement. The system performs the measurements by a Keithley source meter unit. The communication between the software and the measurement unit takes place over local area network, using standard communication protocol, TCP and using SCPI commands. The system's further part is a power supply for the LED-panels of the solar simulator and a central control unit that controls the light intensity and the power supply, performs the switches of the demo PV-module, sets the cells' temperature. The unit communicates over the local area network with the GUI software and the power supply. The users cannot modify the operational parameters of the power supply in remote access mode over the software, to avoid malfunctions.

If the special demo PV-module is not used, the system acts as a solar simulator and I-V curve tracer for measuring any kind of PV device that fits under the solar simulator. Naturally, the system can also be operated in local mode as a conventional PV-device tester.

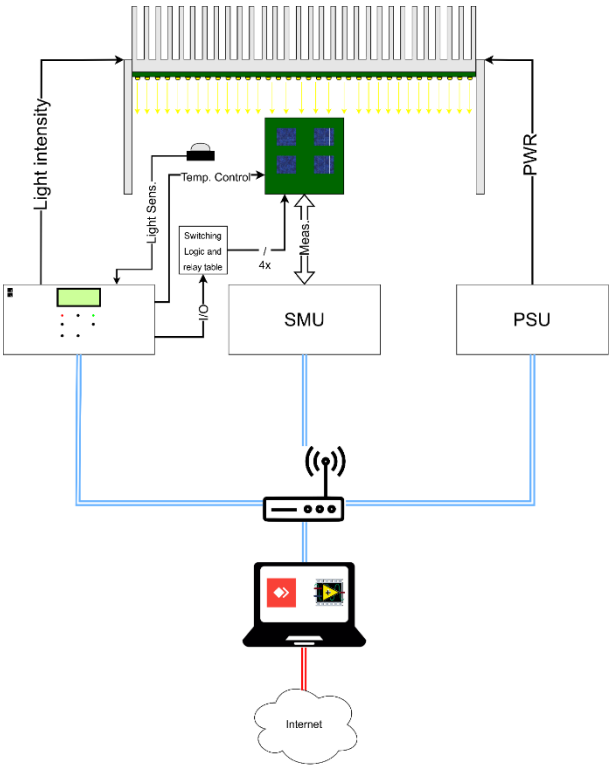

Fig. 1: Schematic system layout

The measurement system's components are the following: illumination unit made of LED modules, source meter unit (SMU), high power power supply, personal computer which contains two network cards and a self-developed control unit. As seen on Fig. 1 the main components of the system communicate through local area network which is realized by a router. The personal computer is responsible for controlling the system, this device is connecting at the same time to the mentioned local area network and to the wide area network. The users can connect via internet with AnyDesk to the computer that runs the GUI software made in National Instruments LabVIEW development environment, performs the measurements. On the figure the local area network is marked in blue (double line), the software is

configured to communicate only on this network. The structure and functions of the special module, the structure and tasks of the self-developed control unit, and the operation of the LabVIEW software will be discussed below.

Solar simulator

The special PV-module illuminated by a solar simulator during the measurements. The solar simulator has a modular design, it consists of 9 LED-moduleswith a size of 110 x 110 mm in a 3 x 3 layout, with a calibrated illuminated area 20 x 20 cm. Thanks to the arrangement of the LEDs, the solar simulator is able to meet the homogeneity criteria of IEC 90604-9 Class A [1] without a special optical solution. Based on our previous work [2] the light homogeneity distribution of an illuminating module is shown in Fig. 2.

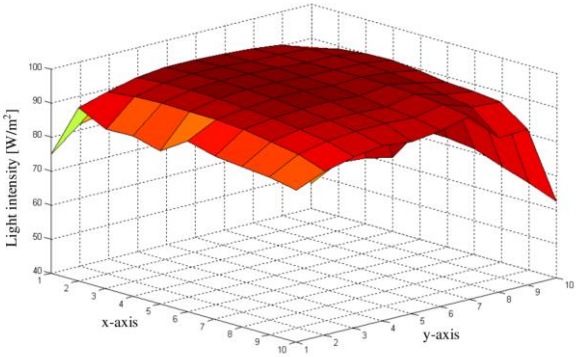

Fig. 2: Light intensity distribution of a single LED-module

The illumination unit can illuminate a 200 x 200 mm area with a light intensity between 100 or 1000 W/m^2 During the illumination, the system measures the intensity with a sensor module. This device consists of a calibrated PV-cell, with an analogue output signal which is proportional to the light intensity, with a sensitivity of 0,01 V / 100 W/m^2. Both the special PV-module and the light sensor fit under 200 x 200 mm homogeneously illuminated area of the solar simulator.

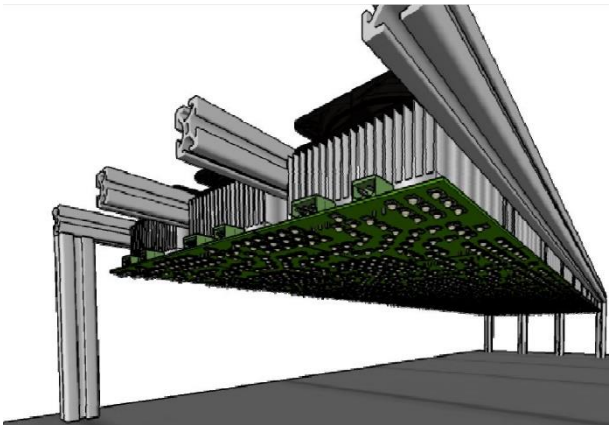

Fig. 3: CAD-drawing of the LED-simulator

Control Unit

This self-developed unit is responsible for several tasks. Previously the control unit of the solar simulator was a current control with an analogue input that received the analogue control voltage from a PC over a D/A converter card. This unit was upgraded to be capable of digital communication and supplemented with additional functions, including the control of the demo module. It controls light intensity by a variable current limiter, that is connected to the 250 V and 2,5 A main power supply. It also contains a power supply that delivers the voltages for the current limiter (symmetric 15 V), the solar simulator's cooling system (12 V), and the digital microcontroller (5 V). The further parts of the control unit are a network module, a microcontroller, and current generators for the PT100 types of temperature sensors. The structure of the control unit is shown in Fig. 4.

One of the main task of the control unit is the communication with the high-power power supply via SCPI commands. The unit enables, disables, and configures the power supply. It also generates the setpoint of the solar simulator. This is an analogue signal which goes to the input of the current limiter. The previous version of the control unit didn't contain a control-loop to sets the light intensity, and it was offline, meaning the user set the intensity with buttons.

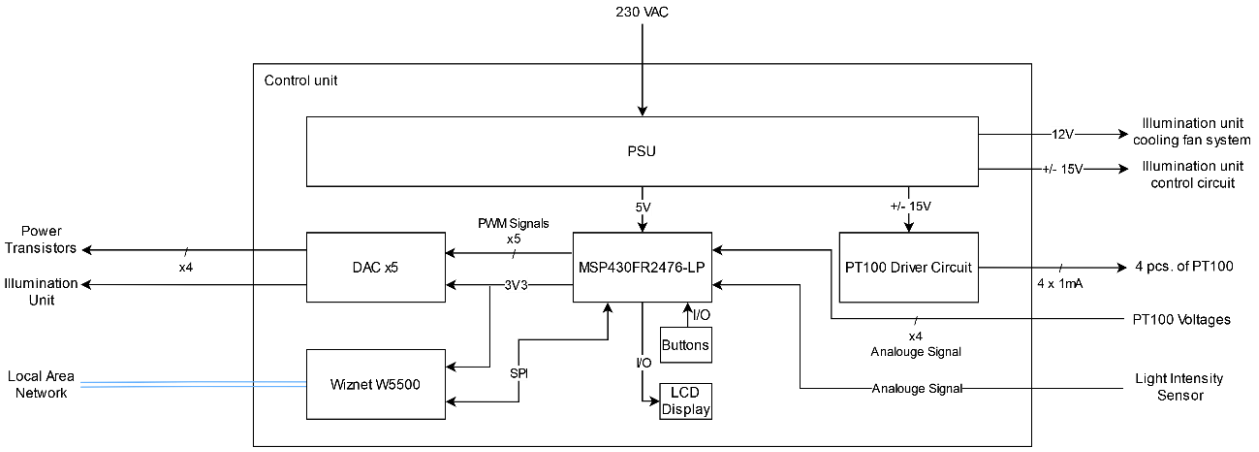

Fig. 4: Control unit architecture

Additional features were added to the control unit. The actual version consists of 5 control loops, one of them is responsible for the light intensity and the other 4 are responsible for the temperature of each cell. The measurement software sends the setpoints of the intensity and the temperatures, the control unit receives it and starts the control. For the control of the light intensity the control unit receives the output signal of the intensity sensor as a feedback. In the unit a PI-type control mechanism is implemented.

An important feature is that the user cannot change the settings of the power supply over the GUI software, to avoid malfunctions. The control unit is also capable to operate in offline mode, meaning that the solar simulator can be operated without GUI software on the main personal computer. In this mode the unit acts as a manual solar simulator.

Special demonstrator PV-module

The special demonstrator module that is used by the students during the remote session consists of 4 solar cells. Due the construction of the module, the connections between these cells can be modified during the remote session, this is how the different module wiring configurations are demonstrated to the students. The PV-module schematic can be seen Fig 5 and the possible cell connection configurations are shown in Fig. 6.

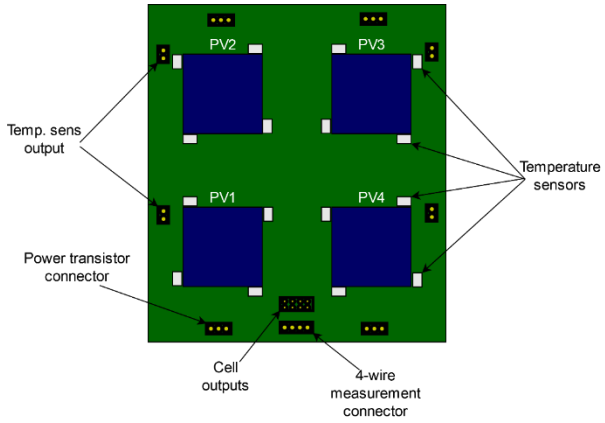

Fig. 5: Layout of the special demo-module

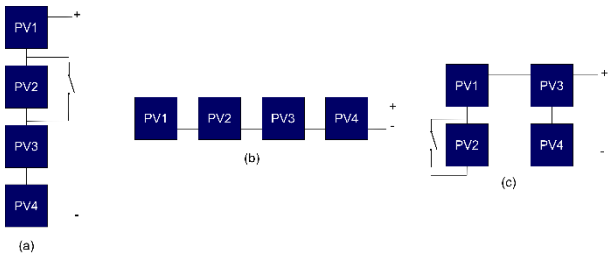

Fig. 6: Possible configuration of the demo module. a) series, b) parallel, c) hybrid (2 strings of 2 cells in parallel)

The anode and cathode of each cell are routed to the connections of the module where the switching logic circuit and relay table are connected to the module. With this switching circuit the user can choose between the connect modes, and can insert a fault to the module via the GUI. This fault is the short circuit of the cell number two. With this function, it is easy to demonstrate the change in the U-I characteristic of the given connection mode in the event of such fault.

As already mentioned, each cell's temperature can be modified. Heating is achieved by high power transistors which have been integrated to bottom side of the PCB, under the cells. The transistors transfer heat through thermal vias to the cells to reach the desired temperature. Four PT100 type temperature sensors are responsible for the temperature feedback for each cell. The location of the thermometers and the module itself have been designed according to design considerations that help to determine the temperature of the component as accurately as possible [3]. The temperature sensors have been placed as close as possible to the cells and there are poured copper surfaces between the cells and the sensors' bottom side to increase the thermal conductivity. The four resistors are connected in such way that their resulting resistance is 100 Ω (T = 0 ° C). Thus, the measurement of the area limited by them, i.e., the average cell temperature, is realized. The temperature sensors and the heating transistors can be contacted over the connectors marked in Figure 5. The location of the transistors in the module is shown in Fig. 7.

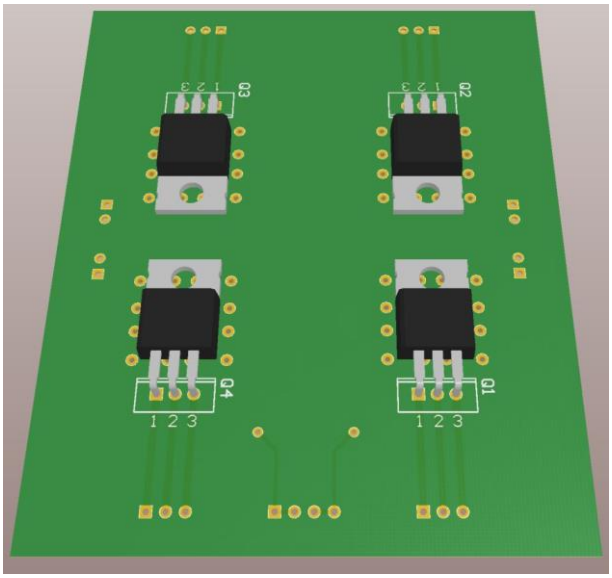

Fig. 7: Transistors for the heating of each cell

MEASUREMENT

The system performs the measurement with a Keithley 2450 source meter unit (SMU) [4] which is marked on Fig. 1. The device performs the measurement in 4-wire measurement mode. For the measurement the voltage

generator mode of the SMU is used that forces different voltage values to the terminals of PV-module and at every value the current will be measured. This device can measure maximum in the range of +/- 20 V modules, and a maximum current of 1 A.

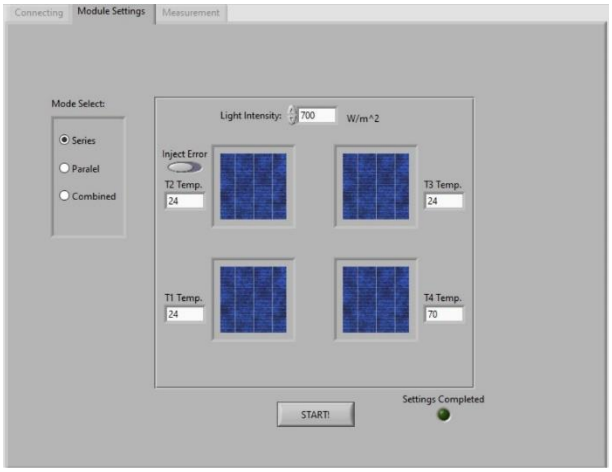

Fig. 8: GUI for setting the measurement parameters

After a measurement is done, its results can be saved before a new one is started. The software saves the result into coma separated values file format. (*.csv) As default the software recommends the actual date as the file name, but the user can modify it. The data saves into the file also contains the cell connecting method, the illumination value, and the temperature values. The GUI for the module settings can be seen in Fig. 8.

Measurement software

The GUI software is responsible for the connection between the user and the measurement system. The software communicates over the local area network with the components of the measurement system. After the start of the application the software tries to connect to the SMU and the control unit. The software can't connect directly to the high-performance power supply, only the control unit is capable of this. The block diagram of the measurement software can be seen in Fig. 9.

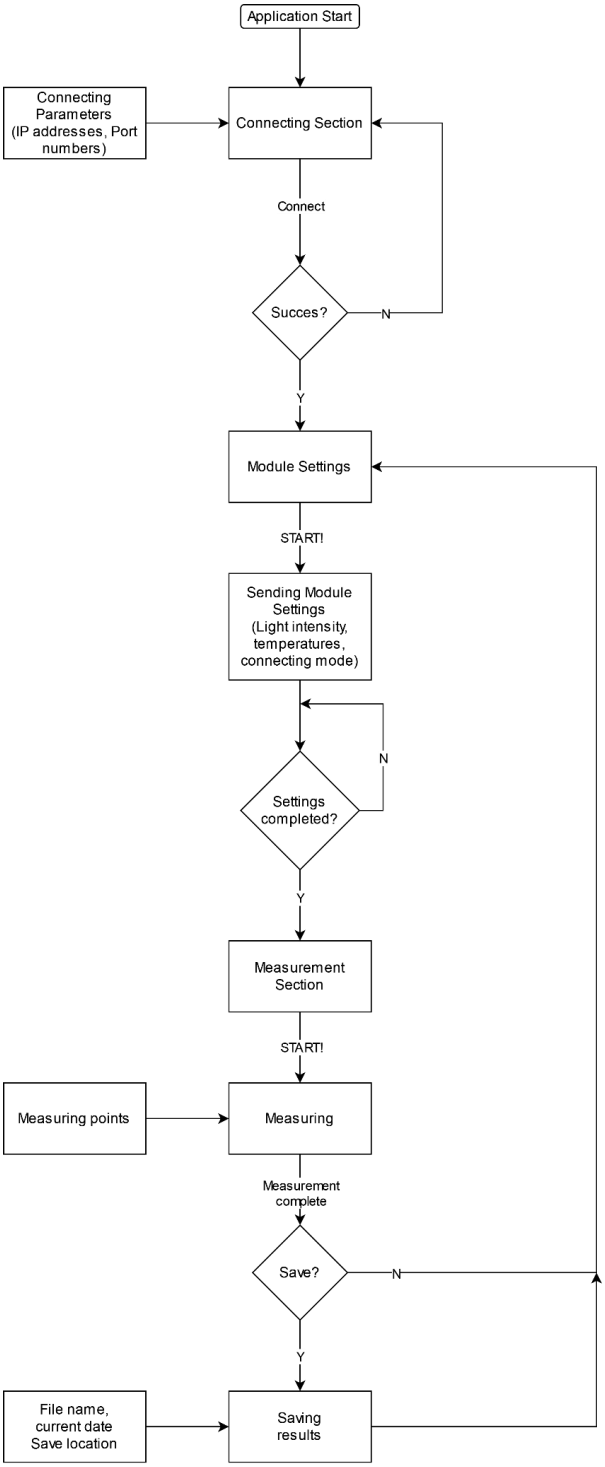

Fig. 9: Block diagram of the measurement software

Measurement results

The I-V curves of the measurement results are displayed in X-Y plots on the screen of the GUI. For comparison reasons it is possible to display more curves in one plot. The user has the possibility to save the I-V curve data after each measurement and use the measurement data for processing and analysis later. Fig. 10 shows some examples for the visualization of measurement data at different module configurations and light intensities.

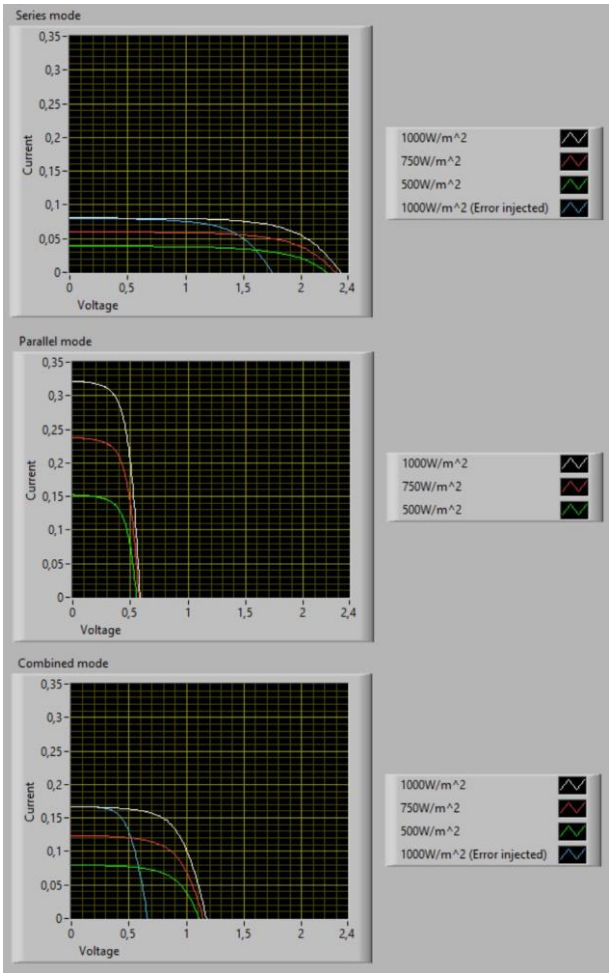

Fig. 10: Displayed results for different configurations of the demo module configurations at different light intensities, with cell failure switched on and of. a) series configuration, b) parallel mode (no cell failure available), c) hybrid mode

Addresses of the authors

Richárd Vági, 1117 Budapest, Magyar tudósok krt. 2, Budapest, Hungary, vagi.richard@vik.bme.hu
Balázs Plesz, 1117 Budapest, Magyar tudósok krt. 2, Budapest, Hungary, plesz.balazs@vik.bme.hu

CONCLUSIONS

To be able to deliver practical laboratory sessions in times of COVID-19 human contact restrictions a fully remote controllable measurement setup was developed for the demonstrations of the effects of the environmental conditions on the behaviour of PV-devices. With the developed setup the I-V curves of solar cell and small modules can be measured in remote control and fully automatedly. The system comprises of a solar simulator and a special demo module. In the demo module the configuration of the wiring of the cells can be change, also faults can be inserted into the circuit over a GUI. In addition, the temperature of each cell can be seat with the help of a heating transistor on the backside of the demo module. This enables students to investigate and evaluate the behaviour of solar cells and modules over a wide range of possible operational conditions remotely. Without the special demo module the system operates as a remote controlled solar simulator.

ACKNOWLEDGEMENTS

This research was partially funded by the EURYDICE project in the framework of the Erasmus+ Programme of the European Union.

REFERENCES

[1] IEC 60904 - 9: 2007: Photovoltaic devices, Part 9: Solar simulator performance requirements
[2] Cs. Berényi, G. Hantos, B. Plesz: Design of a compact modular multifunctional solar cell measurement system, In: Proceedings of the 6th International Workshop on Teaching in Photovoltaics (2012)
[3] Texas Instruments Application Report: Temperature sensors: PCB guidelines for surface mount devices, downloaded from: https://www.ti.com/lit/an/snoa967a/snoa967a.pdf, May 15th, 2022
[4] Keithley 2450 SMU Datasheet, downloaded from: https://download.tek.com/datasheet/1KW-60904-2_2450_Datasheet_082821.pdf, May 15th, 20022

Model for Electricity Generation by Thermoelectric Generators used in Spectrum-Splitting Applications

Ahmed Issa Alnahhal[1,2], Ahmad Halal[1] and Balázs Plesz[1],
[1]Department of Electron Devices
Budapest University of Technology and Economics
Budapest, Hungary

[2]Department of Biomedical Engineering
University of Palestine
Gaza Strip, Palestine

Abstract

A model of solar thermoelectric generator STEG device is presented which consist of a concentrator part, heat collector part, TEG part and heat sink part. A simulation is carried out for the full spectrum, visible light spectrum (380 nm-750 nm) and near infrared spectrum (750nm-3000nm) of solar radiation in term of concentration. The hot side temperature, cold side temperature and their temperature difference are simulated for each spectrum. Also, the generated voltage, current, output power and the efficiency of the TEG have been evaluated and simulated for each spectrum. The effects of the heat transfer coefficient of the heat sink and concentration levels are included and evaluated. With non-concentrated or at the same concentrated light naturally, the full spectrum resulted in the highest efficiency, but higher concentration levels can compensate the lower power density of filtered light. Also compared to PV cells the efficiency is lower with both the full and the visible spectrum, however in the IR-region it can be competitive to PV-cells, due to its broader absorption spectrum. Due to this TEGs can be a viable alternative for solar cells in applications where the lower wavelength parts of the spectrum are used for different purposes or devices (i.e., high band gap solar cells, plant growth, etc.).

Keywords: Thermoelectric Generator, Solar Spectrum Splitting, Concentrated Spectrum, MATLAB.

INTRODUCTION

The most used energy resources are limited resources, and they will be depleted quickly due to their widespread use. The use of these resources is likewise detrimental to the ecosystem. The use of solar energy is becoming increasingly vital as the resource issue worsens. Photovoltaics and concentrated solar power are two of the most common technologies for directly harnessing the sun's energy. Furthermore, a significant portion of these resources are squandered as waste heat rather than being transformed into electrical energy. Solar thermoelectric generator STEG is a power generation technology that converts the incoming solar radiation into thermal energy, and transforms this thermal energy directly into electricity [1]. Thermoelectric generator (TEG) units consist of n- and p-type semiconductor materials which are connected electrically in series and thermally in parallel [2]. A highly efficient TEG device will depend on the electrical and thermal characteristics of the used semiconductor materials as thermal conductivity, electrical conductivity and Seebeck coefficient which define the figure of merit (ZT) of the TEG device as

$$ZT= \frac{s^2\sigma}{K} T \quad (1)$$

Where s, σ, k and T are the Seebeck coefficient, electrical conductivity, thermal conductivity, and average temperature, respectively [3]. The conversion efficiency of TEGs is limited by two major factors; the Carnot cycle efficiency, which establishes a theoretical upper constraint on the efficiency of thermal energy conversion to work and the efficiency of the thermoelectric effect. Carnot efficiency is $\Delta T/T_h$, where T_h is the temperature of the hot side and ΔT is the temperature difference between the hot and cold sides [4]. As a result, the overall efficiency of a thermoelectric device is governed as follows

$$\eta= \frac{\Delta T}{T_H} \frac{(1+ZT)^{\frac{1}{2}}-1}{(1+ZT)^{\frac{1}{2}}-\frac{T_C}{T_H}} \quad (2)$$

Where T_C is the cold-side temperature, T_H is the hot-side temperature, ΔT the temperature difference T_H - T_C and

ZT is the thermoelectric material's figure of merit [5-6]. The lower the thermal conductivity and higher the electrical conductivity and Seebeck coefficient of the material, the higher ZT and the more efficient the TEG device. Higher temperature differences across the TEG terminals also increase the TEG's efficiency. Therefore, concentrated solar thermoelectric generator (CSTEG) is introduced in which the sun's energy is concentrated. The area of the thermoelectric module is substantially less than in flat-plate systems because the focusing optics focus the light. The reduced size of used semiconductor materials results in lower cost, in which the expensive semiconductor materials are replaced by cheap ones, such as glass mirrors or lenses, steel, aluminum, and plastics. Bismuth Telluride (Bi_2Te_3) is a common thermoelectric generator material which can be used up to temperatures of 350°C [7]. Their efficiency is less than 10%. Many thermoelectric materials are currently being investigated to increase and optimize power generation, also recent advancements in ZT offers significant potential in the development of new generation as well [8]. Ideas for solar thermoelectric generators and photovoltaic thermoelectric hybrid systems have been developed in recent years as thermoelectric technology has progressed [9,10]. Thermoelectric devices have several advantages over conventional power-generation methods [11]: TEGs are silent solid-state devices with no moving parts, ecologically friendly, scalable from tiny to large heat sources, and very reliable. They also have a longer lifespan and the ability to create electrical energy from low-grade thermal energy. This paper contains four sections. The second section is methodology, the third section is the results and discussion, and the fourth section is the conclusion.

METHODOLOGY

Fig. 1 shows a schematic diagram of a CSTEG system in which a concentration lens concentrates the solar radiation into the heat collector. The heat collector collects the solar energy and transfer it to the hot side of TEG module. A heat sink is used to remove the heat from the other terminal of the TEG module for temperature gradient establishing.

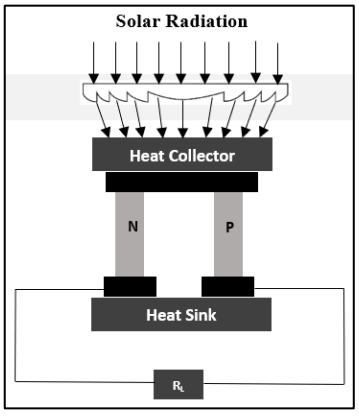

Fig. 1: Concentrated Solar Thermoelectric Generator CSTEG

Thermoelectric Generator Model

The heat collected by the TE module's hot junction can be represented as [12]

$$Q_H = \alpha_{HC} E_{TEG} - Q_{rad} - Q_{conv} \quad (3)$$

Where α_{HC} is the heat collector absorptivity, E_{TEG} is the input solar energy of heat collector, Q_{rad} and Q_{conv} are the heat collector's radiation and convection heat losses respectively. The heat collected by the hot junction which is equal to the heat transferred by heat collector, and the heat removed by the thermoelectric cold junction [12] are as follow:

$$Q_H = K_{HC}(T_{HC} - T_H) \quad (4)$$
$$Q_C = h_c A_{HS}(T_C - T_{Coolant}) \quad (5)$$

Where K_{HC} represents the heat collector conductivity, h_C is the heat transfer coefficient, A_{HS} is area of heat sink, T_{HC}, T_H, T_C and $T_{Coolant}$ are heat collector, hot side, cold side and coolant temperatures. The classic formulae for absorbed and removed heat [13] based on the Seebeck, Thomson, and Peltier effects are as follows:

$$Q_H = (K_p + K_n)(T_H - T_C) - \frac{1}{2} I^2 (R_p + R_n) + (S_p - S_n) I T_H \quad (6)$$
$$Q_C = (K_p + K_n)(T_H - T_C) + \frac{1}{2} I^2 (R_p + R_n) + (S_p - S_n) I T_C \quad (7)$$

Where I is the current supplied by the Seebeck effect voltage, $S_{n,p}$, $R_{n,p}$ and $K_{p,n}$ are the Seebeck coefficient, electrical resistance and thermal conductance of TEG n- and p-type legs respectively [14] in which

$$R_{n,p} = \frac{L}{A_{n,p}\sigma_{n,p}} \quad (8)$$
$$K_{n,p} = \frac{A_{n,p}k_{n,p}}{L} \quad (9)$$

Where $A_{n,p}$ is the n-type and p-type legs cross-section area, $\sigma_{n,p}$ and $k_{n,p}$ are n- and p-type legs electrical and thermal conductivity respectively. The current I supplied by the Seebeck voltage and the TEG output power [15] are as follow:

$$I = \frac{V_{TEG}}{R_L + R_{TEG}} \quad (10)$$
$$P_{TEG} = I^2 R_{TEG} \quad (11)$$

By setting $R_L = R_{TEG}$, the maximum efficiency of the TEG subsystem is as [15]

$$\eta_{TEG} = \frac{P_{TEG}}{E_{TEG}} \quad (12)$$

Spectrum-Based Electricity Generation

A CSTEG model is presented using the forementioned equations in MATLAB. The output power of the CSTEG system is determined by the spectrum and intensity of the incident sunlight, as well as the electrical and thermal characteristics of the TEG thermocouple. The solar radiation spectrum has been divided into three parts, full spectrum, visible spectrum (400 nm-780 nm) and near infrared spectrum (780 nm-3000 nm). The output power

and efficiency of the CSTEG has been evaluated and simulated for each spectrum in terms of concentration levels. The solar spectrum-based energy is calculated in (13) where η_{opt} is the concentrator efficiency, F(λ) the irradiance spectrum, λ_1 and λ_2 are the spectrum wavelengths limits.

$$E_{TEG} = \int_{\lambda_1}^{\lambda_2} \eta_{opt} A_{HC} C_g F(\lambda)\, d\lambda \qquad (13)$$

The simulation has been performed for natural convection heat transfer coefficient of 2.5 W/(m^{2}K) [16] and using the parameters in table I and under the following assumptions; the TEG module's contact resistances are neglected and the Seebeck coefficient, electrical and thermal conductivity of the TEG legs materials are the same at the hot and cold sides.

Sy.	Description	Value
	Optical	
η_{opt}	Optical Efficiency	0.9
C_g	Concentration ratio	50-150 suns
	Heat Collector [12]	
A_{HC}	Surface Area	50 um^2
K_{HC}	Thermal Conductivity	0.2 W/K
α_{HC}	Absorptivity	0.95
ε_{HC}	Emissivity	0.08
	TEG [17]	
$L_{p,n}$	Length of p and n-Type Leg	5mm
W_{pn}	Width of p and n-Type Leg	5mm
$H_{p,n}$	Height of p and n-Type Leg	5mm
σ_p	p - Leg Electrical Conductivity	76103 $(\Omega m)^{-1}$
σ_n	n - Leg Electrical Conductivity	89365 $(\Omega m)^{-1}$
k_p	p - Leg Thermal Conductivity	1.265W/(mK)
k_n	n - Leg Thermal Conductivity	1.011W/(mK)
s_p	Seebeck Coefficient of p-Leg	2.037×10^{-4} V/K
s_n	Seebeck Coefficient of n-Leg	-1.721×10^{-4} V/K
	Heat Sink	
A_{HS}	Surface Area	50 um^2
h_c	Heat transfer Coefficient	1000 W/m^{2}K

Table I. Data Parameters Used in the CSTEG Model

RESULTS AND DISCUSSION

Fig. 2 shows the temperature, heat collector heat flux and efficiency of CSTEG of full, visible light and near infrared spectrums at concentration ratio of 100 suns. Fig. 2 (a) shows hot, cold side temperatures and temperature difference. The hot side temperature of full spectrum is higher than the visible light and near infrared spectrums. Also, the cold side temperature of full spectrum is higher than the others. The difference of hot and cold side temperatures of full, visible light and near infrared spectrums are 218.57 K, 123.96 K and 103.47 K respectively. Fig. 2 (b) depicts that the heat flux of heat collector of full, visible light and near infrared spectrums are 4.1968 W, 2.1887 W and 1.7929 W respectively. While fig. 2 (c) indicates that the efficiency of the CSTEG is the highest with the full spectrum, while the near infrared spectrum has the lowest efficiency, and the visible light has an efficiency in between. Fig. 3 shows the temperature and efficiency of CSTEG of visible light and near infrared spectrums at concentration levels of 50, 75, 100, 125 and 150 suns and a heat transfer coefficient of the heat sink of 1000 W/m^{2}K.

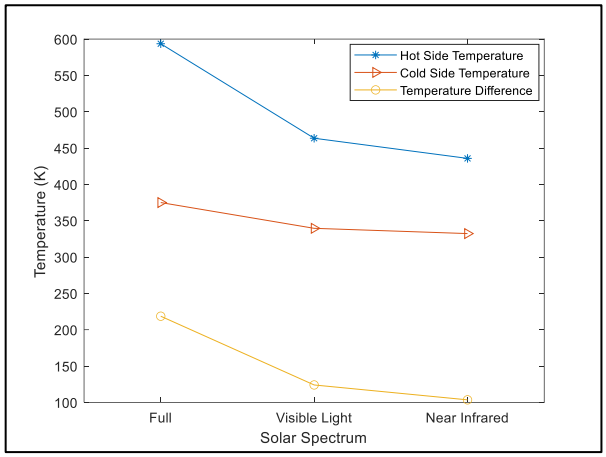

(a)

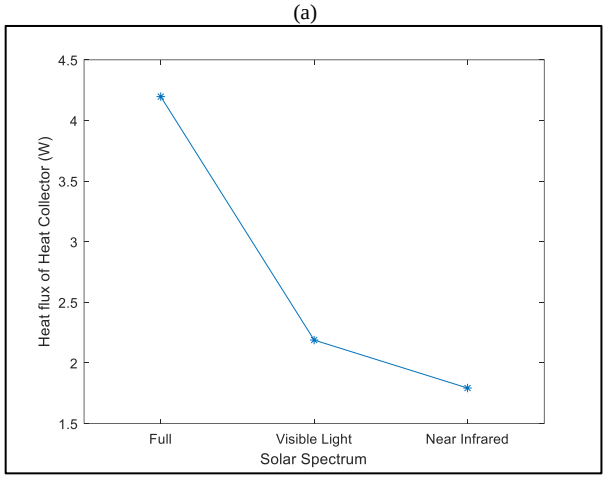

(b)

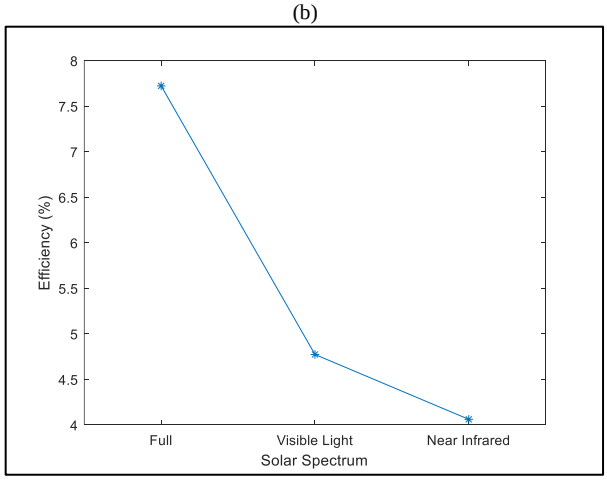

(c)

Fig. 2: Thermoelectric Generator a) Temperature -Solar Spectrums, b) Heat Flux – Solar Spectrums and c) Efficiency-Solar Spectrums at heat transfer coefficient of 1000 W/m^{2}K.

Fig. 3 (a) shows the hot side temperature, cold side temperature and temperature difference of concentrated visible light spectrum. The hot side temperature increases almost linearly with the concertation levels. The cold side temperature shows the same tendency but with a lower slope, thus the temperature difference is increasing. Fig. 3

(b) depicts the hot side temperature, cold side temperature and temperature difference of concentrated near infrared spectrum. The visible light spectrum heats the TEG more than the near infrared spectrum. Therefore, Fig. 3 (c) indicates that the efficiency of CSTEG at visible light spectrum is higher than its efficiency at near infrared spectrum.

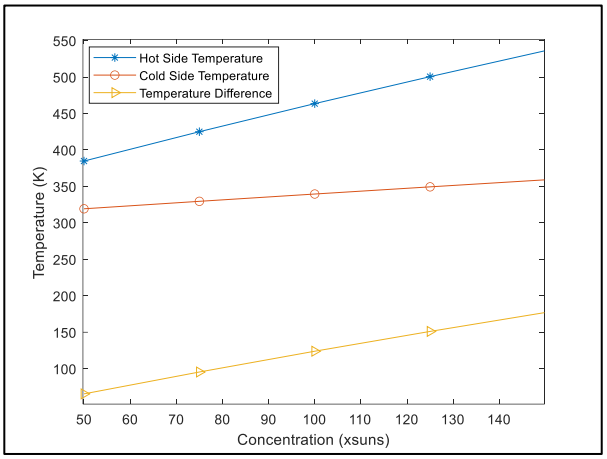

(a)

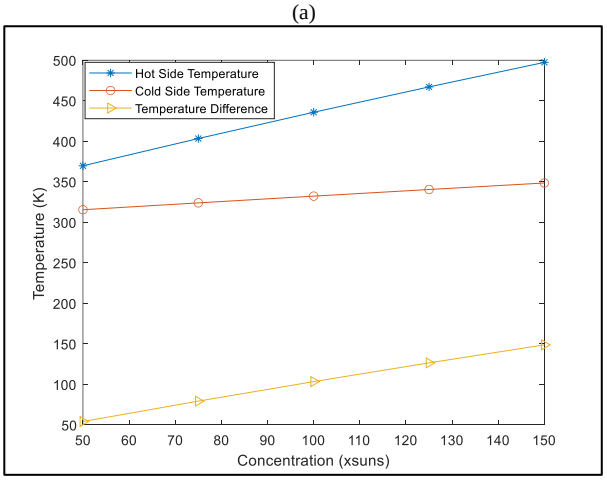

(b)

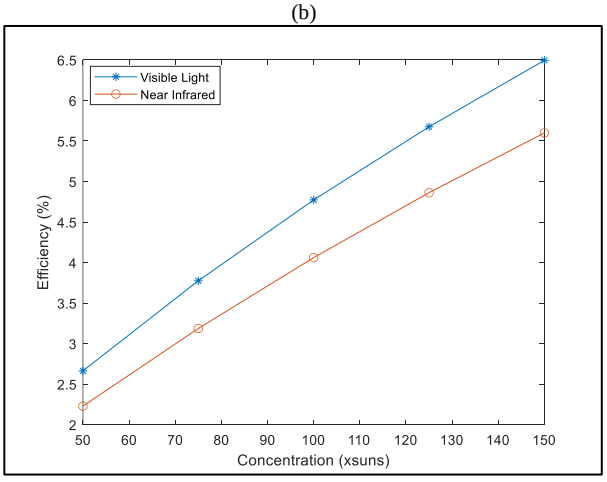

(c)

Fig. 3: Thermoelectric Generator a) Temperature - Concentration of visible light spectrum, b) Temperature – Concentration of near infrared spectrum and c) Efficiency-Concentration at heat transfer coefficient of 1000 W/m^{2}K for the heat sink.

Comparing Fig. 3 (C) with Fig. 2 (C), the efficiency of TEG at visible light and infrared spectrums at concentration of 100 suns are 4.77% and 4.06% respectively, while its efficiencies at concentration of 150 suns are 6.49% and 5.60% respectively. While the efficiency of TEG at full spectrum with concentration 100 suns is 7.72%. It can be seen that the efficiency of the TEG at visible light and near infrared spectrums at concentration level of 150 suns approach the efficiency of TEG at full spectrum with concentration 100 suns. Thus, a higher concentration levels can compensate the lower power density of filtered light. The hot side, cold side temperatures and efficiency values of the three spectrums with concentrations are tabulated in Table II. Fig. 4 reveals the temperature and efficiency of CSTEG of full, visible light and near infrared spectrums at concentration level of 100 suns and a heat transfer coefficient of the heat sink of 1000 W/m^{2}K, 5000 W/m^{2}K and 10000 W/m^{2}K.

	50	75	100	125	150
Visible Light Spectrum					
T_H (K)	384.7	424.9	463.5	500.5	536.1
T_C (K)	319.2	329.5	339.5	349.3	359.0
ΔT(K)	65.4	95.4	123.9	151.1	177.1
η (%)	2.66	3.77	4.77	5.67	6.49
Near Infrared Spectrum					
T_H (K)	369.7	403.3	435.7	467.0	497.3
T_C (K)	315.5	323.9	332.3	340.4	348.5
ΔT(K)	54.2	79.3	103.4	126.5	148.8
η (%)	2.22	3.18	4.06	4.86	5.60

Table II. Hot Side and Cold Side Temperatures and the TEG Efficiency of Filtered Spectrums with Different Concentration Levels.

Fig. 4 (a) and (b) show that the hot side and cold side temperature of full, visible light and near infrared spectrums are decreased as the heat transfer coefficient increases. The decrease in cold side temperature is more significant than the decrease in hot side temperature, thus their difference increases. It also shows that the decrease of hot side temperature and cold side temperature is more significant as the heat sink's heat transfer coefficient is increased from 1000 W/m^{2}K to 5000 W/m^{2}K than if it increased from 5000 W/m^{2}K to 10000 W/m^{2}K.

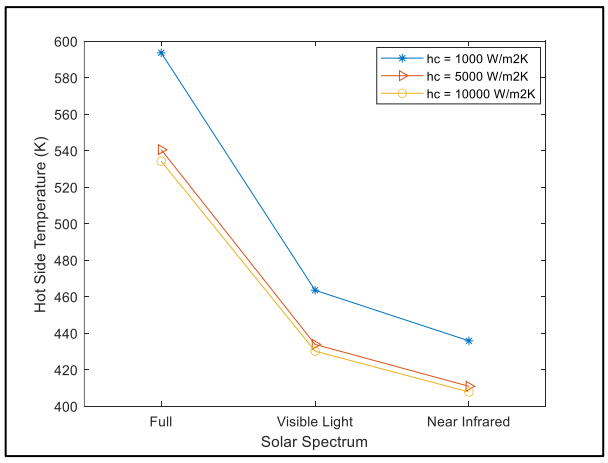

(a)

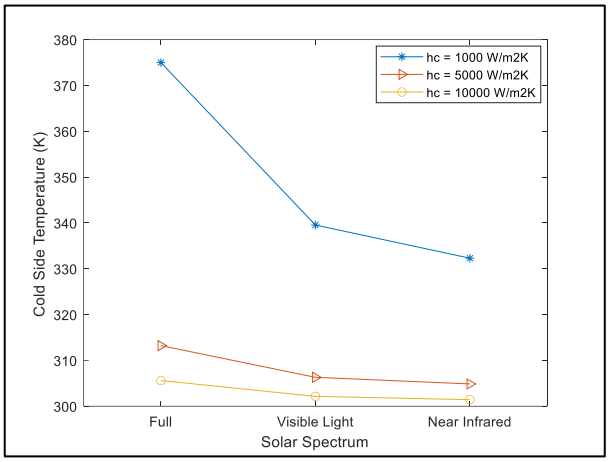

(b)

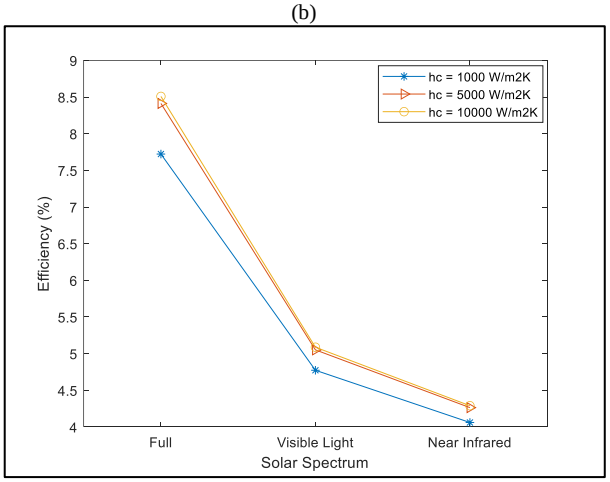

(c)

Fig. 4: Thermoelectric Generator a) Hot side Temperature - Solar Spectrums, b) Cold Side temperature – Solar Spectrums and c) Efficiency- Solar Spectrums at different heat transfer coefficient values.

That is why Fig. 4 (c) indicates that the increase of CSTEG efficiency at each spectrum is more significant as the heat transfer coefficient increased from 1000 W/m^{2}K to 5000 W/m^{2}K. Table III tabulates the hot side and cold side temperatures, their difference and efficiency values of TEG for the three solar spectrums at concentration level of 100 suns and heat sink's heat transfer coefficient of 1000 (W/m^{2}K), 5000 (W/m^{2}K) and 10000 (W/m^{2}K).

	h_c (W/m^{2}K)	T_H (K)	T_C (K)	η (%)
Full Spectrum	1000	593.57	375.00	7.7224
	5000	542.08	313.33	8.5205
	10000	535.72	305.66	8.6184
Visible light	1000	463.50	339.54	4.7731
	5000	433.83	306.30	5.0513
	10000	430.13	302.15	5.0875
Near Infrared	1000	435.77	332.30	4.0608
	5000	410.88	304.86	4.2636
	10000	407.78	301.43	4.2898

Table III. Hot Side and Cold Side Temperatures and the TEG Efficiency of full and Filtered Spectrums at Different Heat Sink's Heat Transfer Coefficient Values.

CONCLUSION

A model of the TEG device is presented which consist of a concentration part, heat collector part, TEG part and heat sink part. A simulation is carried out for the full spectrum, visible light spectrum (380 nm-750 nm) and near infrared spectrum (750nm-3000nm) of solar radiation. The hot side temperature, cold side temperature and temperature difference between them are simulated at each spectrum. Also, the generated output power and the efficiency of the TEG have been evaluated and simulated at each spectrum. The effects of the heat transfer coefficient of the heat sink and concentration ratio are included and evaluated. Increasing the heat transfer of the heat sink decreased the temperature of cold side of the TEG. Thus, it was shown that the heat extraction capacity of the heat sink is one of the most important limitations of TEG system performance. The results showed that higher concentration levels can compensate the lower power density of filtered light. Also compared to PV cells, the efficiency is lower with both the full and the visible spectrum, however in the IR-region it can be competitive to PV-cells, due to its broader absorption spectrum. Due to this TEGs can be a viable alternative for solar cells in applications where the lower wavelength parts of the spectrum are used for different purposes or devices (i.e., high band gap solar cells, plant growth etc.) by splitting the spectrum between them.

ACKNOWLEDGEMENTS

The research reported in this paper and carried out at Budapest University of Technology and Economics was partially supported by the Stipendium Hungaricum Scholarship Program of the Hungarian Government and the project number 2020-1.1.2-PIACI-KFI-2021-00242 of the National Research, Development, and Innovation Office (NKFIH).

REFERENCES

[1] Lee, Ho Sung: *Thermal design: heat sinks, thermoelectrics, heat pipes, compact heat exchangers, and solar cells*, John Wiley & Sons, 2010.

[2] Rowe, David Michael: *CRC handbook of thermoelectrics*, CRC press, 2018.

[3] Rowe, David Michael: *Thermoelectrics handbook: macro to nano*, CRC press, 2018.

[4] Dousti, Mohammad Javad, Antonio Petraglia, and Massoud Pedram: Accurate electrothermal modeling of Thermoelectric Generators, Proc. DATE15 (Grenoble, 2015), 1603-1606.

[5] Kim, Hee Seok, Weishu Liu, Gang Chen, Ching-Wu Chu, and Zhifeng Ren: Relationship between thermoelectric figure of merit and energy conversion efficiency, Proceedings of the National Academy of Sciences 112, 2015, 8205-8210.

[6] Snyder, G. Jeffrey: Application of the compatibility factor to the design of segmented and cascaded thermoelectric generators, Applied physics letters 84, 2004, 2436-2438.

[7] Mamur, Hayati, M. R. A. Bhuiyan, Fatih Korkmaz, and Mustafa Nil.: A review on bismuth telluride (Bi2Te3) nanostructure for thermoelectric applications, Renewable and Sustainable Energy Reviews 82, 2018, 4159-4169.

[8] Zoui, Mohamed Amine, Saïd Bentouba, John G. Stocholm, and Mahmoud Bourouis.: A review on thermoelectric generators: Progress and applications, Energies 13, 2020, 3606.

[9] Scherrer, H., L. Vikhor, B. Lenoir, A. Dauscher, and P. Poinas: Solar thermolectric generator based on skutterudites, Journal of Power Sources 115, 2003, 141-148.

[10] Kraemer, Daniel, L. Hu, A. Muto, X. Chen, G. Chen, and M. Chiesa: Photovoltaic-thermoelectric hybrid systems: A general optimization methodology, Applied Physics Letters 92, 2008, 243503.

[11] Mamur, Hayati, and Rasit AHISKA.: A review: Thermoelectric generators in renewable energy, International Journal of Renewable Energy Research (IJRER) 4, 2014, 128-136.

[12] Ju, Xing, Zhifeng Wang, Gilles Flamant, Peng Li, and Wenyu Zhao: Numerical analysis and optimization of a spectrum splitting concentration photovoltaic–thermoelectric hybrid systém, Solar energy 86, 2012, 1941-1954.

[13] Babu, Challa, and P. Ponnambalam: The theoretical performance evaluation of hybrid PV-TEG systém, Energy conversion and management 173, 2018, 450-460.

[14] Dhoopagunta, Shripad: *Analytical modeling and numerical simulation of a thermoelectric generator including contact resistances*, 2016.

[15] Li, Peng, Lanlan Cai, Pengcheng Zhai, Xinfeng Tang, Qingjie Zhang, and M. Niino: Design of a concentration solar thermoelectric generator, Journal of electronic materials 39, 2010, 1522-1530.

[16] Kosky, Philip, Robert T. Balmer, William D. Keat, and George Wise.: *Exploring engineering: an introduction to engineering and design*, Academic Press, 2015.

[17] Li, Zhi, Wenhao Li, and Zhen Chen: Performance analysis of thermoelectric based automotive waste heat recovery system with nanofluid coolant, Energies 10, 2017, 1489.

Addresses of the authors

Ahmed Issa Alnahhal, 1117 Budapest, Magyar tudósok krt. 2, Budapest, Hungary, aalnahhal@edu.bme.hu
Ahmad Halal, 1117 Budapest, Magyar tudósok krt. 2, Budapest, Hungary, ahmadhalalftesah@edu.bme.hu
Balazs Plesz, 1117 Budapest, Magyar tudósok krt. 2, Budapest, Hungary, plesz.balazs@vik.bme.hu

Teaching PV from basic understanding to global implications

P.P. Altermatt,
Trinasolar Co Ltd, State Key Laboratory for Photovoltaic Science and Technology (SKL),
Changzhou, Jiangsu Province, China, pietro.altermatt@trinasolar.com

Abstract

This paper draws on teaching experiences in three different areas of photovoltaics (PV). Firstly, when teaching the basic understanding of PV, it is efficient for most people if it is taught in such a way that they can briefly summarise the main idea (preferably with a keyword) and assign a picture to this keyword (which best reflects the dynamics of the topic). Secondly, peers in international cooperation are often unaware that they are teaching each other about their contribution to a common project; they tend to think that teaching is something a teacher does. However, if peers spend some time teaching each other, it can improve and accelerate the results of a project. Thirdly, as solar PV becomes a pillar of the energy transition worldwide, it is important to think beyond the technical aspects. To broaden horizons, graphs are presented for group discussions at the beginning of the course, so that participants are not tied into a track, too often prescribed by industrialised countries.

Keywords: teaching photovoltaics, basic knowledge, peer teaching in projects, broaden horizons.

TEACHING BASIC UNDERSTANDING OF PV

How does a solar cell work? To someone who knows that electricity consists of tiny particles (electrons) flowing along copper wires, you may say the following. Sunshine contains energy. In a solar cell, sunlight is absorbed and its energy is given to electrons. These electrons must be transported very quickly to the narrow metal fingers in front of the solar cell, otherwise they lose the energy they have gained. See Fig. 1.

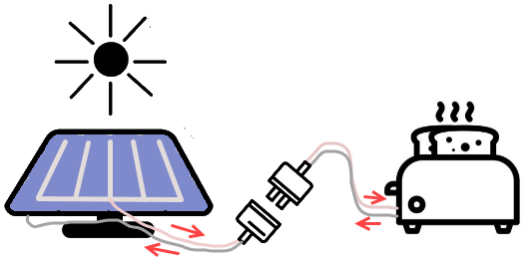

Fig. 1: Electrons get their energy from sunlight and flow through the front wire of the solar cell into your toaster. There, they lose their energy and flow to the back of the solar cell, where they can gain energy from sunlight again.

Once the electrons are in the metal fingers, they flow into the front wire and into your socket, so their energy can be used to power something, for example a toaster. In the toaster, the electrons lose their energy and flow back through the second pole of the plug to the wire at the back side of the solar cell, where they can enter the solar cell and gain energy again. Their roundtrip can start again.

On a next, deeper level, you may talk about more details with the help of Fig. 2, as explained in [1]:

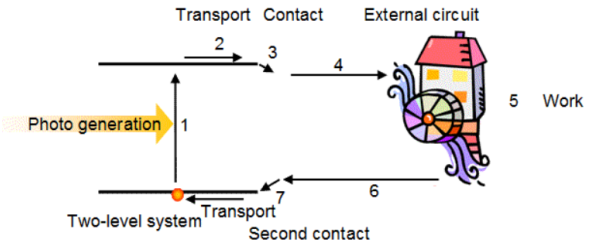

Fig. 2: The pathway in Fig. 1 can be regarded more schematically as a two-level system, with the upper level having more energy than the lower level [1].

From there you may go into more detail. For example, absorption. You may explain that blue light contains a lot of energy (that's why it can cause sunburn), while red and infrared light contains less energy (it warms us up). Then you may show Fig. 3, a two-level system where the upper level has more energy than the lower level:

Fig. 3: Instead of a two-level system in Fig. 2, there must be many levels so that a broad range of colours can be absorbed from sunlight [1].

You may explain that a two-level system (to the left) can only absorb light with a certain energy (or wavelength or pure colour). As the number of energy levels increases (to the right), a wider energy range (or wavelength range or colours) of light can be absorbed. Then you can introduce the conduction and valence band as shown in [1]. Or the advantage of tandem cells. And so on.

The underlying pedagogical method is the following: For most people it is efficient if it is taught in such a way that they can

- briefly summarise the *main idea* (preferably with a *keyword*),
- attach an *image* to this keyword (which best reflects the *dynamics* of the topic), and
- *repeat* it the next day, in a week and in a month so that the new information is memorised.

This underlying pedagogical method is used in the explanations of the photovoltaic principle in [1] as well as in the lecture on the solar spectrum [2] and the lecture on optics for solar cells [3]. These lectures provide small portions of information with a balance between depth (for good understanding) and brevity (to maintain attention).

PEER-TO-PEER TEACING IN INTERNATIONAL COLLABORATION

In international cooperation, peers often have difficulties informing each other about their contribution to a joint project. These difficulties arise when peers cannot visit each other either because they live on different continents or due to covid travel restrictions. Fig. 4 shows a real-life example where a peer describes on three PowerPoint slides how he/she examined samples from the other peers (for confidentiality reasons, some details are asterisked).

The sample structure is simple: there are a maximum of four different layers evenly deposited on a silicon wafer. However, the project was plagued by misunderstandings between the peers who deposited the layers onto the wafers in one country and the peers who examined the results in another. An analysis of the report in Fig. 4 showed that the experiment itself was described in sufficient detail, but both peers were not quite sure about the identity of the samples. Moreover, the peers who had deposited the layers were not sure what the other peers had concluded from their experiment with etching. They were also not sure how to proceed with the next round of samples.

Both peer groups were given the following recommendations to not only inform each other but to teach each other about their own work:

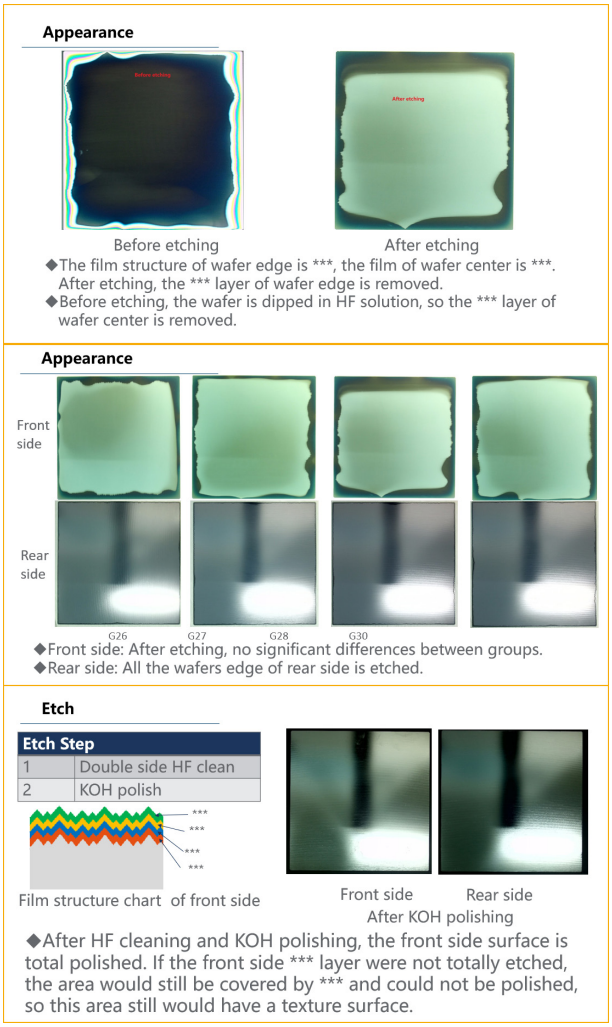

Fig. 4: A real-life example of how peers report instead of teach their experiment on samples treated by peers in another country. While the experiment itself is reported in detail, the context, the goal, the conclusions and the way forward are not communicated, leading to misunderstandings and uncertainties.

1. Give *context* on the first PowerPoint slide. What is your specific *goal* for this series? What is your *problem* that you want to solve? This was missing in Fig. 4.
2. On the second slide, make sure to communicate the *identity* and *structure* of your samples and the *tools* used for a measurement etc. to avoid misunderstandings that can also occur later when comparing different experiments as part of a common project. The structure of the sample was incompletely described on the last page of Fig. 4.
3. Describe your specific *work* (well done in Fig. 4).
4. Add your *results* explicitly (they were only implicitly communicated in Fig. 4).
5. Communicate your *conclusion*, which is your *interpretation* in the context of the first slide. This was missing in Fig. 4.
6. Finally, add instructions or suggestions on *what to do next*, i.e. what you think is *useful* to get closer to your *goal* described in the first slide. This was missing.

If you describe more than just your experiment, it will help the other peers to get closer to your goal. If they don't know what your goal is, they will automatically pursue their own goal.

For an online meeting, all PowerPoint files of the past experiments were sent to all peers again and then discussed one after the other. It turned out that there were not only misunderstandings from the beginning, but also that the goals of the two peer groups diverged over time.

Reflecting on what happened over time, it turned out that the two peer groups were unaware that they were often in a *teaching* situation. Teaching is often seen as something teachers do. However, spending some time on good peer teaching can improve and accelerate the results of a project.

In short, routinely communicate your contributions to a joint project as follows:

Context:
- Goal
- Problem

Experiment:
- Identity of samples
- Methods used

Interpretation:
- Results
- Interpretation
- Conclusion

What to do next:
- What is useful to get closer to the goal

TEACHING GLOBAL IMPLICATIONS OF PV

Photovoltaics is becoming one of the main pillars of the global energy transition to reduce CO_2 emissions and fulfil the Paris Climate Agreement. For this task to be accomplished, it is important not only to think about the technology. As with any technology, it involves people and affects people.

This implies two aspects of teaching:

1. Teaching ourselves how the use of PV affects people, their economy and the environment.

2. Teaching people about PV, its uses and its impact on their lives.

In the following, a very general and open entry for the first point is addressed by presenting a series of simple graphs to a small group, one graph after the other in a time span of about 5 to 10 minutes each. This is intended to stimulate a discussion about the causes of the global energy system and possible impacts of PV.

For simplicity and to avoid being distracted by regional details, all graphs are plotted against geographical latitude, where 0 is the equator and ±90 is the north or south pole.

The first graph compares population with energy consumption:

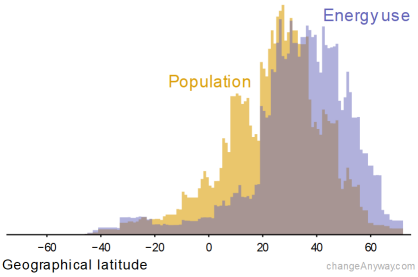

Fig. 5 Energy consumption compared with population across geographical latitude, where 0 is the equator and ±90 is the north and south poles. The area under both curves is made equal.

The first reaction may be that the gap between population and energy consumption is because more heating is needed in the north. But soon a discussion may emerge about rich and poor countries and how to alleviate the world's energy supply problems.

After 5 – 10 minutes, the next graph is handed out, which compares the population with fossil energy production rather than with energy consumption:

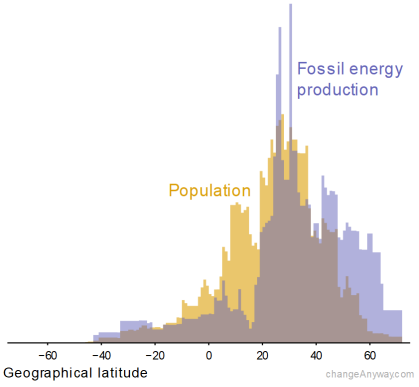

Fig. 6: As Fig. 5 but comparing population with fossil energy production.

People may ask themselves first, where the two different peaks of fossil energy production come from. It is oil production, limited to a very few countries. It is often surprising that there is a disparity between population not only in energy consumption but also in energy production. The populated south not only consumes less energy, but also produces less energy. A discussion may arise about how energy production will develop in developing and emerging countries and what impact this will have on the Paris Climate Agreement.

The next graph is about the realistically assessed potential of PV in each country in terms of connection to a grid or the distribution of stand-alone systems, the distribution of the population within the individual countries, the locations for industry, etc. (which differs considerably from "country area times annual irradiance"):

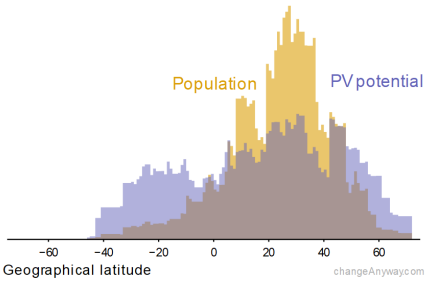

Fig. 7 As Fig. 5 but comparing population with the realistically achievable PV potential.

At first, one might be surprised at the low PV potential compared to the population between 0° and 40° north latitude, and the high PV potential at high latitudes. An important clue for the group could be that we do not need to exploit a large part of the PV potential to be fully provided with energy, and that at high latitudes the PV potential is high relative to the population density because the population density is very thin. There may be discussions about seasonality, or whether Australia's high potential can be used in a hydrogen economy, or what happens in India (which stretches from about 10° to about 30°). The peak of population density is where India and China overlap in latitude, both fast-growing economies with a high share of coal power.

From there, more detailed and specific discussions may develop and the teacher may begin to teach more concrete elements with more concrete graphs and topics.

If you teach more concrete topics after these graphs, you have to expect that people will criticise you for leaving out this or that topic. This is a good sign: The graphs shown here are intentionally less concrete in order to *broaden* the horizon in group discussions and to think of all possible aspects that you as a teacher cannot cover all. If you start the lesson right from the beginning with the usual graphs about the global state of energy, population, industrialisation, etc., people are already tied into a track. A non-specific introduction broadens the perception, and as long as you don't spend too much time on it, people won't find it too vague, but an open introduction to a complex topic that is too often taught in a limited way, prescribed by industrialised countries.

ACKNOWLEDGEMENTS

I am very grateful for the inspiration and knowledge I have received from the people I have taught.

REFERENCES

[1] Altermatt, P.P., Lecture on the principle of PV, at PV Lighthouse, Australia: https://www.pvlighthouse.com.au/cms/lectures/altermatt/principle/the-pv-principle :

[2] Altermatt, P.P., Lectures on the solar spectrum, at PV Lighthouse, Australia: https://www.pvlighthouse.com.au/cms/lectures/altermatt/solar_spectrum

[3] Altermatt, P.P., Lectures on optical for solar cells, at PV Lighthouse, Australia: https://www.pvlighthouse.com.au/cms/lectures/altermatt/optics

Research at the University Centre for Energy Efficient Buildings in the field of photovoltaic

Petr Wolf, Sofiane Kichou
Czech Technical University in Prague, University Centre for Energy Efficient Buildings
Trinecka 1024, 273 43 Bustehrad, Czech Republic

Abstract

University Centre for Energy Efficient Buildings is a new research centre build in 2014. It was established by 4 faculties (Faculty of Electrical, Civil, Mechanics and Biomedical engineering) and focuses on research project, certain type of R&D for private companies and student projects. There is a strong and tight relation and cooperation with the faculties, not only concerning trainings and student projects (mostly final bachelor, master, doctoral thesis). The expertise and devices are shared among the institutes. Many graduated students find at UCEEB their first job; this way they learn how to use their knowledge for solving practical tasks. At UCEEB we offer positions for student from foreign universities either within the IAESTE program or just based on their direct application and interview. In this paper we will describe the opportunities which UCEEB offers for collaboration, and student participation and trainings. We will also present the Laboratory for Photovoltaics and Energy Systems in its present state and expected expansion in the near future.

Keywords: student internships, photovoltaics, energy systems

INTRODUCTION

University Centre for Energy Efficient Buildings (UCEEB) was founded as an independent institute of the Czech Technical University in Prague under the auspices of four departments – Civil engineering, Mechanical Engineering, Electrical Engineering and Biomedical Engineering. The Centre's goal is to leverage synergy effects of research activities of the individual departments which are related to energy efficient buildings.

UCEEB is a reaction to one of the European Union's largest priorities aimed at optimisation of energy efficiency of buildings. The new centre should also have better opportunities to participate in European scientific projects, such as the Joint Technology Initiative on Energy Efficient Buildings, which is based on the EU's targets for carbon dioxide emissions.

It is clear that sustainable building is not just a trend or fashion, but a necessity. That is why we look at energy efficient buildings as a whole.

COLLABORATION WITH THE UNIVERSITY

Figure 1 shows in a simple way the link between UCEEB and the university. There is no standard education program at UCEEB, nevertheless the students build a remarkable part of its stuff. They work on various tasks within the running projects or their own final projects and thesis. After graduation, they often get a job offer at UCEEB which is a great chance to gain experience before working in private sector or doing a consequent (e.g. Ph.D.) study. If there is an overlapping topic, their work can be combined with such study as well.

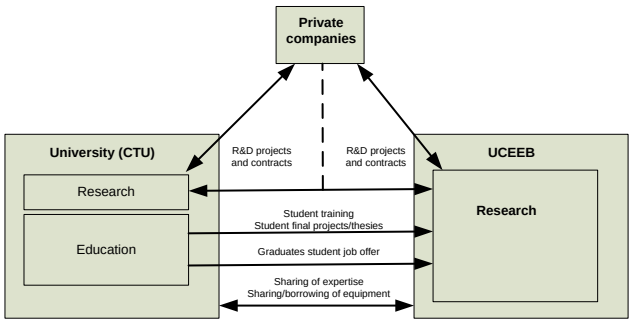

Fig. 1: Link between UCEEB and the Czech technical university.

The researchers are working within five teams – Architecture and the environment, Energy systems in buildings, Materials and structures, Indoor environmental quality and Control and monitoring of intelligent buildings. Current running research projects include those supported by the Czech and EU state policy and those completely financed by private companies as contractual research. Such projects provide the major costs for running the centre.

The unique competence of the centre lies in the holistic approach with the main focus on buildings. This can be

demonstrated on project where several (or even all) groups take part. For example, within H2020 project MORE-CONECT we solved a method for refurbishment of old houses taking into account the civil engineering, architecture, inhabitant aspects, energy needs and PV integration.

PV RESEARCH GROUP

Currently, there are 10 people in the photovoltaic research group, 8 of them working full time. The vision of a high penetration of renewables is the common topic, nevertheless the projects deal with different areas such as:

Photovoltaic energy forecasting

This topic started already 3 years ago by the need of a structured and robust cloud service providing the forecasting irradiance and PV power profile for the pilot projects of smart energy control. Firstly, a middle term service has been developed, based on worldwide free available models together with on place feedback. Since 2020 this service in its basic mode was released for free use.

The main focus of the team is currently on short-term forecasting models utilizing computer vision and machine learning techniques. Taking high resolution sky images, the clouds can be tracked and deliver a precise irradiance forecast for a very short term, up to 45 minutes. All forecasting services currently cover Czech Republic only, but can be expanded to other countries on request. There are first attempts to use this service for intraday energy trading together with commercial partners.

PV systems simulation and analysis

Often, we are asked from companies or municipalities to prepare concepts for energy management on the scale of a building up to a small district. Sometimes they already have a documentation of PV and battery installation and would like somebody to prepare an impartial review. Recently, there is an increased request from international companies to “go green”, establishing concepts for carbon free production and renewable energy usage. We already worked on several studies in order to achieve this. Currently, the European strategy aims for designing and piloting of positive energy districts. Within the centre for advanced photovoltaics project we work on preparing such a concept for a new constructed Prague district (part of Zizkov quarter), Fig. 2.

PV systems and battery control

Within four projects we have gained experience on innovative energy management and battery control based on PV and load prediction and flexible energy pricing. In this way, since 2017 we control an administrative building with PV and battery system, Fig. 3. Recently, we started developing a control algorithm for a family house that is equipped with various technologies (e.g. PV, battery system, EV charger, indoor quality sensors, attendance monitoring).

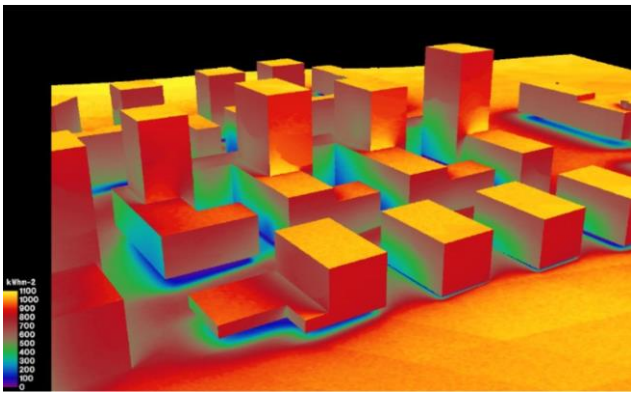

Fig. 2: Solar irradiation map of the neighbourhood.

Fig. 3: Hybrid PV system with battery used for balancing the administrative building energy needs.

PV systems laboratory

The PV systems laboratory is equipped with devices enabling testing inverters and batteries under various conditions (Figs. 4 and 5). On the input side, there is a power source simulating the grid where voltage and frequency can be adjusted. The PV source is pretended by a PV simulator. Parameters such as PV technology and possible shadowing have to be defined together with irradiance and temperature profiles. During the tests, voltages, currents and power is being measured using a precise five-channel power analyser.

Typical tasks we can do are:

- checking inverter behaviour when voltage or frequency is out of the limits,
- measuring maximal power point tracking (MPPT) and inner efficiency of the inverter in static or dynamic conditions,
- measuring the battery charge and discharge profiles, checking the battery management system (BMS),
- measuring the inverter output power quality e.g. harmonics, flicker), measuring of transient states, such as switching on/off or going to back-up mode.

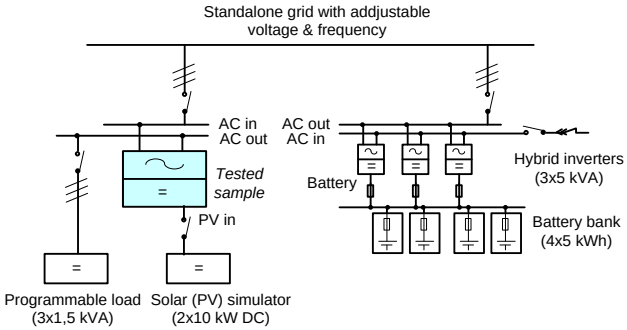

Fig. 4: Principal scheme of the PV systems laboratory

Fig. 5: Main test room for PV systems at UCEEB

INTERNSHIP

We have mostly positive experience with taking students for internship. They mostly address us via IAESTE program, but recently a high percentage of them contacted us directly. The students also share their experience with each other, so from the French university ISAE – SUPAERO we already have the third student based on recommendation.
The students mostly spend 3-6 months at UCEEB, we prefer longer term internships as it takes one or two first months till they get into the topic and can contribute to the project work.

CONCLUSION

Since its start in 2014, UCEEB research centre works in the field of complex R&D in various fields related to buildings. The tight relation with Czech Technical University in Prague is essential on sharing expertise, equipment, trainings and internships of students. Within the photovoltaic research group, the researchers work on simulations and studies as well as perform test in the laboratory. As R&Ds are on the application level, it is often requested and linked to a private company, which can act as a client or a research project partner. Last but not least, we should mention the internships of students from other, mostly foreign universities, who deliver useful work to the projects.

ACKNOWLEDGEMENTS

This work has been supported by the Operational Programme Research, Development and Education of the European Structural and Investment Funds, project CZ.02.1.01/0.0/0.0/15_003/ 0000464 Centre for Advanced Photovoltaics.

REFERENCES

[1] University Centre for Energy Efficient Buildings, http://www.uceeb.cz

[2] OP VVV Project Centre for Advanced Photovoltaics, http://cap.fel.cvut.cz/en/

Addresses of the authors

Petr Wolf, CTU UCEEB, Trinecka 1024, Bustehrad, Czech Republic, petr.wolf@cvut.cz
Sofiane Kichou, CTU UCEEB, Trinecka 1024, Bustehrad, Czech Republic, sofiane.kichou@cvut.cz

Photovoltaic education and alternative energy teaching

M. Stoev

Solar Energy Centre, Faculty of Mathematics and Natural Sciences,
South-West University "Neofit Rilski", Blagoevgrad, Bulgaria

Abstract

The photovoltaics education as a part of alternative energy teaching is discussed. The lecture courses on renewable energy sources and systems, chemistry of solar cells and applied photovoltaics are oriented to BSc. The new MSc "Innovative technologies for renewable energy" is for students from University of Chemical technology and Metallurgy and South-West University "Neofit Rilski" in Bulgaria. The courses are presented in the fields of natural and technical sciences university education in Europe and Asia. The impact on the society of PV demonstration projects as a BIPV and a smart home managing, water purification system powered by PV, growing seedlings by PV and photosynthesis are discussed.

Keywords: PV BSc and MSc education, renewable energy sources, chemistry of solar cells, applied photovoltaic, alternative energy teaching, PV demonstration projects

Introduction

The fast growing of alternative energy in energy mix is a fact and it is an energy politic in every country in Europe and Asia. Now is easy to see online by Internet the deal of alternative energy in the country energy mix [1-2]. It is easier solar PV firms to install 100 MWp PV plant for a year than universities to educate students at that time in photovoltaics responsible to produce PV materials, solar cells, PV modules, electronics, mechanical constructions, monitoring, PV systems engineering etc. and to support practically PV education as a demonstration projects oriented to the society. This is really a challenge to university natural and technical education to create a new infrastructure for alternative energetic and in particular PV solar with a practical contacts with solar firms, alliances of producers of eco energy and RES clusters. The goal of presented lecture courses is to educate basically students in renewable energy sources and systems, chemistry of solar cells and applied photovoltaics as a lectures, seminars, laboratory exercise, and demonstration projects and to provide a practical training in solar firms.

Lecture courses for BSc students

The main lecture courses are Renewable energy sources and systems, Chemistry of solar cells and Applied photovoltaics are presented in English, Russian and Bulgarian languages oriented to BSc students from faculties of Natural and Technical sciences. The university education as a lecture courses, seminars and laboratory exercises are provided from Solar Energy Centre, South-West University [3] and a practical training on PV plants, small hydro, biomass utilization etc. is from RES cluster [4]. The students are involving in demonstration projects with a real impact on the society and partially to a family home and a small business as a building integrated PV, managing energy mix at home, smart home with PV generator, energy efficiency at home, utilization of solar energy by photovoltaics and photosynthesis for a small family business, energy efficiency applications for grooving seedlings indoor at a controlled atmosphere powered by BIPV and a protection outdoor from solar radiation by shedding from PV aria, 7 stages water purification system with reverse osmosis and UV disinfection for drinking and technical water supply. The products from applied photovoltaics projects are green energy as a part of a home energy mix to power energy efficiency applications, seedlings, drinking water, RO technical water and etc.

The lecture courses on photovoltaic education, alternative energy teaching and seminars are presented in Bulgaria at SW University, Technical University Sofia and Chemical and Metallurgical University Sofia, in Czech Republic at Faculty of natural sciences, Charles University, Prague, in Poland at Faculty of mechanic and mechatronics, West Pomeranian University of Technologies, Szczecin in Kazakhstan at Karaganda State University Buketov, Karaganda Technical University, Faculty of energetic at Pavlodar State University, Ekibastuz Technical and Engineering Institute and Faculty of electrical engineering at Afyon Kocatepe University, Turkey. The recommended literature is [5 - 9].

The main points of discussion during lecture courses and seminars are:

Lecture course: **Renewable energy sources and systems**
Lectures 30 hrs and 15 hrs seminars

- Energy: sources, lows and conversion
- Energy mix: Past from fossil fuels to renewable energy
- Solar energy: Photovoltaic, thermal conversion and photosynthesis
- Wind energy
- Hydroelectric energy
- Biomass energy
- Geothermal energy
- Tidal energy

Lecture course: **Chemistry of Solar cells**
Lectures 30 hrs and 15 hrs laboratory excises

- Solar energy: Characteristics and measurements
- Photovoltaic effect, materials, solar cells design and characteristics
- c-Si, mc-Si, μc-Si and a-Si solar cells
- GaAs solar cells
- CdS/CdTe solar cells
- Cu_2S solar cells
- $CuInSe_2$, $CuInS_2$ solar cells
- Dye solar cells
- Organic solar cells
- Third generation solar cells
- Life cycle of PV cells, degradation and utilization of solar cells

Lecture course: **Applied photovoltaics**
Lectures 30 hrs and 15 hrs laboratory exercise

- Solar radiation: characteristics, measurements, software and solar audit
- Photovoltaic effect and materials for photovoltacs
- Solar cells: design, parameters and losses
- PV modules: design and structure
- PV electronics: inverters, solar chargers
- PV aria: design
- PV mechanical constructions
- Battery package
- PV systems: stand alone, grid connected, BIPV and hybrid
- PV system design: PV system engineering
- Life time of PV systems and recycling
- Good practice of PV systems

Lecture courses for MSc students "Innovative technologies for renewable energy" is a part of the project "Modernization, digitalization and internationalization of education at the University of Chemical Technology and Metallurgy, BG05M2OP001-2.016 Modernization of higher education, BG05M2OP001-2.016-2.016-0013-C01

I semester
Obligatory courses:

- Innovative bioelectrochemical systems
- Innovative methods for energy storage and conversion
- Hydrogen power generators
- High temperature electrochemical technologies

Electable courses:

- Innovative solar cells
- Electrode materials for microbiological electrolysis systems
- Ecological and environmental impact assessment
- Metrology

II semester
Obligatory courses:

- Geothermal waters for renewable energy
- Basics of entrepreneurship
- Photolysis and photoelectrolysis
- Oxygen-Hydrogen technologies with RES

Electable courses:

- Solar Energy Audit
- Innovative and entrepreneurial approaches in the hydrogen economics
- Technologies for storage and transport of high energy gases.
- Energy and eco-affectivity of Renewable Energy Systems

The Internship is oriented to the solar firms in South-West Bulgaria. The Thesis are in the fields of innovative technologies for renewable energy.

REFERENCES

[1] https://www.energy-charts.de
[2] http://www.tso.bg/default.aspx/page-707/bg
[3] www.swu.bg
[4] www.res-cluster.com/en/home/
[5] www.pveducation.org
[6] S. Kaplanis, El. Kaplani, Renewable Energy Systems: *Theory, Innovations & Intelligent Applications*, Nova Science Publishers Inc., New Yotk, 2013.
[7] Kl. Jager, Ol. Isabella, Ar. Smets, R. M. van Swaaij, M. Zeman, *Solar Energy: Fundamentals, Technology, and Systems*, Delth University of Technology, 2014.
[8] M. S. Imamura, P. Helm, W. Palz, *Photovoltaic System Technology: A European Handbook*, EC, Publ. H. S. Stephen & Associates, UK, 1992.
[9] T. Markvart, L. Casatener, *Photovoltaics: Fundamentals and Applications*, Elsevier Ltd., 2003.

Addresses of the author
M. Stoev, Solar Energy Centre, Faculty of Mathematics and Natural Sciences,South-West University "Neofit Rilski", Blagoevgrad, Bulgaria, e-mail: mstoev@mail.bg

Solar Energy Research & Education @TU Delft/PVMD

Miro Zeman and Olindo Isabella
Photovoltaic Materials and Devices group
Delft University of Technology
The Netherlands

Abstract

Delft University of Technology aims to become global academic leader in Solar Energy research and education. Utilization of solar energy is a crucial step in executing the energy transition towards sustainable energy. Success of the energy transition execution depends on technicians, engineers and leaders who have skills and knowledge to do it. The Electrical Sustainable Energy (ESE) department at Delft University of Technology focuses on educating their students to prepare them for taking an active role in the energy transition. Photovoltaic Materials and Devices group is a part of the ESE department and carries out research and education in the area of photovoltaic technology (PV).

Keywords: photovoltaics; research; education

INTRODUCTION

Delft University of Technology aims to become global academic leader in Solar Energy research and education. Utilization of solar energy is a crucial step in executing the energy transition towards sustainable energy. Success of the energy transition execution depends on technicians, engineers and leaders who have skills and knowledge to do it. The Electrical Sustainable Energy (ESE) department at Delft University of Technology focuses on educating their students to prepare them for taking an active role in the energy transition. Photovoltaic Materials and Devices group is a part of the ESE department and carries out research and education in the area of photovoltaic technology (PV).

ENERGY TRANSITION

The Energy Transition aims to transform the present energy system that is based on fossil fuels into one based on renewable energy sources (RES). The main challenge is to realize this transition at the lowest possible cost without compromising the system's reliability. Since the most important RES, such as solar- and wind energy, deliver electricity, the primary challenge is to accommodate RES in the existing electrical power system or to design and build new ones. Consumers are becoming electricity producers by installing their own photovoltaic (PV). In this way, micro-grids with its own electricity generation are formed where power management and market mechanisms can be controlled locally. By interconnecting the micro-grids, the stability and resilience of the entire electrical power system can be increased, and conversion and transport losses can be minimized. When consumers mutually exchange electricity or deliver electricity to the distribution network, new market design and regulations have to be developed and put into place.

THE ELECTRICAL SUSTAINABLE ENERGY DEPARTMENT

The ESE department's research activities aim at accelerating the energy transition towards sustainable energy. The research covers conversion of RES into electricity, its transmission, distribution and storage. The department designs and fabricates high-performance, low-cost photovoltaic (PV) cells and power electronics devices for integration in future power networks. It studies systems with electricity generation using PV and wind technologies, high-voltage and direct-current transmission, and intelligent power management for increasing energy efficiency.

In anticipation of the large-scale introduction of renewable and distributed energy sources, the technical, economic and societal performances of the future electricity system are studied through multidisciplinary "system of systems" approaches. Working on this energy transition, the ESE department contributes to tackling important societal challenges such as climate change and environmental pollution.

THE PHOTOVOLTAIC MATERIALS AND DEVICES GROUP

Research

The PVMD group has a long history of research on thin-film silicon solar cells and advanced opto-electrical modelling of solar cells. The research program of the PVMD group has been recently expanded towards crystalline Si and hybrid tandem devices, intelligent and multi-functional modules, X-IPV systems, circular photovoltaics and multi-scale modelling. The group focuses on five application areas; (1) crystalline silicon solar cells, (2) thin-film and tandem technology, (3) photonics and Si-based storage, (4) photovoltatronics, (5) and urban energy (see Fig. 1).

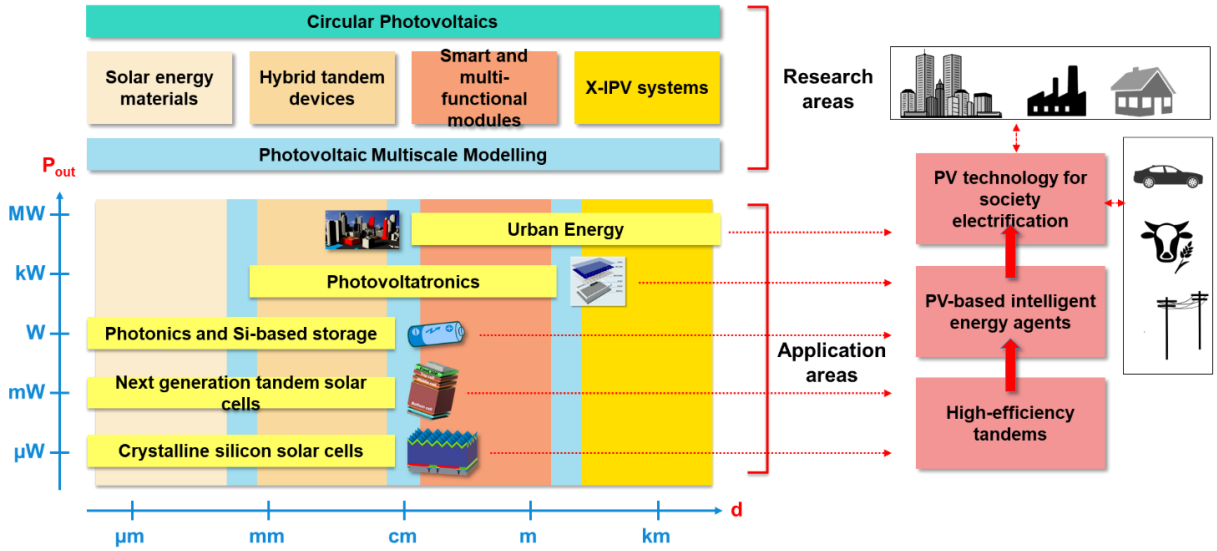

Fig. 1: Research topics and application areas of the PVMD group @TU Delft.

Education

PVMD group has developed a package of PV-related courses for MSc programs that is called PV profile (see Fig. 2). In addition to standard PV courses such as PV Basics, PV Technologies and PV Systems, new courses such as PV Modelling, PV Processing and Virtual PV Lab were added. We have developed a digital twin of the PV profile so that both on-campus and ex-campus students can learn about the whole PV value chain from solar energy materials to devices, modules, and systems. In addition, the PVMD group organizes annual PV Systems Summer School.

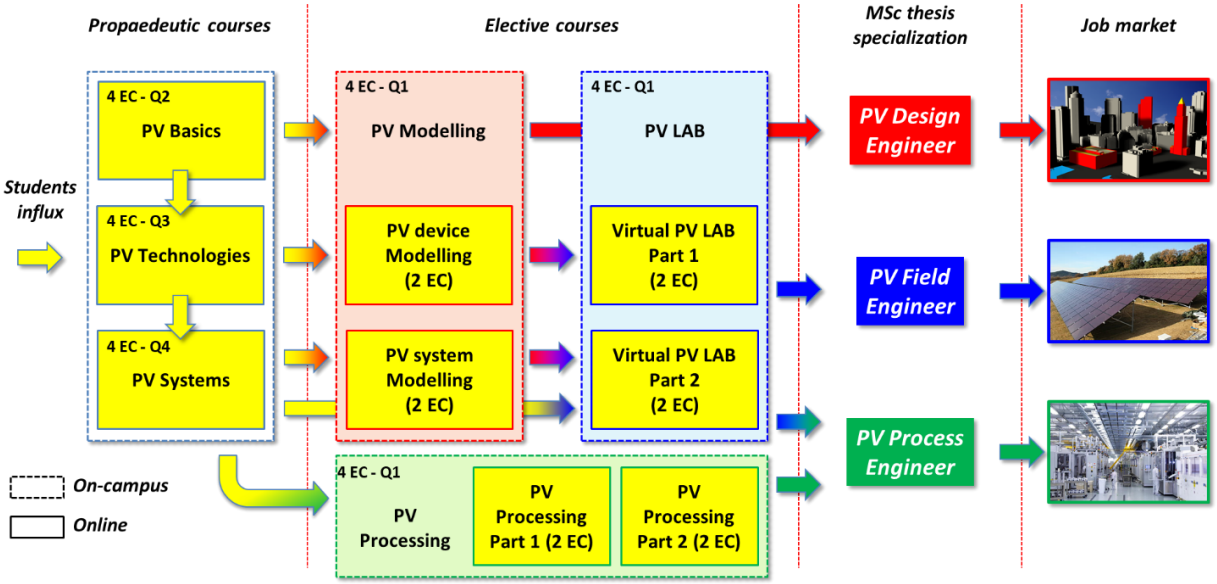

Fig. 2: PVMD group educational activities

CONCLUSION

Our academic mission is to deliver excellent young engineers and future leaders in the field of energy transition. Therefore, we believe that PhD candidates, PostDocs, R&D people and engineers who work in the area of sustainable energy should have knowledge in how real PV systems operate. In these times of fast changes in the way we use electricity, the penetration of photovoltaic systems in the electricity grid is literally booming. Our Summer school offers theoretical knowledge and practical training in design, installation, understanding, and monitoring of PV systems.

Addresses of the authors

Miro Zeman, M.Zeman@tudelft.nl
Olindo Isabella, O.Isabella@tudelft.nl

Present trends in crystalline silicon photovoltaic cells and modules

V. Benda
Department of Electrotechnology
Czech Technical University in Prague, faculty of Electrical Engineering
Prague 6, Czech Republic

Abstract

Photovoltaics (PV) is expected to play an important role in the future global energy system. Advances in technology have led to an impressive reduction in the price of photovoltaic modules and other parts of photovoltaic systems, so that the cost of electricity produced by photovoltaic systems has fallen close to the long-term cost of electricity in the grid. The key components are PV modules, which are basic devices that are capable of long-term operation in outdoor conditions. PV modules can be implemented from different materials with different production technologies. Innovative driving forces are module cost, module efficiency and module life. At present, wafer-based crystalline silicon technologies best meet the criteria due to their high efficiency, low costs, and long service life, and in the current production of photovoltaic energy they represent almost 95% of the total module production. The article discusses trends in crystalline silicon technologies.

Keywords: PV modules technology; PV module efficiency; LCOE; PV module service life

INTRODUCTION

Photovoltaics (PV) is expected to play a key role in the future global energy system. Advances in technology have led to a significant reduction in the price of PV systems, so that the cost of electricity produced by PV systems has fallen almost to the level of the long-term cost of electricity in the grid.

The impressive development in photovoltaics during last ten years can be characterised by very fast increase of both annual installed power and cumulative installed power [1; 2], as demonstrated in Fig.1.

PV cells and modules can be made of different materials by different production technologies. The conditions that any technology for a wide range of applications should meet are: low production cost, high efficiency, high operational reliability, and availability of input materials.

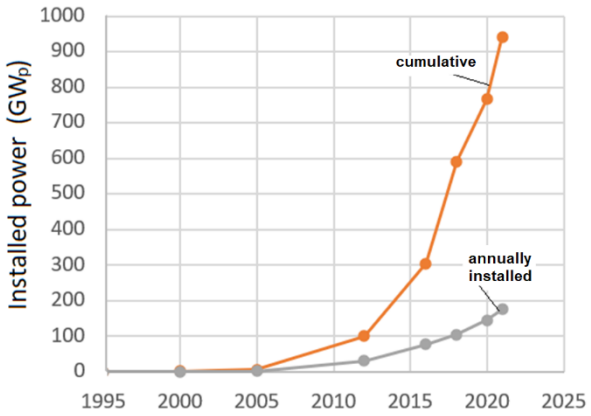

Fig.1. The developments of the PV cumulative installed capacity and annual production

During the 50 years of development of photovoltaic technologies, many materials and technologies have been studied (3 generations [3] are listed in Table 1). Regarding technological and economic aspects (high efficiency requirements, low prices, long life, wide availability of materials), crystalline silicon cells and modules predominated [4], accounting for 95% of total production [5], as demonstrated in Fig. 2. Although some thin film technologies (CdTe, CICS) can compete both in terms of efficiency and price, resources (Te, In) are limited and their annual production could hardly exceed 20 GW_p [6]. Other technologies have not yet reached the

1st generation *– wafer-based technology (mostly crystalline silicon solar cells)*

2nd generation *- thin film solar cells amorphous silicon (a-Si) and microcrystalline silicon (μc-Si), cadmium telluride/cadmium sulfide (CdTe/CdS) and copper indium gallium diselenide (CIGS) solar cells, kerstenits*

3rd generation *- technologies based on newer compounds including nanocrystalline films, active quantum dots, tandem or stacked multi-layers of inorganic based on III-V materials, organic (polymer)-based solar cells, dyed-sensitized solar cells, perovskites, etc.*

Table 1. PV cell generations [3]

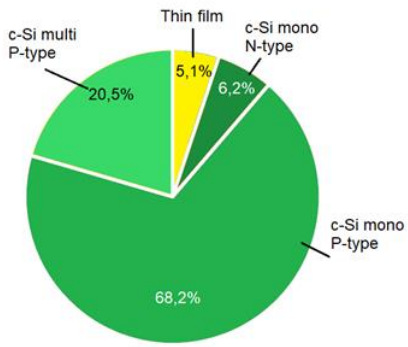

Fig.2. PV module technology share in 2020

level of series production. The current development of photovoltaic cells and modules is therefore connected mainly with wafer-based crystalline silicon technologies.

PROGRESS IN CRYSTALLINE SILICON TECHNOLOGIES

The impressive development of crystalline silicon module technology in the last decade can be demonstrated by the development of annual production (see Fig.1), price, and efficiency, as shown in Fig. 3.

The most important drivers of the technology developments [7] are:

- The module cost
- The module efficiency
- The module service life

The expansion of technology on a gigawatt production scale also requires:

- No material constrains
- Environment friendly fabrication processes

Wafer-based crystalline silicon technologies best meet the criteria of high efficiency, low cost and high service life, and currently account for about 95% of total module production.

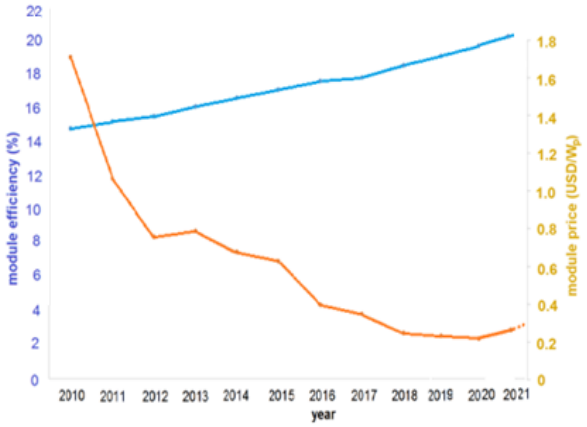

Fig.3. Development of average price and average efficiency of c-Si modules

The main technological changes in mass production technology can be observed in the last 5 years. These changes, which lead to an increase in the efficiency and service life of the modules, can be observed in the field of the starting crystalline material, in the field of the structure and technology of PV cells, in the field of the construction and technology of the modules. New technologies, new materials, and highly productive manufacturing equipment are required to reduce production costs.

Changes in starting material. In the period 2008-2016, the main trend was to improve the starting multicrystalline material as to reduce the cost of the starting material. However, the introduction of the continuous Czochralski pulling method in 2016 has reduced the cost of mono-crystalline silicon rods and due to lower losses in wafering by diamond-plated wire also the cost of wafers.

The changes in mono/multi c-Si cells ratio are shown in Fig.4. Replacing boron doping with gallium doping in monocrystalline silicon [8] results also in an efficiency improvement. Currently mono-crystalline gallium doped wafers of thickness of 0.17 mm predominate as the starting material for cell production [9]. The transition to the initial N-type material may further increase the efficiency of PV cells.

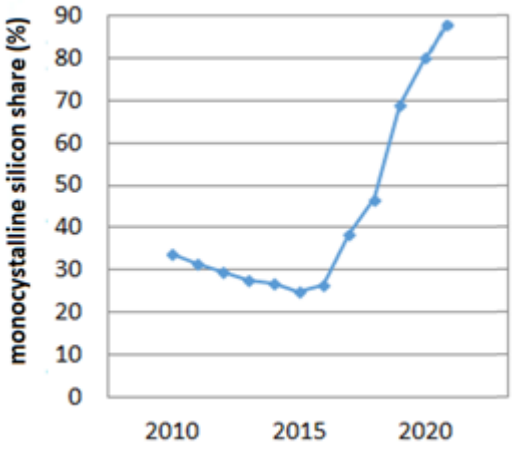

Fig.4 . Development of the share of monocrystalline silicon in the total production of c-Si cells

Module cost reduction

Cost reduction is associated with the steps of techno-logical breakthroughs, the expansion of production plants and increasing the level of automation, and the costs of materials and components (silicon, glass, polymer films, etc.) and energy in the production chain. Efficiency improvements in PERC technology and the deployment of larger wafers in larger module resulted in higher average module efficiencies. Development in average module efficiency and average module price in the last decade is demonstrated in Fig.3. The rise in module

prices started in 2020 is related to the lack of polycrystalline silicon resources, which is likely to last throughout 2022 [10].

One of the tools for reducing the cost of PV cells and modules was also to increase the wafer area (from 164x164 mm^2 in 2016 to 210x210 mm^2 in 2020). This increase in cell area was followed by an increase in module power [11]. The maximum module power development is shown in Fig.5. Increasing module power can also help reduce BOS [12] costs and reduce costs for other components, including racks, foundations, and cabling.

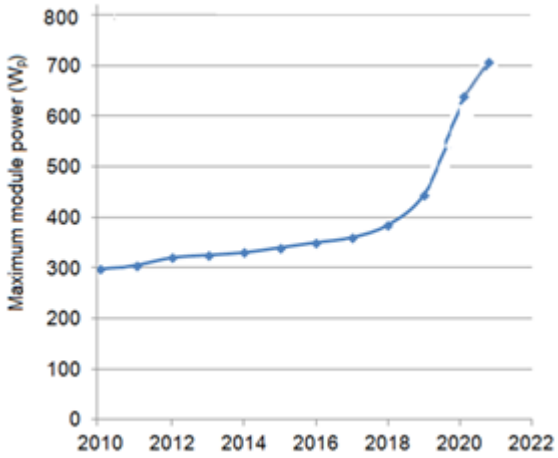

Fig.5. Maximum module power development

The module efficiency increase

The increase in the efficiency of the module is usually associated with an increase in the efficiency of the cells from which it is composed. The efficiency improvements are reached by decreasing all types of losses – both optical loses, recombination losses and electrical losses. Individual loss components are minimized by using new physical design principles, optimizing technological tools and materials. After reducing the volume recombination losses to an acceptably low level, the surface recombination on the rear contact was reduced by switching from all-area contact used in Al BSF cells to the local contacts on the passivated rear surface used in PERC cells. The next step is a fully passivated surface realizing the all-area contact by tunneling the carriers through a very thin passivation oxide layer - TOPCon cells. This technology development is indicated in Fig.6.

At the module assembly level, there are used construction improvements to decrease inner resistive losses (half cut cell configuration, shingled construction improvements to decrease inner resistive losses (half cut cell configuration, shingled cell configuration), optical losses (using AR coated glass, white EVA, wire cell connection).

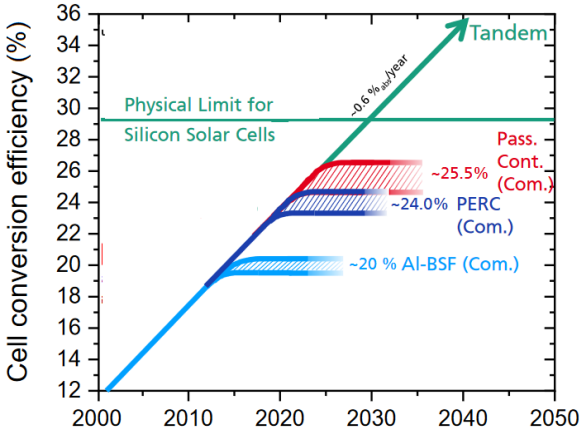

Fig.6. Development of the efficiency of c-Si cells depending on the technology [5]

The possibility of making better use of solar radiation has led to the development of bifacial cells and modules, which currently account for about 30% of total production and their market share is expected to grow.

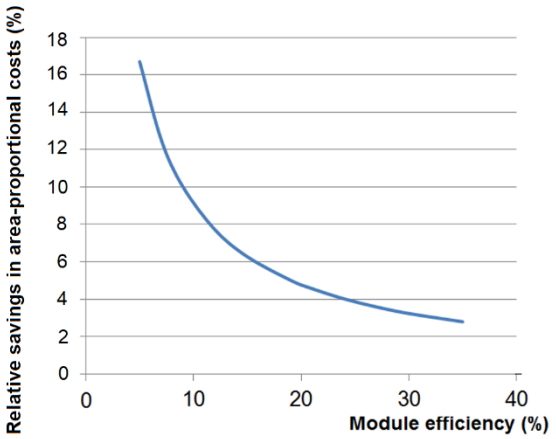

Fig.7. The relative savings of area-related costs caused by a 1% increase in module efficiency

Improving module costs and module efficiency are very important for reducing the investment costs of a PV system, which consist of module costs, BOS costs and soft costs. Part of the non-modular costs is proportional to the area and is therefore inversely proportional to the efficiency of the module. In this way, increasing the efficiency of the module leads to a reduction in the area-dependent part of the investment [7, 12]. However, the relative changes in these parts of the investment costs decrease with the increasing efficiency of the module. Fig. 7 shows the relative savings in area-proportional costs due to a 1% increase in module efficiency. In order to maintain the module efficiency as an effective innovative driver, the savings from efficiency gains should be greater than the increase in module technology costs associated with this efficiency gains.

The module service life extension

Due to the environment, the efficiency of the module decreases over time. The service life n is often taken as the number of years until the efficiency of the modules is reduced to 80% of the initial value and in this form is often used as the warranty period of the PV modules specified by the manufacturer.

The encapsulation material and the back cover materials are key module components to ensure long time stability. Intensive development efforts have been (and are) being made to optimize these components in terms of performance and cost.

Foils will stay mainstream as back cover material, but glass is expected to gain a significant higher market share as backside cover material especially for bifacial c-Si module applications. Polyolefins are a forthcoming alternative to EVA especially for bifacial products in glass-glass combination and for SHJ [13].

The module service life influences resulting cost of electrical energy generated (the LCOE of photovoltaic systems). For constant investment cost and the energy output, the module service life prolongation results in a decrease of the LCOE. Some results can be obtained using a simplified model [7]. In Figure 7, the relative decrease of LCOE caused by an increase in the module service life of 1 year (from *n* to *n*+1, e.g., from 20 to 21 years) are plotted as a function of module service life *n*.

In addition to the effect of module degradation, described by the expected decrease in module efficiency, faults can also occur on both modules and other parts of the installation causing accidental malfunctions of the PV system. The repair of these faults increases the operating costs of the system, which results in an increase in the ratio ε between the annual operating costs of the PV system and the investment costs with a consequent decrease in the relative LCOE reduction, as shown in Fig. 8.

Present service life of c-Si modules is usually declared 25 years (or more). For example, bifacial modules with double-sided glass with polyolefin (POE) encapsulation have a service life of well over 30 years [13]. However, it is also important to increase the service life of the other components of the PV system to a similar level in order to take advantage of the savings resulting from extending the service life of the modules [14].

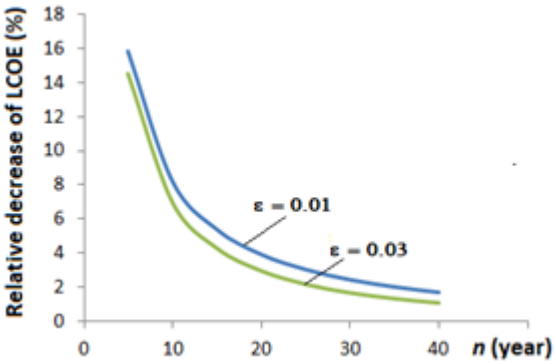

Fig.8. The relative decrease of LCOE caused by an increase in the module service life of 1 year for different ε - ratio between average annual operating cost and the investment cost

THE TECHNOLOGY ROADMAP

Global demand for photovoltaics as a source of electricity is growing and certain scenarios assume that annual production will approach 1 TW_p over the next decade. In principle, silicon technology has the potential to handle this volume of production.

Further development of photovoltaics requires

- Improve module efficiency without significantly increasing processing costs.
- Further optimize unit costs throughout the value chain by increasing the overall efficiency of the installed production capacity equipment, implementing upgrades and new production capacities, more efficient use of Si and non-Si materials and ensuring high efficiency of newly installed capacities.
- Prepare specialized product modules for various market applications (e.g. specialized for hot and wet environment)

Large-scale production of some structures may have problems in terms of the availability of some materials [15] (e.g., lack of indium can significantly reduce the production of cells using ITO), which needs to be taken into account at the development stage.

High hopes are associated with the development of perovskite PV cells and modules which, due to their high efficiency and expected low cost, could replace crystalline silicon modules in the future. Perovskite modules have undergone rapid development, but there are still some stability and longevity issues that prevent the rapid introduction of mass production.

REFERENCES

[1] 2022 Snapshot of Global PV Markets, Report IEA-PVPS T1-42:2022 April 2022

[2] Global Market Outlook For Solar Power 2022 – 2026, Solar Power Europe 2022

[3] M. A. Green, Third generation photovoltaics: Ultra-high conversion efficiency at low cost, Progress in Photovoltaics, vol. **9**, no. 2, pp. 123-135 (2001)

[4] Wim C. Sinke, Development of photovoltaic technologies for global impact, Renewable Energy **138**, p. 911-914 (2019).

[5] Photovoltaics report , February 2022, https://www.ise.fraunhofer.de/content/dam/ise/de/documents/publications/ studies/Photovoltaics-Report.pdf

A. Feltrin, A. Freundlich, Material considerations for terawatt level deployment of photovoltaics. Renewable Energy **33**, p. 180–185 (2008)

[6] Benda V. and Cerna L., A Note on Limits and Trends in PV Cells and Modules, Applied Sciences, 2022

[7] S.W. Glunz, S. Rein, J. Knobloch, W. Wettling and T. Abe, *Comparison of boron and gallium doped p-type Czochralski silicon for photovoltaic application*, *Progress in Photovoltaics: Research and Applications* 7(6), 463-469 (1999)

[8] International Technology Roadmap for Photovoltaic

[9] (ITRPV) Results 2021 Thirteenth Edition, March 2022

[10] Shashinger, M.: Module prices set to rocket back to 2019 levels, PV magazine, 11, 2021, p.10-11

[11] S. K. Chunduri, M. Schmela:,Very High-Power Solar Modules, TaiyangNews Report 2021

[12] Wang, X.; Barnett, A. The Evolving Value of Photovoltaic Module Efficiency. *Appl. Sci.* **2019**, *9*, 1227

[13] S. K. Chunduri, M. Schmela, Advanced Module Technologies, TaiyangNews Report 2021

[14] Review of Failures of Photovoltaic Modules, Report IEA-PVPS T13-01:2014

[15] Y. Zhang, M. Kim, L. Wang, P. Verlinden and B. Hallam, Design considerations for multi-terawatt scale manufacturing of existing and future photovoltaic technologies: challenges and opportunities related to silver, indium and bismuth consumption, (Analysis) *Energy Environ. Sci.*, 2021, 14, 5587-5610

[16] Urbina A., The balance between efficiency, stability and environmental impacts in perovskite solar cells: a review, *Journal of Physics: Energy* 2, Number 2 (2020)

Address of the author:
Czech Technical University in Prague,
Dept. Electrotechnology, Technicka 2, 166 27 Praha 6,
Czech Republic
E-mail: benda@fel.cvut.cz

Enhancing photovoltaic systems with shortest time storage to compensate feed-in gaps caused by cloud shadows

E. Harzfeld
Department of Electrical Engineering and Computer Science
Stralsund University of Applied Sciences
Stralsund, Germany

Abstract

As a result of the transition of energy systems towards regenerative solutions, the share of PV power will increase considerably. Voltage stability of PV systems is becoming increasingly important as the feed-in peak is during the period of peak load and short-term weather phenomena will increase as a result of climate change, here in particular cloud draught. By using short-term ultracapacitor systems and expanding these storage systems with battery and methanol storage systems, it is possible to stabilise the grid and consumer voltage even under conditions of high PV feed-in. Voltage fluctuations that occur as a result of surplus or deficit feed-in can be limited or prevented by storage systems adapted to the feed-in power.

Keywords: PV unit, weather phenomena, grid stability, ultracapacitor, batteries and power to methanol.

SUMMARY

The expansion of renewable energies, especially photovoltaics, creates new problems regarding grid stability. For this reason, new solutions for maintaining grid stability are presented here, which are combined with a description of shortest-time storage systems. Knowledge of the structure and mode of operation of short-time storage systems supports their further development and optimisation regarding their use in PV systems and combinations thereof.

1. INTRODUCTION

1.1 Energy transition and PV expansion requirements

PV systems use the sun's solar radiation and feed enormous amounts of energy into the connected grids in Europe, preferably in the summer months. The prospective development of PV expansion is shown in Fig. 1 and Fig. 2, starting from 2020 to 2070, using Europe and Germany as examples. The high PV expansion targets result from the enormous annual energy demand and the far too low full load hours of photovoltaics.

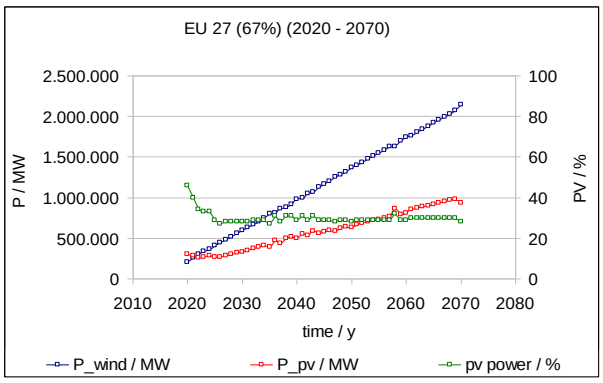

Fig. 1. Expansion of photovoltaics (932 GW; 2070) in EU27

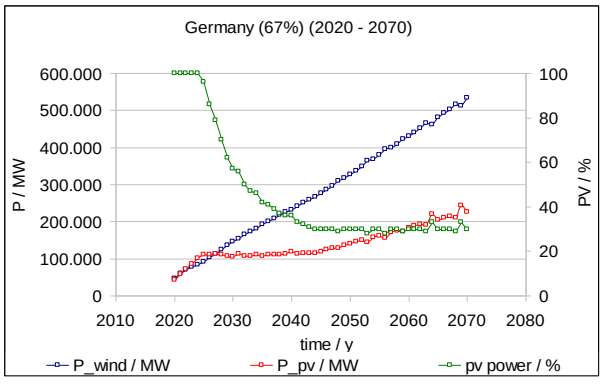

Fig. 2. Expansion of photovoltaics (226 GW; 2070) in Germany

1.2 Climate change and weather phenomena

As a result of climate change, weather phenomena such as heat waves, hurricane-like storms, thunderstorms and increased cloudiness will occur very frequently in the near future, all of which will influence both feed-in power and consumer behaviour. While heat waves are relatively slow-moving events, hurricane-like storms, thunderstorms and increased cloudiness are short-lived events. In particular, cloudbursts, see Fig. 3, place special demands on the installed storage systems. The storage systems required here must respond extremely fast and have low losses in the case of extreme current gradients. Furthermore, the storage systems should have an extremely high number of cycles and operate in summer and winter with almost the same internal resistance.

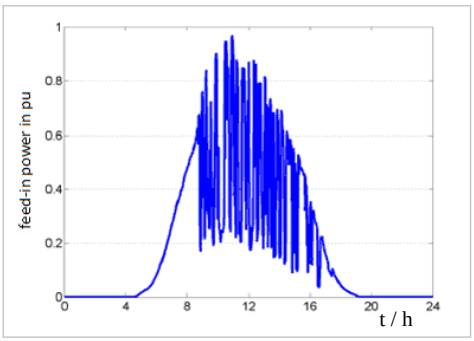

Fig. 3. Effect of clouds on PV feed-in

1.3 Impacts on grid stability

Grid stability has so far only been influenced by internal and external disturbances. Internal disturbances include switching operations. These switching operations affect generator and consumer units equally. External disturbances concern weather events, short circuits or line interruptions. While short-circuits can usually be remedied by briefly disconnecting and then reconnecting the short-circuited line, this is not possible in the case of line interruptions. Here, only redundant lines can mitigate the failure. Taking into account a changed feed situation as a result of the expansion of renewable energy generation, additional switching operations or feed fluctuations, for example due to PV systems, are added. The frequency of switching operations can lead to premature ageing of equipment such as cable sleeves (see Fig. 4) in cable networks.

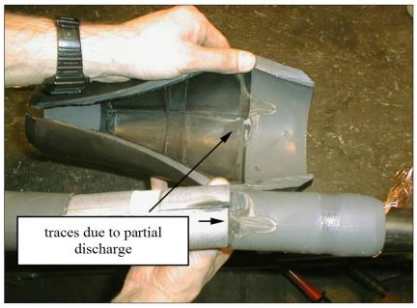

Fig. 4. Incorrectly mounted sleeve damaged by partial Discharge [1]

1.4 Storage systems

The storage of electrical energy from PV systems, see also Fig. 5, is today primarily accomplished by battery storage. Sooner or later, when grid stability plays a greater role, ultracapacitors and methanol storage will supplement battery storage. While ultracapacitors and battery storage belong to the short-term storage category, methanol storage belongs to the long-term storage category. Methanol storage units are continuous storage units that are not dependent on charging and discharging processes.

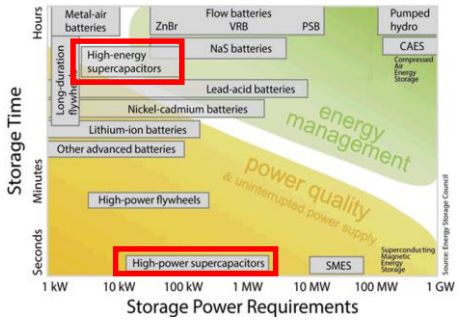

Fig. 5. Energy storage technologies [2]

1.4.1 Ultracapacitors

Ultracapacitors belong to the shortest time storage devices. Their construction is relatively uncomplicated, which is why they also have enormous long-term stability. In terms of stored energy and their charging and discharging behaviour compared to batteries, they could be considered power storage devices. Unlike batteries, ultracapacitors can store less energy. On the other hand, they can deliver the stored energy to the consumer more quickly and at much higher currents. This advantage over batteries makes them very interesting for short-term events. Fig. 6 shows the structure of an ultracapacitor.

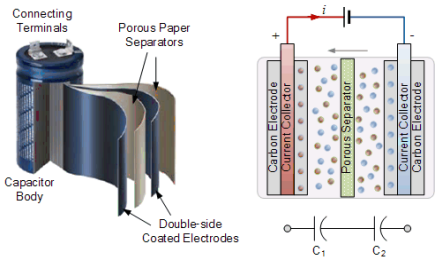

Fig. 6. Design of an ultracapacitor [3]

1.4.2 Batteries

Batteries belong to the group of short-term storage devices, see Fig. 7. It is known that batteries can achieve relatively long operating times if properly maintained and operated. This is especially true for car batteries. The use of Li-ion batteries also shows that batteries show a considerable energy density at a favourable weight, which is why they are currently being used for e-mobility applications. Nevertheless, there are specific requirements that must be taken into account. This applies in particular to voltage balancing, cell temperatures and charge / discharge management.

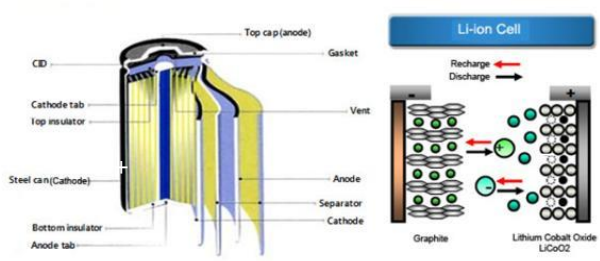

Fig. 7. Design and operating principle of a Li-ion battery [4]

1.4.3 Power to Methanol storage

With Power to Methanol, see also Fig. 8, a Power to X solution, it is now possible to store large quantities of energy. While ultracapacitors and battery storage can compensate for short-term fluctuations in the generator or consumer area, power to methanol storage is considered seasonal storage or long-term storage. Seasonal storage of PV energy becomes interesting whenever there is a very large excess supply of PV power in the upstream grid. Preferably in the summer months, feed-in power may exceed demand and the excess energy must be supplied to suitable storage facilities. Power to methanol storage take surplus electricity from PV systems and convert it into a liquid energy carrier. Methanol is now a synthetic energy carrier that can be used in many different ways. It is both an excellent fuel for all vehicles with combustion engines and a basic chemical for C1 to C4 chemistry.

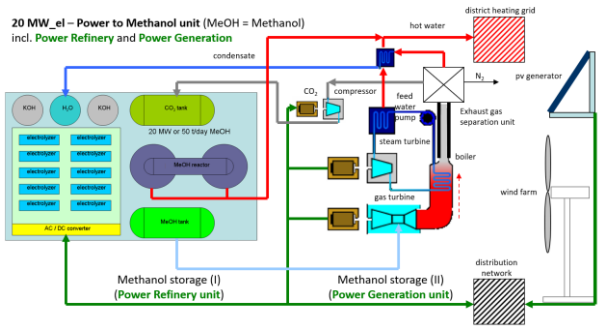

Fig. 8. Power to Methanol storage

2. PV SYSTEMS

Photovoltaic systems are largely state of the art. Their base material, silicon, is the second most abundant element available on earth after oxygen. Looking at the progress of mankind's social development, we see in many places that we are already in the midst of the information age, in which large-scale communication systems and computers have conquered our working and leisure worlds.

The use of high-purity silicon for microelectronic circuits requires large quantities of silicon. The incurring excss material can be re-used to produce PV cells thereby contributing to an efficient material flow. Photovoltaic users produce renewable electricity, which is paid for by all citizens through the kilowatt hour price. This keeps the price of microelectronic products low and enables everyone interested in information technology to purchase microelectronic products.

In the context of the energy transition, which demands a rapid expansion of renewable energies, measures must be taken to maintain grid stability. These include the use of batteries, ultracapacitors and power to methanol units.

While batteries and ultracapacitors belong to short-term storage, power to methanol storage can be grouped among long-term storage. The efficient use of Power to Methanol storage requires an additional interconnection of the energy storage units via HVDC system.

2.1 PV-unit (PVU)

Simple PV units, see Fig. 9a, consist of a PV generator and an inverter. The PV unit is connected via an inverter to the power grid or to an isolated grid with alternating current. Such units have a rated power from 5 to 50 kW. A converter connected between the PV generator and the DC busbar provides voltage matching and system control.

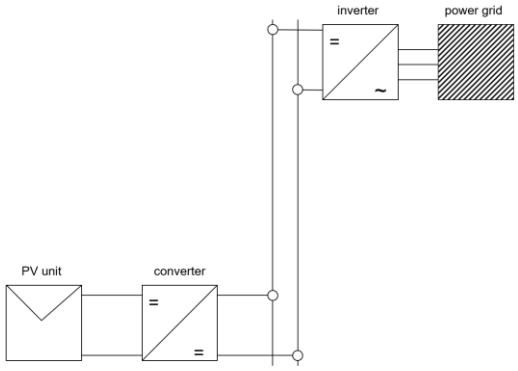

Fig. 9a. Simple PV unit without storage

These simple units are not in a position to stabilise the grid voltage. Due to the lack of storage elements, they rather contribute to risking the grid stability.

Furthermore, a large number of small units can contribute to increasing the nominal voltage above the permitted level, see Fig. 9b. The voltage increase, see Fig. 9c, at the feed-in point and the feed-back of the surplus energy into upstream grids contribute to an increased stress on the operating system.

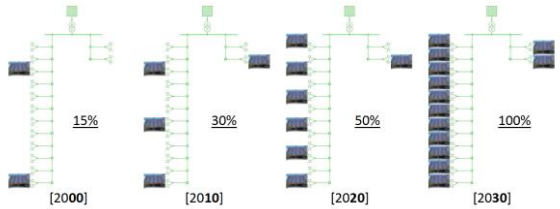

Fig. 9b. PV unit penetration

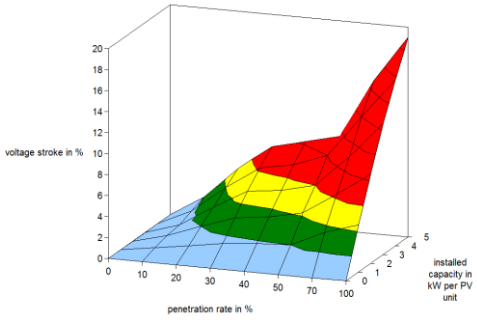

Fig. 9c. Voltage stroke

2.2 PV-battery-unit (PVBU)

The expansion of PV systems with battery storage, see Fig. 10, is always advantageous when the PV electricity cannot be directly utilized at the time of generation and must be fed into the power grid for relatively low returns. The electricity stored in the battery can be used in the evening or early morning by the owner of the PV unit. The installed battery should have a unit capacity adapted to the PV unit. Furthermore, the capacity should be related to the actual demand.

In a future grid supporting smart meter operation, the battery management can also ensure that the battery is charged or discharged depending on the current electricity price. No PV feed-in is required for this. If the PV unit owner owns an electric car, the electric car can be charged via the battery of the PV unit.

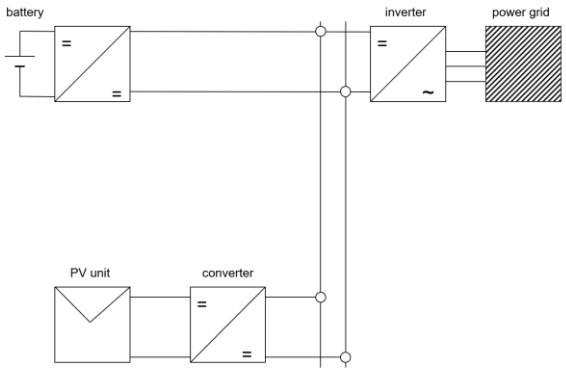

Fig. 10. PV battery unit

2.3 PV-battery-ultracapacitor-unit (PVBUU)

While PV battery units can be classified in the power range from 5 to 50 kW, PV battery ultrapacitor units, see Fig. 11, can be assigned to a power range from 50 to 1000 kW. Here, questions of grid stability play a significant role. Smaller grids would be very sensitive to voltage fluctuations due to the weather event with clouds. For this reason, ultracapacitors must react very quickly to voltage fluctuations and compensate as far as possible. The downstream battery storage is connected via a slower DC/DC converter. Only after the ultracapacitor has been fully utilized, the battery is subjected to the disturbance event and included in the voltage stabilization.

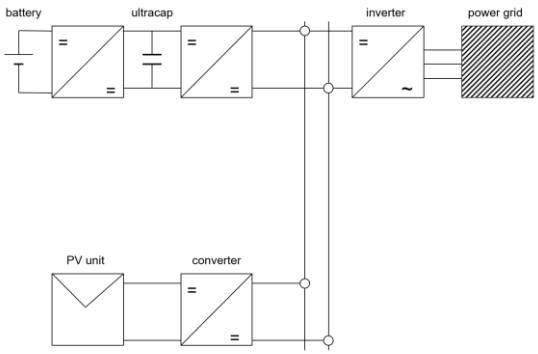

Fig. 11. PV unit with battery and ultracapacitor

2.4 PVBUU with power to methanol unit

PV units above 1 MW installed capacity can have additional storage and grid connections. The feed-in power, especially in the summer months, could be used for long-term storage of PV electricity. While surplus PV electricity can be converted into methanol during the day via a power to methanol unit, see Fig. 12, a battery storage system could ensure that the power to methanol unit does not have to be switched off immediately after sunset, but instead runs through the night at low output. In order to avoid excessive battery power for larger systems, an HVDC connection could be used to take inexpensive surplus electricity from other regions and convert it into methanol. In return, the PV battery ultracapacitor and power to methanol unit could also

convert methanol back into electricity and provide grid support when the ultracapacitor and battery are no longer able to do this. The feedstock required for the storage system is provided by a recovery system. The water and CO2 contained in the flue gas are separated and stored.

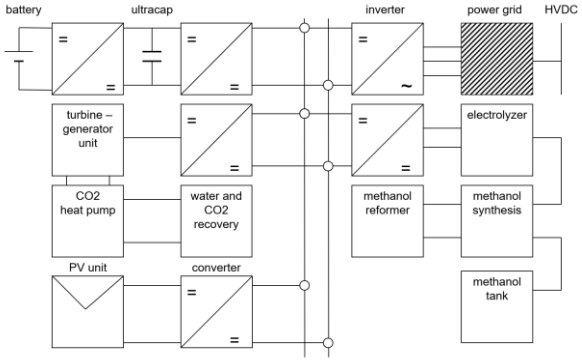

Fig. 12 PVBUU with power to methanol unit [5, 6, 7]

3. ULTRACAPACITORS

Ultracapacitors should be used in such a way that the storage capacity is utilised efficiently. Since ultracapacitors, in contrast to batteries, have a lower energy density, ultracapacitors should always be used when a short charging process is to be expected in addition to a short discharging process. Oscillations, as represented by clouds, are short-term events in which both processes take place at short intervals within seconds. The special design and physical properties of ultracapacitors make these special capabilities possible.

Whereas in batteries, for example, Li-ions are conducted from one electrode to the other by an electric field between the electrodes and must pass through a separator that protects the electrodes from a short circuit, the situation is completely different in an ultracapacitor. Here, the salt ions dissolved in a solvent, e.g., acetonitrile, are separated by a cyclic process and stored in tiny pores of activated carbon. If charging and discharging processes take place after a completed charge carrier separation, in this case cyclisation, the salt ions embedded in the pores of an activated carbon matrix move only minimally. In principle, no more charge carrier transports, here salt ions, take place within the ultracapacitor. Only the much lighter and smaller electrons are now absorbed by the ion fields within the pores of the activated carbon matrix or released into the activated carbon matrix.

3.1 Structure and mode of action

The ions enclosed in activated carbon pores with a diameter of approx. 100 nm form virtual ion electrodes. While the electrode precharged with positive ions binds electrons in its environment, the electrode precharged with negative ions binds positive holes in its environment. Since the ions no longer leave the pores, any number of charging and discharging processes can be carried out. During the cycling process, which after all involves charge separation, in this case positive and negative ions of a salt, as many electron-hole pairs are formed in the respective electrodes during cycling as it is possible for the salt ions in each electrode to bind via their field forces. While the ions remain in the pores, electron-hole pairs can form at all locations within the activated carbon matrix of the electrodes. Since their number is balanced and in equilibrium with the respective number of ions in each electrode, a shift of charge carriers from one electrode to the other can now take place by applying a charging voltage. It is interesting to note that up to half of the maximum voltage (2.5 V), i.e., 1.25 V, an almost linear charging process takes place. In the range from 0V to 1.25V, virtual ion electrodes form within the pore region, creating an additional capacitance, a pseudo-capacitance. Above 1.25V, the formation of the ion electrode within the pore spaces is completed and the virtual ion electrode now moves very slowly towards the activated carbon surface of the pore. Shortly before reaching the maximum charging voltage (2.5V), a limit is reached where no further approach to the activated carbon matrix is possible, and the ions are pushed into each other. These processes, nearing and concentration, also result in the formation of pseudocapacities. This process is exemplified by a simulation of the ion distance from a fictitious activated carbon surface in Fig. 13b. Here it can also be seen that after a stagnation of the approach process, a concentration process presumably takes place, whereby the distance increases somewhat. If further charge carriers are added via a charging process, the distance decreases again.

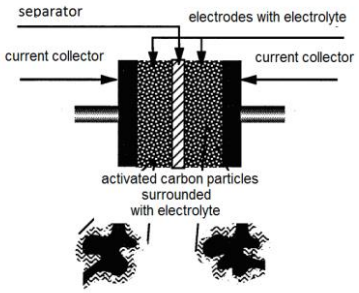

Fig. 13a. Ultracapacitor assembly

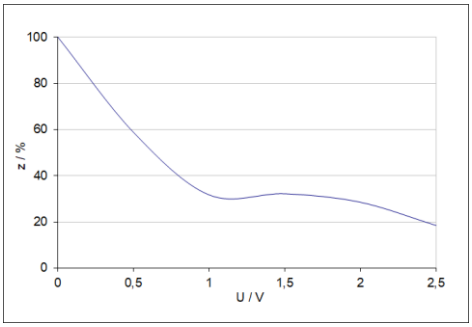

Fig. 13b. Simulation of the ion distance from a fictitious activated carbon surface and the formation of the pseudo-capacitance during the charging process (e.g.: z = f(U) in % starting with initial distance of 100 %)

Fig. 13a shows the basic structure of an ultracapacitor. It consists of a current collector, activated carbon surrounded by electrolyte and a separator.

3.2 Modeling

The modeling is based on the idea of generating large surfaces, which correspond to the well-known capacitor plates from physics. If we try to make a reference to biology, we could imagine that large surface areas could be created, for example, by pyrolysis of wood. If the question is asked, how do trees grow, two interesting stages of development can be observed. While young trees show almost linear growth, older trees grow exponentially at a certain stage of development. Since these growth phases can also be transferred to the fruits of the trees, linear and exponential growth take place here within a few weeks. For example, in a coconut there are shell sections from linear and exponential growth phases. While shell sections from a linear growth phase have small surface areas, the surface areas from the exponential growth phase are very large. Using this knowledge for a new and interesting technology, natural raw materials can be used to achieve interesting physical effects. Activated carbon produced in this way has enormous surface areas within the existing pores. Fig. 14 shows an activated carbon layer on a current collector with a film thickness of s = 150·10^-6 m and particles with a diameter of d_{Pa} = 15·10^-6 m. The particles obtained via pyrolysis have macro-, meso- and micropores. The largest pores have often a diameter of d_{Po_max} = 100·10^-9 m and the smallest of d_{Po_min} = 10·10^-9 m.

Due to the consideration of an exponential growth, model equations also result for the capacitors examined here, which take this special feature into account. Using exponential growth functions, parameters can now be determined that describe both the situation in the capacitor and the behaviour of the capacitor within an electrical or electronic circuit. It is of great interest that the deviations of the impedance spectra from the model and the original are as small as possible, see also Fig. 14a) and 14b). The method used here varies the parameters of the growth functions step by step until an optimal model has been found with minimal deviations.

a)

b)

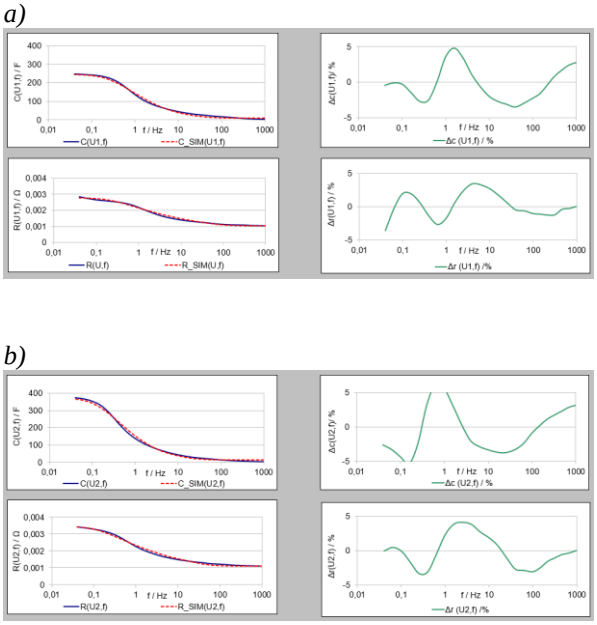

Fig. 14. Capacitance and resistance spectra of an Ultracapacitor and associated relative errors for
a) U_1 = 0V and
b) U_2 = 2.5V

The capacitance and resistance distribution within one of the two almost identical electrodes of an ultracapacitor, see Fig. 15, clearly shows that during the charging process of the ultracapacitor there are changes within the activated carbon matrix or the activated carbon particles. While almost no changes can be detected in the higher layers, there are significant changes in the lower layers near the current collector. Since most of the salt ions have been absorbed into the particle pores here, the ions react very sensitively to the applied voltage and the influx of charge carriers, in this case electrons. In particular, in Fig. 15a) it is noticeable that in the lowest particle layers the capacitance increases continuously up to 1.25V, then remains unchanged, and then gradually increases again. These effects, which can be attributed to the pseudocapacitance, presumably take place within the particles and there in the pores. If the resistance spectrum is consulted, it is noticeable that a considerable increase in resistance takes place in the deeper-lying particles in the region of the maximum charging voltage. This increase in resistance in combination with a slight drop in capacitance indicates that shortly before the maximum charging voltage is reached, there are less freely moving electrons available in the activated carbon matrix, which can explain the increase in internal resistance, see also Fig. 15b)

a)

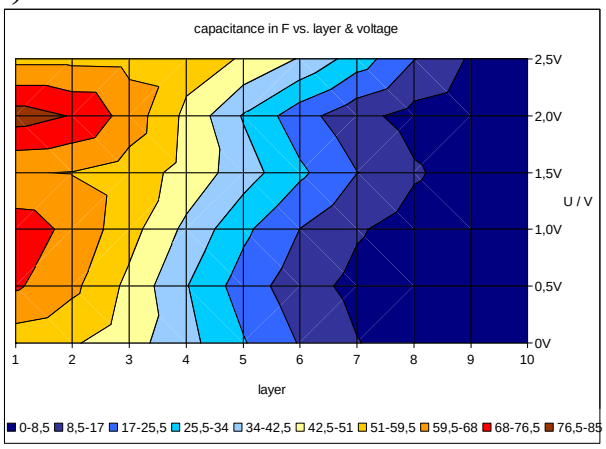

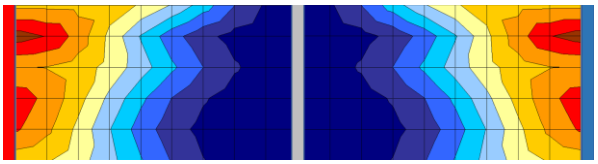

b)

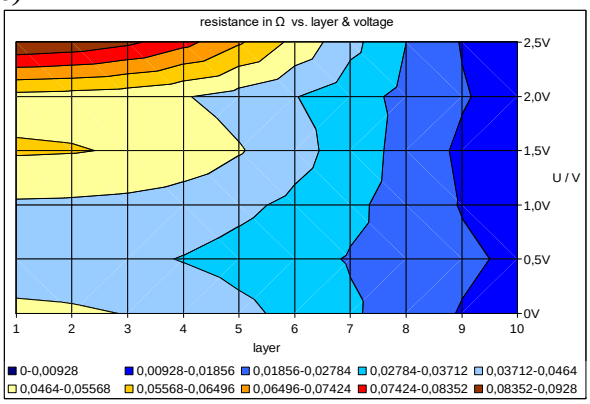

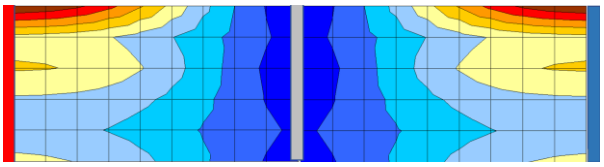

Fig. 15. Capacitance a) and resistance b) distribution as a function of the number of layers n=10 and the charging voltage U=[0...2,5]V

3.3 Simulation

Based on the capacitance and resistance distributions from the ultracapacitor parameter determination, a simulation model can now be created. The simulation model is subjected to a charge and discharge test and the results of the simulation are compared with a measurement on the real ultracapacitor. These tests are demonstrated here using a 1F ultracapacitor as an example. An optimum number of layers of n=10 particle layers was also found for the ultracapacitor used, see also Fig. 16.

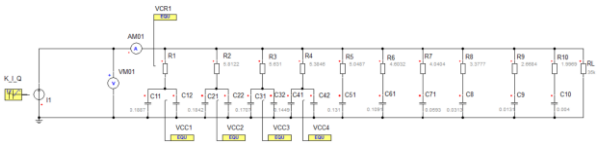

Fig. 16. Simulation model of a 10-stage RC model for a 1F ultracapacitor [8]

For the parameterization of the 10-stage model, 2 x 20 parameters were taken from the ultracapacitor parameter analysis and preset according to the required voltage control.

To validate the ultracapacitor parameters, an original ultracapacitor is charged and discharged with a suitable measuring system. The charging and discharging currents as well as the charging and discharging voltages are measured, recorded, stored and displayed graphically, see Fig. 17 and 18.

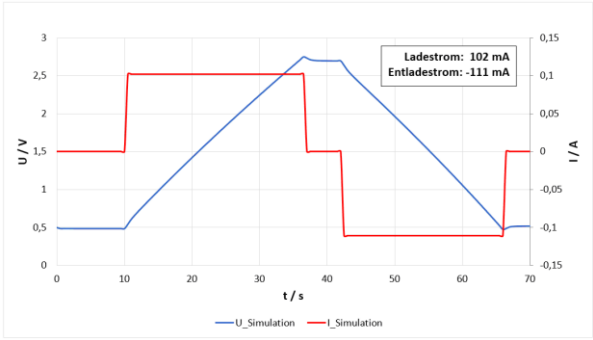

Fig. 17. Simplorer simulation of charging and discharging a 1F ultracapacitor using the ultracapacitor equivalent circuit shown in Fig. 16

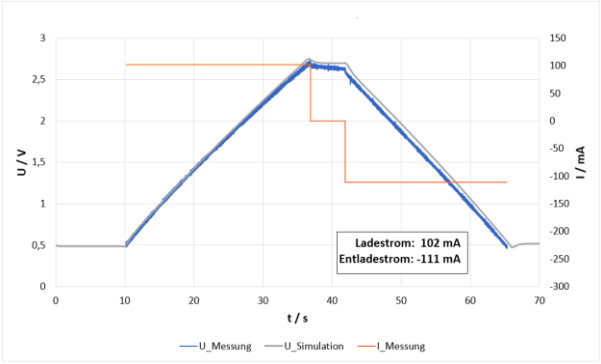

Fig. 18. Comparison of simulated and measured charge and discharge voltage

As can be seen in Fig. 18, the simulation and the measurement of the charge and discharge voltage is well matched. From this it is concluded that the method used to determine ultracapacitor parameters, see Fig. 14 and 15, is correct and that the actual physical conditions within the electrodes have been correctly described.

In this way, a new and innovative method was presented and verified that allows both the description of electrode

processes within the activated carbon matrix of an ultracapacitor and the dynamic simulation of an ultracapacitor on the basis of an ultracapacitor parameter determination.

The advantages of the method are to find out new knowledge about the internal ultracapacitor processes. Furthermore, the materials used and their efficiency can be optimised.

With regard to the application of ultracapacitors to compensate grid instabilities caused by fluctuating feed-ins from regenerative energy generation systems, it is now possible to generate very accurate equivalent circuits for ultracapacitors.

Using the equivalent circuits, a wide variety of weather scenarios and the effectiveness of the ultracapacitors can be investigated.

4. RESULTS

The decline of fossil energy sources requires a rapid expansion of renewable energies. While wind energy provides annual full-load hours significantly higher than those of photovoltaics, the feed-in from the latter is better tuned to the demand over the day. Furthermore, photovoltaics can be installed close to consumers, as the operating conditions do not have a harmful effect on humans and animals.

However, the installation of photovoltaic systems close to the consumer also means at the same time that the supply systems must not be stressed additionally by photovoltaic systems. Serious problems occur when enormous back-feeding takes place, for which the existing supply systems are not designed.

Furthermore, weather phenomena such as heavy cloud cover can occur more frequently in conjunction with other harsh conditions due to climate change. This is currently being discussed very intensively, as it can lead to an additional stress on the energy supply systems as a result of switching operations.

While a few photovoltaic systems do not pose any problems for the power grid, a clustered installation of photovoltaic systems leads to a significant voltage increase in the consumer area.

Based on these challenges, this paper described what storage solutions could look like to fulfil long-term objectives.

4.1 Internal voltage stabilisation

New storage solutions for photovoltaic systems require measures that contribute to both internal and external voltage stabilisation.

Only when it has been ensured that internal voltage stabilisation is guaranteed can external voltage stabilisation also take place.

The storage systems to be used must therefore be designed for both internal and external requirements.

While smaller systems can be equipped with ultracapacitors and batteries with little effort, larger systems require more attention in terms of internal and external compliance with supply stability.

Photovoltaic systems in the higher power range must be kept connected to the grid under all circumstances to avoid supply interruptions.

Power-to-methanol photovoltaic systems provide long-term storage for electricity, heat and fuel supply to residential areas, hospitals, airports and other consumers, even as stand-alone solutions.

4.2 External voltage stabilisation

With the expansion of renewable energy generation, fluctuations within the supply grids will increase and, under certain circumstances, critical supply situations will occur when either too much or too less energy is available. In this context, PV systems with storage could take on a grid-supporting function. This requires the use of storage in PV systems.

The concrete contribution to grid support results from the installed storage systems and their characteristics.

Furthermore, it is assumed that powerful high-voltage direct current transmission systems will be used, which also provide night-time electricity from wind energy. This night-time electricity could be stored by PV systems with storage and used for long-term storage of electricity in methanol.

In addition, PV systems with storage could help supply the industry with basic chemicals, in this case methanol.

5. OUTLOOK

The expansion of renewable energies requires the simultaneous expansion of short- and long-term storage. The efficient use of renewable energies is only possible through the use of storage. Shutdowns of renewable energy producers mean losses in sustainability and economic success.

The use of ultracapacitors can help to remedy the fluctuations generated by renewable energies and make renewable energies stable sources of energy supply.

REFERENCES

[1] Pepper, D.: Grundlagenuntersuchungen zum Teil-entladungsverhalten in kunststoffisolierten Mittel-spannungskabeln bei Prüfspannungen mit variabler Frequenz und Kurvenform, Dissertation, 2003, S.39

[2] Conover, D., Rosewater, D.: Energy Storage System Overview and Addressing System Safety (US DOE, 2015)

[3] HTTPS://SEMIENGINEERING.COM

[4] https://www.electronics-tutorials.ws/de/kondensatoren/ultrakondensatoren.html

[5] Harzfeld, E.: Patent document: EP 2 100 869 A1 Process for the production of methanol by utilization of carbon dioxide from exhaust gases of fossil-fuelled power generation plants

[6] Harzfeld, E.: Patent document: EN 10 2018 105 643 B3 Method for uninterruptible power supply by means of a rapid standby system

[7] Harzfeld, E.: Patent document: US 2021/0052926 A1 Method for preventing fires in tank systems and tank system for methanol fuels with a fire protection device

[8] Harzfeld, E.: Patent document: DE 10 2007 039 941 A1 Method for determining the capacitance, resistance and energy density distribution in devices with electro-chemical double layer

Address of the author
Harzfeld, Edgar; Stralsund University of Applied Sciences; Zur Schwedenschanze 15; 18435 Stralsund; Germany; edgar.harzfeld@hochschule-stralsund.de

Agro-Forestry and Photovoltaics: Innovative Production and Utilization of Energy for Autonomous Agricultural Processes

Ladislava Černá[1], Jan Weger[2], Kamila Vávrová[2], Petr Wolf[3]
[1]Department of Electrotechnology
CTU in Prague, Faculty of Electrical Engineering
Prague, Czech Republic
[2]Silva Tarouca Research Institute for Landscape and Ornamental Gardening, Publ. Res. Inst.
Section of Phytoenergy
Průhonice, Czech Republic
[3]University Centre for Energy Efficient Buildings
Czech Technical University in Prague
Buštěhrad, Czech Republic

Abstract

Since the beginning of the solar boom, photovoltaics has expanded to a previously unsuspected extent due to a significant drop in prices. As the area for installation is limited and the occupation of agricultural land for installation is undesirable, experiments have begun with a combination of agricultural production and photovoltaics - agrophotovoltaics. However, a further reduction in the price of photovoltaic components means that even where the installation does not seem to make sense, it is possible today to build a system that finds its use. Such an example can be the installation of modules between trees of agroforestry systems, which are innovative and multifunctional farming managements aimed at adaptation of agriculture to impacts of the climate change.

Keywords: agrovoltaics; agroforestry; agricultural production

INTRODUCTION

While the price of photovoltaic installations in 2010 was around 3,200 EUR / kWp, today's costs can be estimated at around 600 EUR / kWp. Thanks to its easy availability, users who would not have considered it before also became interested in photovoltaics. An interesting concept may be the installation of modules within agroforestry systems, as will be described below.

AGROVOLTAICS AND AGROFORESTRY WITH PHOTOVOLTAICS

Agrovoltaics, or agrophotovoltaics is a term referring to photovoltaics installed on agricultural land without stopping agricultural production. This concept was first described by A. Goetzberger in 1981 [1]. There are basically two concepts used:

- classic orientation of modules on increased construction with larger spacings
- vertical construction

While in the past the rather classic orientation of the modules was used, thanks to the development of bifacial technologies, the vertical construction is starting to catch up with the second group.

Agroforestry systems (ASF) are agricultural or land use system in which trees are grown in combination with conventional agriculture on the same land plot (EU regulation no. 1305/2013). Modern agroforestry systems are considered as one of the promising adaptation and mitigation measures to minimise impacts of the climate change in agriculture [2]. In addition to having a positive effect on the yields of some crops or of quality of their products, this approach also has a positive effect on ecosystem services of agriculture including erosion control, buffering extreme weather (heavy rains, heat waves, strong winds), biodiversity improvement, or carbon (humus) sequestration [3], [4]. Within agroforestry, several planting scheme are applied including silvoarable alley cropping where trees are planted in the form of lines, and therefore it is possible to place photovoltaic modules between them.

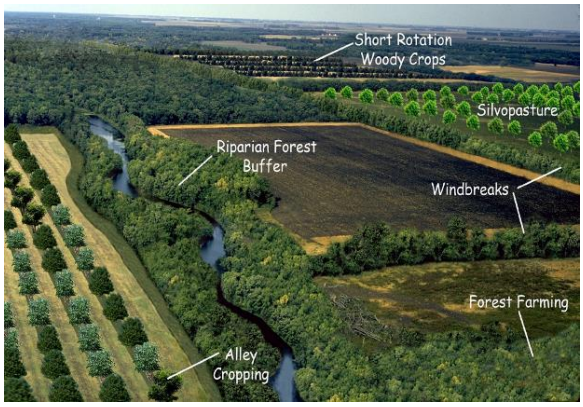

Fig 1: Main types of agroforestry systems USDA, 2010

Although placing modules between trees seems seemingly pointless due to the frequent shielding and minimal performance that such installations can provide compared to standard installations, there are a number of low-power applications where even a small amount of power can be useful. Such applications include, for example:

- post-drying (energy chips from fast-growing woody plants),
- pumping water into watering tanks,
- operation of small agricultural (mobile) facilities (slaughter, milking, etc.),
- charging stations for (micro) electromobility,
- charging stations for telephones and portable devices for e.g. agritourism.

Requirements are being collected and communication with farmers is underway as to whether and what applications they would be interested in.

EXPERIMENTAL SYSTEM AT RILOG

In order to investigate the interactions between the agroforestry system and photovoltaics, an experimental agroforestry-photovoltaic (AGFPV) system of 6.72 kW_p was launched last year at the Silva Tarouca Research Institute for Landscape and Ornamental Gardening (RILOG) complex in Průhonice within the experimental station Michovky (see Fig. 2). This system consists of panels installed on an inclined plane as well as on a vertical structure. Conventional monocrystalline silicon modules, bifacial PERC modules and CIGS modules are installed to compare technologies. This year, the system will be supplemented by bifacial HJT modules Meyer-Burger.

Irradiance and temperature sensors are installed to monitor the parameters of the photovoltaic system, and the performance is monitored via SolarEdge power

Fig. 2: Experimental AGFPV system at RILOG

optimizers. Other monitored parameters include, in addition to the temperature of the modules, the soil temperature around the modules and the growth of crops in comparison with areas without photovoltaics. First results of electricity production are shown on Fig. 3. During year 2021, 381 MWh of energy was produced, which represents energy yield of approx. 570 kWh/kW_p.

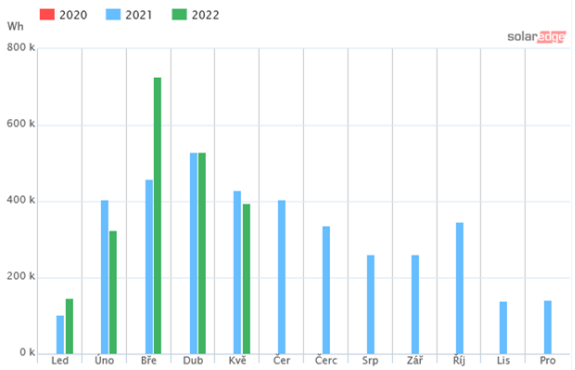

Fig. 3: Production from experimental AGFPV system in Michovky

CONCLUSION

The basic concept of the agroforestry photovoltaic system was described in the article. The first experiments showed about half the yield compared to conventional PV systems. Experiments on the RILOG system will continue in order to determine the appropriate configuration and technology of PV modules in combination with woody plants and the impact on agricultural production.

ACKNOWLEDGEMENT

This work was supported by TACR project No. TK04010166 (Comprehensive solutions of local and regional energy systems as part of GreenDeal's measures to achieve sustainable agricultural and forestry management)

Addresses of the authors

Ladislava Černá, Technická 2, 166 27 Praha - Dejvice, Czech Republic, ladislava.cerna@fel.cvut.cz
Jan Weger, Květnové nám. 391, 252 43 Průhonice, Czech Republic, weger@vukoz.cz
Kamila Vávrová, Květnové nám. 391, 252 43 Průhonice, Czech Republic, vavrova@vukoz.cz
Petr Wolf, Třinecká 1024, 273 43 Buštěhrad, Czech Republic, petr.wolf@cvut.cz

REFERENCES

[1] A. GOETZBERGER & A. ZASTROW (1982) On the Coexistence of Solar-Energy Conversion and Plant Cultivation, International Journal of Solar Energy, 1:1, 55-69, DOI:10.1080/01425918208909875

[2] KOTRBA, Jiří. Selská revue. p. 36–39. *agrolesnictvi.cz* [online]. Asociace soukromého zemědělství ČR. Praha, November – December 2014 [cit. 2022-05-21]. p. 36–39. Available at: https://agrolesnictvi.cz/wp-content/uploads/2015/06/Selsk%c3%a1_revue_2014.pdf

[3] Lojka B, Martiník A, Weger J, Houška J, Doležalová H, Kala L, Szabó P, Kotrba R, Krčmářová J, Chládová A, Vávrová K, Jobbiková J, Ehrenbergerová L, Snášelová M, Králík T. Zavádění agrolesnických systémů na zemědělské půdě. Praha, Česká Republika: Česká zemědělská univerzita v Praze; 2020. 72 p.

[4] Nedej se! Kladno bez Uhlíku (v čase 18:00-20:00 je ukázka Agrolesnické fotovoltailky VUKOZ Michovky: https://www.ceskatelevize.cz/porady/1095913550-nedej-se/221562248420002-kladno-bez-uhliku/

Teaching Photovoltaics for Children

Pavel Hrzina, Ladislava Černá and Tomáš Finsterle
Department of Electrotechnology
CTU in Prague, Faculty of Electrical Engineering
Prague, Czech Republic

Abstract

In recent years, there has been little interest from students in technical fields and the industrial sector thus suffers from a significant shortage. This shows the importance of motivating future students to study technical disciplines from an early age. Within the CTU in Prague, a very successful event is organized every year - the Children's University, where children spend a week at the university and get acquainted with the world of technology. One of the fields they come into contact with is photovoltaics. The form of teaching for children is described in the article.

Keywords: photovoltaics teaching; children

INTRODUCTION

Although it may seem that it may be early to educate students from primary school or kindergarten, it is precisely the primary school from which children go to fields according to their preferences. According to [1], the main motivator for choosing a future career is the family: *"Parents communicate to children their expectations and ideas about their professional future. Children learn from their parents' attitudes, behavior at work and how they talk about work. Career choice is then further significantly influenced by the socio-economic status of the family, its cultural capital, the profession pursued and the educational attainment of the parents."*

Therefore, it is very important to address the parents and children from early age to show them possibilities. As the university is well aware of that, it cooperates with kindergartens and basic schools on special events for them.

As part of pre-school education, the CTU operates its own kindergarten, which is then followed by a primary school, where children are in contact with technology from the beginning. For other children, CTU organizes a suburban camp called "Children's University", which is visited by about 150 children every year.

In the field of photovoltaics, other cooperation runs with Czech Solar Association, which organizes events focused on connection of photovoltaics with teaching physics on basic schools and other events. As an example, there were a few workshops in cooperation with National Technical Museum where basic principles of photovoltaics were introduced to children. Similar programmes are organized by other CTU's employees in other technical sectors.

CHILDREN'S UNIVERSITY & PHOTOVOLTAICS

This year, a photovoltaic group is also involved in the Children's University.

There are several issues to be faced when teaching young children:

- lack of knowledge
- the short time the child stays
- a short interval during which the child is educated in the field
- the need to capture and preserve in memories

Although the last point is well covered by the University in the form of matriculation and graduation ceremony (every child gets a graduate diploma), other points must be solved within the course.

In the field of photovoltaics, we decided to make a workshop, where every child can produce its own solar lamp. Children will get acquainted with the basic functions of photovoltaics and take home something they can be rightfully proud of. Since the teaching takes place as a production, there is no need to worry about lack of attention, because the child is automatically focused on doing his job to the best of his ability.

PV LAMP DESCRIPTION

To produce solar lamp, standard circuit diagram utilizing commercially available circuit QX5252 is used [2]:

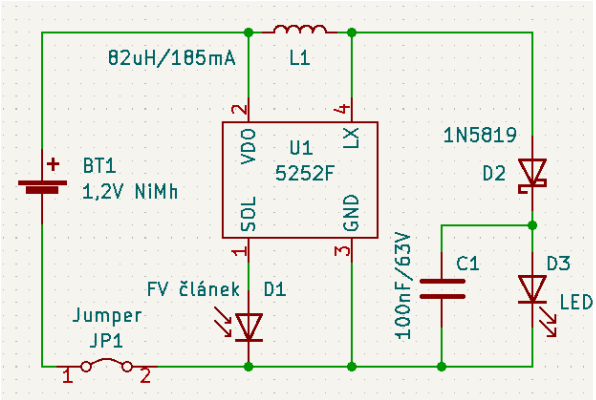

Fig. 1: Solar lamp circuit diagram

List of Components

Component	Value
PV cell (sub-module)	2V, min. 150 mA @STC
Chip	QX5252
Secondary cell (battery)	NiMH/NiCd, min. capacity of 600 mAh
inductance	According to LED colour, we used 82 µH
LED	High luminous white LED, bigger jacket, sufficient radiation angle, we used 10mm shite LED with 100° angle and approx. 2000 mcd luminosity
Rectifier diode	e.g. 1N5819
Capacitor	Ceramic, 100 nF/63V (or 50V)
Single row PIN Header	V/T type, 2 used pins, 2.54 mm distance
Jumper as a switch	2pin switch

Addresses of the authors

Pavel Hrzina, Ladislava Černá and Tomáš Finsterle, CTU in Prague, FEE, Dpt. Of Electrotechnology, Technicka 2, 166 27 Prague 6, Czech Republic
Pavel Hrzina – hrzinap@fel.cvut.cz
Ladislava Černá – ladislava.cerna@fel.cvut.cz
Tomáš Finterle – finsttom@fel.cvut.cz

Fig. 2: Prototype construction

The prototype (see Fig. 2) with a standard layout was tested by high school students. According experiences with these students, the design will be adapted for children:

- longer distances between component terminals,
- suitably bent component terminals,
- easy handling,
- sufficient time for production.

CONCLUSION

This year the prototype of solar lamp for students was tested by high school students. In next month, children will produce same lamp with adjusted design.

Thanks to a useful product, the child sees the result of his work every day and will think about photovoltaics long after graduating from university which may help to motivate it to technical studies in the future.

REFERENCES

[1] HLAĎO, P. *Svět práce a volba povolání: studijní text pro učitele*, Brno: Masarykova univerzita, 2008.
[2] http://jirky.webz.cz/index.php?page=led-solarni-svetylko

Sun Movement Demonstrator

J. Holovský, G. Colombo Chiari, J. Ehrlich and R. Petit Pralon de Miranda
Centre for Advanced Photovoltaics
Department of Electrotechnology
Faculty of Electrical Engineering, Czech Technical University in Prague.
Prague, Czech Republic

Abstract

Sun movement demonstrator is an electromechanical device that visualizes movement of the sun on the sky for chosen geographical location and season. This device was designed and built in the framework of student projects, also including Brazil-Czech academic internship program UNIGOU. This project combined skills of project management, celestial mechanics, geometry, mechanical design by CAD, 3D printing, mechanical technology, mechanical assembling, assembling of electronic components, including soldering and Arduino programming. The device is now fully working and serving mainly for teaching and advertising the topic of solar energy. It nicely demonstrates the potential of solar energy and its seasonal variability.

Keywords: celestial mechanics, solar energy, 3D printing, mechanical design, Arduino programming

INTRODUCTION

Considering sun movement and solar energy, one might ask for example whether sun can ever shine on the back side of photovoltaic modules, if they are ideally oriented toward south. Or as another example, whether there could be shadow during a summer day on south side of a house. Answer is surprisingly affirmative. This is because in summer, sun is not rising at east, as one would say, but at north-east and setting not at west, but at north-west.

To better understand this behaviour and to learn more about sun movement on the sky [1,2], it is useful to transform the observer's time into a sidereal time. The sidereal time is the time in which we count sunsets and sunrises of stars and not Sun. In that time, the year has one day more (366 days). On Prague's astronomical clock sidereal time is indicated by a small star, see Fig 1.

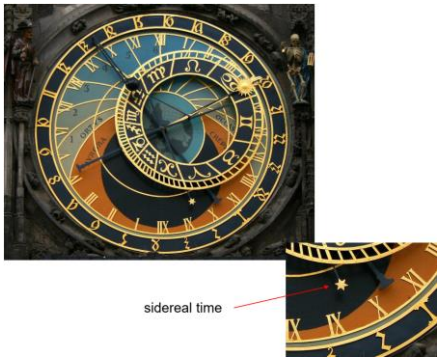

Fig. 1 – Astronomical clock in Prague shows four different times including sidereal time.

We remain in the coordinates of Earth (we are rotating with Earth), but we move far away, so that we can see both Earth and Sun in front of us. Then the situation is as shown in Fig. 2 and Fig. 3.

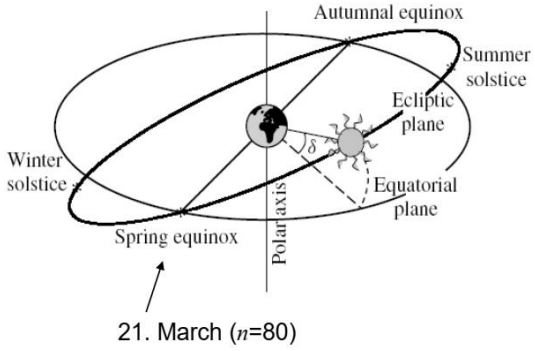

Fig. 2 – Thick lines shows the set of points given by the positions of Sun at *sidereal noon* during a year.

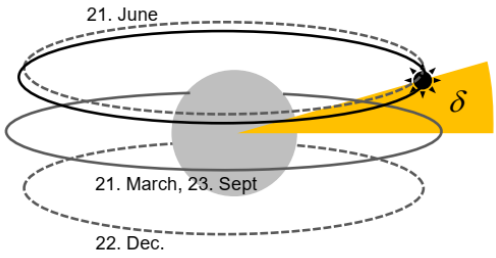

Fig. 3 – Thick lines shows the set of points given by the positions of Sun during one day. Thin and dashed lines represents special days: equinox and solstices.

When we move our coordinate system back to Earth's surface then only sections of the circles depicted in Fig. 3 are visible above horizon. Also, the latitude of the observer's location affects the tilt of the circles. The situation is now shown in Fig. 4.

MECHANICAL CONCEPT

To simulate the sun movement it is necessary to define latitude Φ, declination δ (season), and Earth rotation ωt (time), see Fig. 4.

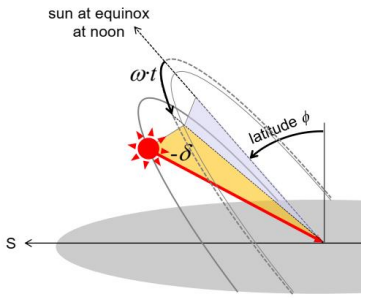

Fig. 4 – Motion of the sun on sky is defined by three independent parameters.

Mechanical concept had to be determined at the very beginning. The key decision was that ωt motion would be realized by individually controlled LEDs on a LED strip formed into a circle. The latitude Φ would be realized by rotating the circle and declination δ would be realized by mutual shift of the observer (model of a house) and the rotation axis of the circle. Because this mutual shift has a direction dependent on latitude, it had to be realized by a combination of vertical and horizontal movements.

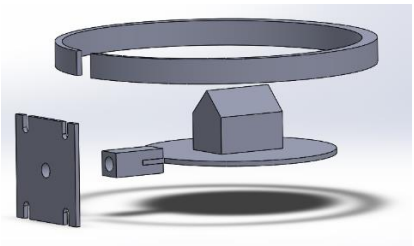

Fig. 5 – Realizing the horizon (circular plate), observer (model of the house) and sun (circle where LEDs will be attached).

MECHANICAL DESIGN

Together with mechanical concept, the method of control and human interface were determined. The choice was to use Arduino microcontroller, LCD display and four navigating buttons.

Once the mechanical design and human interface had been defined, all the commercially available components were selected from the market and eventually purchased, see Fig. 6 (LCD display, navigating buttons and LED strip is missing).

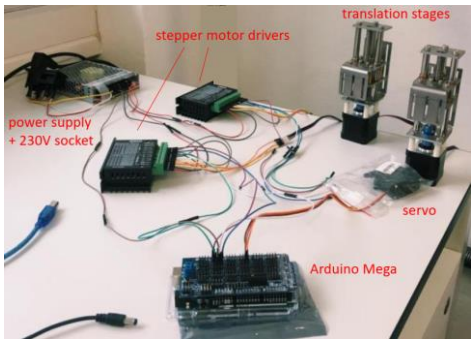

Fig. 6 – Commercially available components being tested and their dimensions and positions being defined.

After all commercial components were known with their exact dimensions, the aluminium frame was designed including positions of all the holes and protrusions, see Fig. 7. The aluminium parts were then machined by water jet from aluminium sheets. Minimum mechanical adjustment was necessary to do afterwards. Aluminium parts were painted black by aloxing.

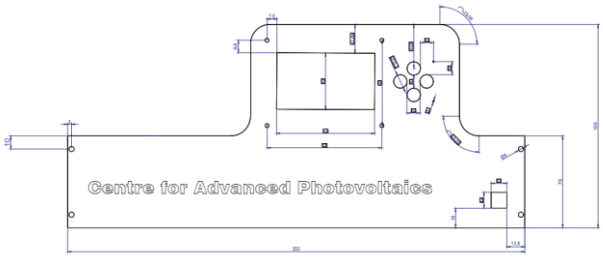

Fig. 7 – Metal parts were precisely designed including all details and hole drilling.

Remaining plastic parts such as the circular LED holder (adjusted according to dimensions of commercial LED strip), model of a house, platform and many other small ones were designed in 3D CAD software and 3D printed.

ASSEMBLY

The assembly represented one of the largest problem for students because still few remaining questions needed to be solved: the problem of position referencing of the translation stages or the problem of shaft bearing of the circle rotation (because servo provided only motion but

not bearing). These skills were definitely beyond the competencies of master students. Also soldering of electrical contacts was a considerable problem for some students. Finished sun movement demonstrator is shown in Fig. 8.

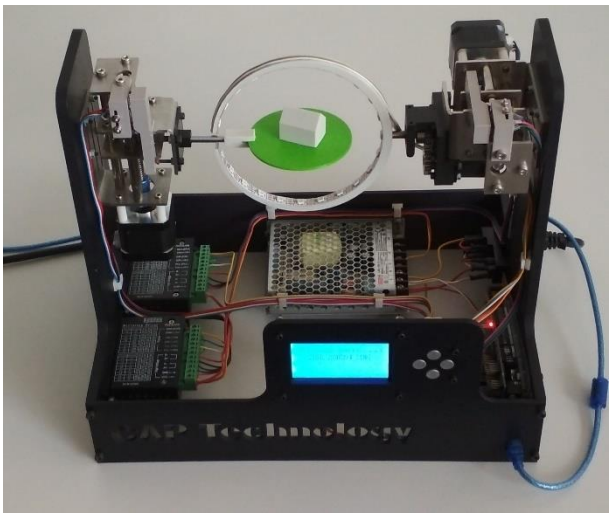

Fig. 8 – Finished sun movement demonstrator.

PROGRAMMING

The chosen microcontroller was original Arduino MEGA2560 REV3 equipped with an Arduino MEGA Sensor shield v2.0. Additionally, a set of libraries was installed for controlling all the other peripheries.

Stepper motors

hardware: Machifit CNC Z Axis Slide Table 50-60mm, fed by driver TB67S109AFTG

libraries: Stepper.h, AccelStepper.h, MultiStepper.h

initialization: AccelStepper

setup: setMaxSpeed, setAcceleration

commands: digitalWrite(pin, HIGH);
delayMicroseconds(500);
digitalWrite(wahl2, LOW);

Referencing was done by while loop and reading microswitch value:

do{ …*stepping commands*…
} while(digitalRead(pin) == false);

Servo

hardware: Servo with metallic gears MG996R

libraries: Servo.h

initialization: Servo

setup: attach

commands: write

LCD display

hardware: ST7920 128x64

libraries: U8g2lib.h, U8x8lib.h, two other libraries are combined as follows: #ifdef U8X8_HAVE_HW_SPI
#include <SPI.h>
#endif
#ifdef U8X8_HAVE_HW_I2C
#include <Wire.h>
#endif

initialization: U8G2_ST7920_128X64_F_SW_SPI u8g2

setup: u8g2.begin //defines navigating buttons

commands: u8g2.clearBuffer, u8g2.sendBuffer
8g2.setFont, u8g2.drawStr
u8g2.userInterfaceMessage,
u8g2.userInterfaceSelectionList

Important: all commands should be inside while cycle as follows: u8g2.firstPage();
do{
…*display commands*…
} while (u8g2.nextPage());

LED strip

hardware: WS2812B, the strip is sensitive to the end where it is fed

libraries: FastLED.h

initialization: CRGB leds

setup: FastLED.addLeds

commands: leds //sets colour of given LED
FastLED.show();

RESULTS AND DISCUSSIONS

After switching on, the demonstrator performs calibration when the translation stages and servo go to their initial positions. Then the demonstrator performs cycle of simulations of randomly selected combinations of latitude and seasons until a right navigating button is pressed. Then the user is given a choice whether the selection will be from a list of pre-defined cities or by a numerical value of latitude. Choosing the first option will then follow selection of city and season, see Fig. 9.

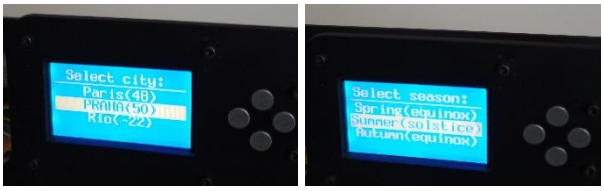

Fig. 9 – User definition of city (latitude given in bracket) and season.

After performing the selection, the servo goes to corresponding angle and consequently stepper motors go to corresponding vertical and horizontal positions. Individual LEDs start lighting up in a sequence from east to west, while LCD display shows corresponding local time, see Fig. 10.

Fig. 10 – Sun movement simulation sequence being performed.

The model of a house is producing a shadow on the platform, which is nicely visible when looking from top, see Figure 11. The two examples demonstrate that in Prague in summer, many places on north side of the house receive no shadow, if they are in a sufficient distance from the house, while on the south side of the house there are many places that receive shadow in the morning and in the evening, no matter how far they are from the house.

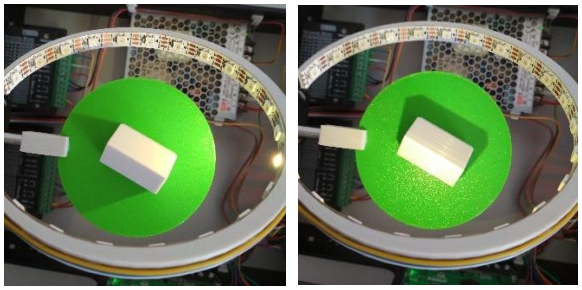

Fig. 11 – Observing the places receiving shadow on north side (direction up) and south side (direction down) during summer in Prague. Left: morning, Right: noon.

CONCLUSIONS

Solar movement demonstrator is an electromechanical device that interactively and instructively demonstrates the sun movement on the sky for selected location and season. The process itself of building such device might be interesting as a student project, because many skills and new technologies can be learned. The device uses many commonly available components that are currently highly popular for hobby 3D printers, RC models, and entertainment and combines them in a new and original way. The device behaves as expected and so far we have not identified any noticeable weaknesses.

ACKNOWLEDGEMENTS

This work was only possible thanks to Brazil-Czech academic internship program UNIGOU. The work was also supported by Czech Ministry of Education, Youth and Sports grant no. CZ. 02.1.01/0.0/0.0/15_003/0000464 – "Centre of Advanced Photovoltaics".

REFERENCES

[1] Approximate Solar Coordinates (2012) https://web.archive.org/web/20160303200632/http://aa.usno.navy.mil/faq/docs/SunApprox.php (accessed March 8, 2021)
[2] Motion of the Sun Simulator https://ccnmtl.github.io/astro-simulations/sun-motion-simulator/ (accessed June 4, 2022)

Addresses of the authors

J. Holovský, Technická 2, 166 27, Prague, Czech Republic, jskub.holovsky@fel.cvut.cz

G. Colombo Chiari, Brazil, guscochi@gmail.com

J. Ehrlich, Czech Republic ehrlijon@fel.cvut.cz

R. Petit Pralon de Miranda, Brazil, rp-miranda@uol.com.br

Using challenge-based approaches for teaching PV: case study of solar communities

J.M. Serra and M.C.Brito

Faculdade de Ciências da Universidade de Lisboa/IDL
Lisboa, Portugal

Abstract

The traditional way of teaching, based on a centred approach around the teacher, must be questioned and new alternatives can be used to actively engage students. WE present here a challenged based approach applied to teaching of PV.

Keywords: photovoltaics teaching; challenge-based approach

INTRODUCTION

The society is not a static entity but it changes over time. This means that the students background knowledge and mindset is also changing. This has important consequences in the way higher education institutions (HEI) fulfill their mission. The traditional way of teaching, based on a centered approach around the teacher must be questioned and new alternatives can be used with very good advantages to actively engage students in the learning process.

One learning approach in HEIs, described as "challenge based", is to manage theory into the test of addressing real problems in collaboration with actors of society.

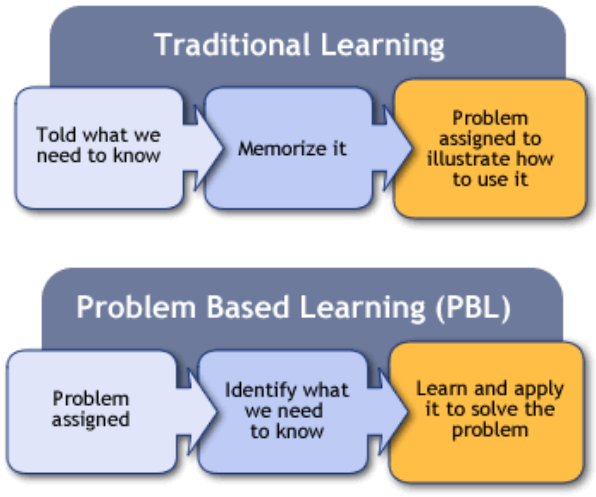

"Challenge Based Learning is an engaging multidisciplinary approach to teaching and learning that encourages students to leverage the technology they use in their daily lives to solve real-world problems." [1]

CHALLENGED BASED TEACHING

In Challenge-Based Learning, students are given challenges, resources, the opportunity to collaborate, tasks with multiple options for solutions and assessment based on real projects. Real-life challenges are interdisciplinary and this requires one to cross the boundaries encountered in single discipline-based courses. Inter-disciplinary approaches bring groups of students with different backgrounds together to understand the various angles from which a specific discipline looks at such challenges. They also help to develop interdisciplinary communication and collaboration skills. In addition, entrepreneurial/managerial skills and market knowledge can be used to enable students to develop technologies and services with the societal appropriation always in mind.

This approach implies changing the role of the teacher to that of a facilitator. Student paths then develop more around self-study and shared or individual experiences giving them the opportunity to explore areas of interest in more detail. Challenge-based programmes that focus on developing robust, coherent and holistic energy solutions, shift away from the more common focus on a single energy technology, or group of energy technologies that only cover a specific part of the energy system.

However, we must not forget that some degree of specialization must be kept. Meeting the need for specialization enhanced by a broader energy systems perspective can be achieved through the adoption of "T-shaped" skills-profiles into the developed

courses/programmes. The essence of such model is that it combines essential, in-depth knowledge in specific, core disciplines (vertical bar of the T) with the broader perspectives of context and impact (the horizontal bar of the T) such as societal or technical aspects to support the energy transition.

The extent of such alternative approaches can be synthetized in

Case-based modules	Challenge-based modules
• Students analyze an existing case/practice emerging from a real-life problem. • they propose solutions, improvements to the existing ones or new/innovative solutions. Students acquire knowledge about real cases and the existing solutions to a problem.	• A combined approach of engineering, societal and business implications and impacts is adopted • Students are invited to work on a non-solved, real-life challenge/problem. • Students are expected to propose solutions/ approaches to solve the challenge/problem. The result is the proposal of a non-existing product.

SOLAR COMMUNITIES

As an example of this approach we designed a challenged based problem students have to solve as part of their assignments related to PV systems in a broader context [2].

Challenge

A group of neighbors in a condominium decided to study the opportunity of setting up a solar PV system to reduce their energy bills.

In the following meetings, they discussed the benefits and issues for individual and shared PV project. Your role in this project is to help on the decision, assessing costs and revenues of the two options.

Data available

The partners in the project included six residential dwellings, a small coffee house and the street restaurant. Luckily, they're all equipped with smart meters and have long term records of electricity demand (c.f. attached file with hourly electricity demand data for one year for each of the 8 meters).

The neighborhood is located in Lisbon (c.f. attached file with hourly solar irradiation data for the same period, measured in the plane of the roof, hence with the inclination and orientation of the future PV system).

The electricity tariff in force at the time of the study is basically a self-consumption mechanism where self-consumed electricity is valued at 0.17 €/kWh (as it avoids consumption at that rate from the grid, including taxes) while exported electricity to the grid is valued at 0.05 €/kWh (which is the retail price for electricity).

The costs of PV system equipment is … €/kWp and of the battery bank is … €/kWh, both including installation costs. The system technical details are listed in Table 1.

TABLE 1. RELEVANT TECHNICAL PARAMETERS

You may use a software tool to simulate the economic revenue, including running costs (battery replacement, etc.), for a PV system, given the specifications of the modules, inverter, etc.

Questions

Determine the optimum PV system/battery capacity for

a) each of the residential and service customers, in the scenario of individual PV systems

b) all residential dwellings, in the scenario of shared PV system

c) all residential buildings and the coffee shop, in the scenario of shared PV system

d) all residential buildings and both service costumers, in the scenario of shared PV system.

For each, indicate the return on investment and payback time as well as the self-consumption and self-sufficiency rates.

What is the expected outcome of the challenge

You will have to write a report for your friends explaining in detail your design calculations, based on the available data, and proposing the system configuration.

REFERENCES

[1] M. Nichols and K. Cator (2008), Challenge based learning white paper. Apple, Inc.

[2] J. M. Serra and M.C. Brito, Case study development: "Solar community: sizing a PV-storage system for aggregated consumers", UNISET Bridging Activity 2018

Addresses of the authors
JM Serra, 1749-016 Lisboa, Portugal, jmserra@fc.ul.pt
M.C.Brito, 1749-016 Lisboa, Portugal, mcbrito@fc.ul.pt

Luminescent solar concentrators – reabsorption and fundamental principles of thermodynamics

B. Dzurnak[1], T. Markvart[1, 2]
[1] - Centre for Advanced Photovoltaics, Faculty of Electrical Engineering
Czech Technical University in Prague
Prague, Czech Republic
[2] - School of Engineering Sciences, University of Southampton, Southampton, UK

Abstract

We report on subject of luminescent solar concentrators as an introductory topic related to education on photovoltaics. Employing of luminescent solar concentrators in any photovoltaic systems possess a plethora of practical and theoretical issues that can be separated into several partial projects and systematically investigated by undergraduate students (without prior knowledge of photovoltaic technologies). Focusing of major mechanism of optical losses, which is phenomena of reabsorption, it is possible to bridge basic functionality and experimental observations of concentrators with theoretical aspects of light conversion and concentration originating in fundamental thermodynamic laws. We show how simplified thermodynamical analysis of radiation flows can lead to estimation of practical parameters of luminescent concentrators.

Keywords: solar cells, photovoltaics, luminescence, fluorescence, concentrators, thermodynamics

INTRODUCTION

Luminescent solar concentrators (LSC) attracted interest for photovoltaic (PV) applications with their potential to reduce costs by concentrating the sunlight onto small area. LSCs were studied extensively already in 1980s [1], however due to the recent interest in new materials and approaches for photovoltaics they are gaining research attention again [2].

From the pedagogical point of view, LSC present an attractive topic for undergraduate (and masters) students of technical fields and can act as an entry topic to the area of photovoltaic research. Moreover, LSC can be used as a demonstrative system of fundamental PV physical principles.

LSC FOR TEACHING AND EDUCATION

Principle of LSC

LSC consist of a plate implanted or covered by luminescent dye molecules. Molecules absorb incident solar radiation from relatively large surface and generate luminescence in all directions. Due to higher refractive index of LSC material, total internal reflection can guide the emitted luminescence towards thin edge of the LSC where solar cell is placed, see schematics on Fig. 1. Although collecting concentrated light from smaller area leads to saving materials, the significant advantage of LSC relies in ability to concentrate diffuse sunlight in contrast to conventional solar concentrators (parabolic mirrors, Fresnel lenses) which can concentrate direct sunlight only.

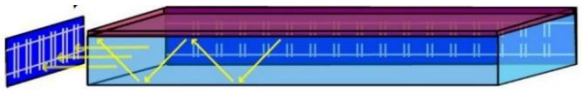

Fig. 1: Schematics of thin dye-layer LSC with solar cell at the edge

Losses in LSC – challenges for improvement

Historically, LSCs are known for low optical efficiencies due to significant losses [3], [2]. There are two critical places for losses – interface of LSC and solar cell, where any inaccuracy results in unwanted outcoupling of the light; losses through escape cone from the front surface, present all over the length of LSC. The latter is mostly a consequence of reabsorption losses which arises from the overlap of absorption and emission spectral bands, see Fig. 2.

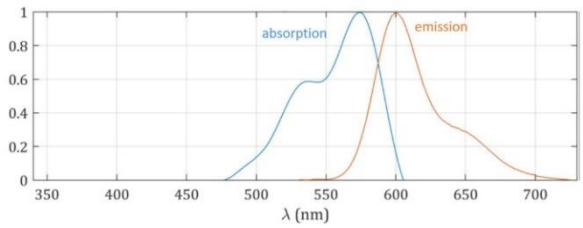

Fig. 2: Normalized absorption and emission spectra of a luminescent dye (BASF R305)

As a part of the LSC research topics, students can decide which of the efficiency issues they aim to tackle, depending on their individual skills. Interface between LSC and solar cell requires focus on coupling optimization by either designing antireflective coatings or index matching layers, as well as optimizing the size and contacting of attached cells and developing convenient opto-electo-mechanical setup for illumination and electrical characterisation of the whole LSC-cell system.

Optimizing reabsorption losses requires deeper understanding of theoretical principles of light conversion and propagating. Students can focus on simulating absorption/emission spectral bands and calculating reabsorption probability along the propagation direction, either with simplified analytical models [4], [5] or by ray-tracing simulations [6]. Moreover, operation of LSC with regards to reabsorption phenomena can act as a demonstrative system for fundamental thermodynamical principles of light conversion.

Reabsorption – linking with fundamentals

Losses of LSC due to escape cone emission are closely related to fundamental laws of thermodynamics. The process of continuous absorption, emission and reabsorption along the propagation of photons within the LSC leads to formation of equilibrium between photons and absorbing molecules. Photons then act as a photon gas and can be described by black body-like distribution with characteristic temperature T and chemical potential μ [7]. This can be directly observed by recording spectra emitted from the edge of LSC and fitting black body curve to the overlapping part of emission spectra with absorption band.

The assumption above leads to the possibility of looking at LSC operation (even without solar cell attached) as of a heat engine – it converts solar black body radiation at fixed temperature to "colder" black body radiation with finite chemical potential. Such an approach then leads to evaluation of limits of LSC operation, e.g., by relating chemical potential to maximum achievable open-circuit voltage [8]. Moreover, limitation of LSC on maximum concentration ratio can be evaluated by considering simple analyses of entropy fluxes related to incident and emitted light, see schematic in Fig. 3. The total entropy change ΔS (which must be non-zero according the second law of thermodynamics) can be expressed in terms:

$$\Delta S = -S_{INC} + S_{EM} + {}^{E_S}/_{T} \qquad (1)$$

where S_{INC} and S_{EM} are entropy fluxes of incident and emitted beam respectively and E_S is the Stokes shift, characteristic for used molecular dye. The term E_S/T is then representing heat loss to the reservoir, originating form thermalization processes within molecules. Assuming constant photon fluxes and describing spatial distribution of incident and emitted photons in terms of etendues $\mathcal{E}_{INC}$ and $\mathcal{E}_{EM}$ respectively, we can write equation (1) as:

$$k_B ln \frac{\mathcal{E}_{EM}}{\mathcal{E}_{INC}} + \frac{E_S}{T} \geq 0 \qquad (2)$$

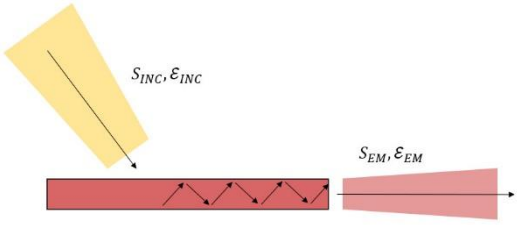

Fig. 3: Schematics of entropy flows in LSC

Equation (2) above can be used to evaluate maximum concentration ratio for two specific cases:

Diffuse incident light – etendues of incident and emitted light are equal (full hemisphere) and C_{MAX} is then given by

$$C_{MAX} = e^{{}^{E_S}/_{k_B T}} \qquad (3)$$

Direct incident light – analogous case to conventional geometrical concentration (where C_{MAX} is given by solid angle ratio), we obtain:

$$C_{MAX} = \frac{\pi}{\omega_S} e^{{}^{E_S}/_{k_B T}} \qquad (4)$$

ACKNOWLEDGEMENTS

Centre for Advanced Photovoltaics is supported by the Czech Ministry of Education, Youth and Sport. CZ.02.1.01/0.0/0.0/15_003/0000464.

REFERENCES

[1] M. G. Debije and P. P. C. Verbunt, "Thirty years of luminescent solar concentrator research: Solar energy for the built environment," *Advanced Energy Materials*, vol. 2, no. 1. pp. 12–35, Jan. 2012. doi: 10.1002/aenm.201100554.

[2] J. Roncali, "Luminescent Solar Collectors: Quo Vadis?," *Advanced Energy Materials*, vol. 10, no. 36. Wiley-VCH Verlag, Sep. 01, 2020. doi: 10.1002/aenm.202001907.

[3] W. G. J. H. M. van Sark *et al.*, "Luminescent Solar Concentrators – A review of recent results," vol. 16, no. 26, pp. 21773–21792, 2008.

[4] W. H. Weber and J. Lambe, "Luminescent greenhouse collector for solar radiation," 1976.

[5] J. S. Batchelder, A. H. Zewail, and T. Cole, "Luminescent solar concentrators. 2: Experimental and theoretical analysis of their possible efficiencies," 1981.

[6] B. Zhang *et al.*, "A luminescent solar concentrator ray tracing simulator with a graphical user interface: Features and applications," *Methods and Applications in Fluorescence*, vol. 8, no. 3, Jul. 2020, doi: 10.1088/2050-6120/ab993d.

[7] T. Markvart, "Detailed balance method for ideal single-stage fluorescent collectors," *Journal of Applied Physics*, vol. 99, no. 2, Jan. 2006, doi: 10.1063/1.2160710.

[8] B. Dzurňák, T. Feng, L. Danos, and T. Markvart, "Hot photons and open-circuit voltage in molecular absorbers," *Semiconductor Science and Technology*, vol. 34, no. 12, Oct. 2019, doi: 10.1088/1361-6641/ab419f.

Addresses of the authors

B. Dzurnak, Centre for Advanced Photovoltaics, Faculty of Electrical Engineering, Czech Technical University in Prague, Technická 2, 166 28, Prague, Czech Republic, branislav.dzurnak@fel.cvut.cz

T. Markvart, School of Engineering Sciences, University of Southampton, University Road, Southampton, SO17 1BJ, UK t.markvart@soton.ac.uk

Remote Laboratory Concept for Renewable Energy Education in South Africa

M.-O. Otto (1), B. Plesz (2), W. Commerell (1), C. Csapo (1), M. Tabacovic (3), Johan Raath (4), Nicolaas Luwes (4)

1 Ulm University of Applied Sciences, Prittwitzstraße 10, 89075 Ulm, Germany
2 Budapest University of Technology and Economics, 1117 Budapest, Magyar tudósok krt. 2, Hungary
3 University of Applied Sciences Technikum Wien, Giefinggasse 6, 1210 Wien
4 Central University of Technology, Free State, Bloemfontein 9300, South Africa

Abstract

The EURYDICE project, funded by the Erasmus + program, is focusing on renewable energies to support the energy system transition to a sustainable one in South Africa and to increase the employability of the graduates of Universities of Technology. The overarching goal of the project is the improvement of the renewable energy education at Universities of Technologies in South Africa with a special focus on photovoltaics. The project wants to achieve these goals by a closer collaboration between universities and industries and the establishment and implementation of remote and mobile labs. Three Universities of Technology in South Africa and three Higher Educational Institutions in Europe work on the project. This paper presents the first results.

Keywords: Laboratory, PV System, Remote Control, Remote Access

MOTIVATION

Technical engineering education at Higher Education Institutes (HEI) is focusing on theoretical education in the classroom and practical education in the laboratory (lab). Education in energy related subjects need especially a highly sophisticated lab infrastructure to demonstrate and visualize the transformation and distribution of energy.
Not every University can afford such an expensive infrastructure.
It can also be said that the movement to Industry 4.0 can be translated into a teaching 4.0 protocol, this could include remote labs that incorporate IOT etc.
For the students, a real world test shows the deviations between pure theoretical calculations and real world measurements better than simulations, because they get an impression on dimensions, sounds e.g. of motors and background information as necessary mechanical installation technologies.
Within the EURYDICE project, an infrastructure was developed where Universities can share their energy experiments due to mobile labs and due to remote accessible infrastructure. A remote lab will be installed and implemented at each of the three South African Universities. The paper will present the remote method and a lab for off-grid and micro-grid PV systems.

LABORATORY INFRASTRUCTURE

PV Micro-Grid System

The lab contains a micro-grid system, which is powered by a combination of solar, wind and battery power. Figure 1 shows the basic system layout with the following specifications: 5 kW stand-alone inverter; 1.3 kW Solar PV grid-tie inverter; 1.0 kW Wind turbine with grid-tie inverter; 1.8 kW Solar PV battery charging system; 24 V / 200 Ah GEL battery storage.
The shown infrastructure can be used in education to show different system configurations and the impact of each component to the overall system performance. The students can analyse, control the power flow within the system, and analyse different system configurations for different applications or locations etc.

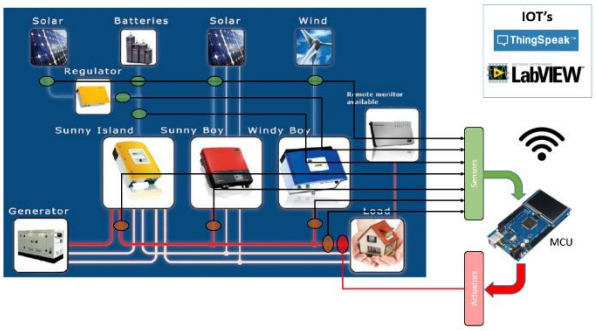

Figure 1: Infrastructure of the PV micro-grid system

PV Mobile Lab System

The mobile lab is a challenging prospect as all components will have to be installed in a cross-terrain trailer/unit. The trailer comes along with basic specifications. Integration between the existing trailer systems and proposed renewable power sources must be accomplished and IoT devices must be monitored and reported to the on-board PC with a LabView platform. Figure 2 illustrates the concept with the proposed system ratings.

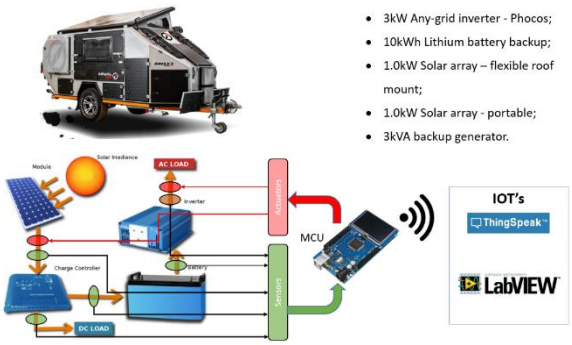

Figure 2: Infrastructure of the PV mobile lab system

REMOTE ACCCESS

Use Cases for a Remote Lab

The concept of a Remote Lab can be seen in Figure 3. The technical experiment equipment or test bed consists of its controller and Human-Machine Interface (HMI). A remote twin is made of the HMI that can control the test bed via the internet the same way as the on-site HMI, if control is handed over to the remote HMI twin.

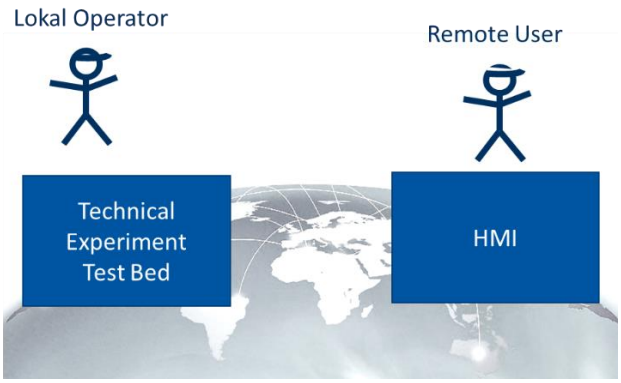

Figure 3: Remote Lab Operation

There are several Use Cases for the local operator of the remote lab, the technical expert for the test bed and on the remote side for the student or researcher using the infrastructure remotely.

Use cases for the operator or researcher at the university following use cases can be identified:

- Remote control of offsite long-term tests
- Remote control of field tests (same as industrial applications)
- Easy to supervise the experiment
- Keeping experiment in a safe operation with software and firmware limits.
- Large class of students can be handled
- Flexibility of controllable access rights that can include flexible access rights (read only, control)

Students use cases are:

- Lab exercise with fully remote control on HMI but a HMI remote twin
- Preparation of face-to-face Lab experiment on physical equipment
- Post processing of data
- Safety of remote-control twin such as that of dangerous experiments. (Remote twin for industrial applications such as remote control of wastewater pipes, disassembling of nuclear reactors, signal disruptor, underground machining)
- Distant education that could include case of high travel costs, illness or pandemics
- Automated report generation of experiment values via e-mail
- ^Exercises with flexible timeframe

Safety and Security Concept

Safety concept on-site. Accessing and especially controlling an energy system remotely is in general a safety critical topic. On-site experiments need either an intensive safety education and test for researchers and a safety responsible person, which is in general the lab

engineer, when students doing experiments on-site in the lab.

Safety concept remote. As a minimum, the same safety level should be achieved when using the infrastructure remotely. Therefore, safety requirements must be defined and implemented into the remote control. It must be ensured that the experiment only runs in a safe operation area. The operator should be able to switch on and off the experiment at any time. The access to the experiment must be in a legal way concerning the university security system.

Safety requirements for remote operation:

- The remote user must identify him or herself
- The remote system should be able to distribute and withdraw access rights between all remote user
- The remote access should not create an unsecure portal on the university access system
- The operator defines safety limits, within the remote user can control the system
- The remote user cannot exceed safety or test bed limits and hardware limits must be hardcoded in firmware.

Implementation

To match the listed requirements, a solution was implemented where centre accessed cloud data storage is used to exchange measured values from the test bed as well as the control values from the remote user. Figure 4 shows the implementation using Google sheets, for this solution and for data exchange based on the remote control of a motor – generator test bed as a starting point for the PV exercises.

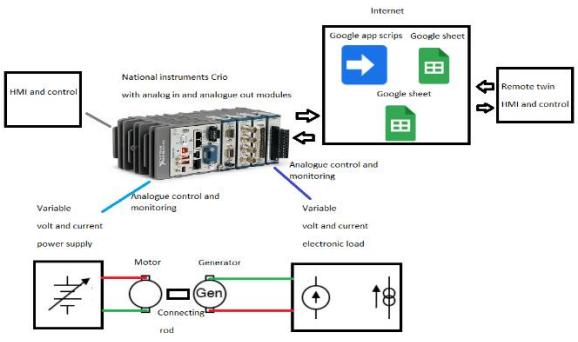

Figure 4: Remote Lab Implementation motor test bed

The motor-generator test bed consists of a controllable power source controlling the motor, and a controllable power load setting a load on the generator side. These devices are controlled via the cRIO with custom control firmware and the HMI.
Thus, this local automation hardware, consists of flexible analogue and digital IO systems with a built/in controller and measures the system states with sensors. The local HMI shows measured values and is able to set control signals to the system's hardware peripherals. In this case these are the controllable source and load.
The local automation hardware uses the local internet to get access to the Google sheet and writes values in the sheet's cells via URL GET commands and corresponding written and published google cloud scripts.
The URL with values updates a google sheet.
The remote user gets an executable file of the remote twin HMI with a similar cloud connection to the google sheet commands programmed in (via written and published) google cloud scripts. When the remote HMI executable is run on a remote system, the user is asked to identify him- or herself for access control and level to the hardware. After successful identification, the remote HMI reads cells from the Google sheet and shows the measured values of the real system in the lab. If the remote user wants to make changes control input settings to the real system in the lab, then the control inputs are set as it would on the onsite HMI. These are written into the cloud Google sheet, then read by the local automation hardware and subsequently controlling the onsite system. The delay time of the communication between the online control was measured as approx. 2 seconds, which is appropriate for many systems.
If the experiment needs faster reaction times one can add a feature in which a test set is send, then the local automation hardware can take measures at higher measuring rates and transmit the test results corresponding to the test set afterwards for remote analysis.

The micro-grid lab remote access is shown in Figure 5. The user gets information about the single values such as PV voltage or PV current. Based on the experimental level, the remote HMI can provide calculated information like PV power. The remote user can switch loads or additional auxiliary energy sources on and off, he can analyse recorded values and make calculations on e.g. state of charge of the battery, power losses within the system.

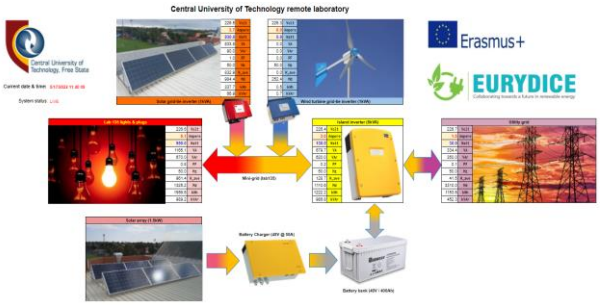

Figure 5: Remote Lab Implementation micro grid lab

CONCLUSION

The purpose of the paper is to show how a remote access to energy related labs can be established on a safe and easy way. The solution shows an easy and safe way to get

remote access to laboratory infrastructure at a different location. A first trial use was done to identify some minor problems.
In the beginning, the focus is on the observability. As a next step the project moves on to the controllability of the system. In systems with higher complexity, the operator has to think about all possible combinations the remote user can do and limit or exclude critical combinations.
The paper shows that remote laboratory infrastructure in PV energy systems is an alternative for onsite laboratory and can enable students and researcher to get access to infrastructures at other locations.

ACKNOWLEDGEMENTS

The EURYDICE project is funded by the Erasmus+ Programme of the European Union (Erasmus+ project 609689)

REFERENCES

[1] Tabakovic, Momir & Commerell, Walter & Otto, Marc-Oliver & Csapo, Csilla & Vermaak, Herman. (2021). Industry – University cooperation in the renewable energy field in south Africa- Gap analysis and enhancement proposals.
[2] Tabakovic, Momir & Otto, Marc-Oliver & Commerell, Walter & Csapo, Csilla & Vermaak, Herman. (2020). Increase in Cooperation Between Industry and Postgraduate Education via Open Labs and Mobile Labs in South Africa. 10.1007/978-981-15-5584-8_53.

Addresses of the authors

Marc-Oliver Otto, THU Technische Hochschule Ulm, Prittwitzstrasse 10, 89075 Ulm, Germany, Marc-Oliver.Otto@thu.de

Balazs Plesz, Budapest University of Technology and Economics, 1117 Budapest, Magyar tudósok krt. 2, Hungary

Walter Commerell, THU Technische Hochschule Ulm, Prittwitzstrasse 10, 89075 Ulm, Germany, Walter.Commerell@thu.de

Csilla Csapo, THU Technische Hochschule Ulm, Prittwitzstrasse 10, 89075 Ulm, Germany, Csilla Csapo@thu.de

Momir Tabakovic, University of Applied Sciences Technikum Wien, Giefinggasse 6, 1210 Wien, momir.tabakovic@technikum-wien.at

Johan Raath, Central University of Technology, Free State 20 Pres. Brand street, Private Bag X20539, Bloemfontein, 9300, South Africa, jraath@cut.ac.za

Nicolaas Luwes, Central University of Technology, Free State 20 Pres. Brand street, Private Bag X20539, Bloemfontein, 9300, South Africa, nluwes@cut.ac.za

DIALOG SESSION

Numerical Simulation Based Physical Parameter Analysis of Perovskite/c-Si Tandem PV Cells

Ahmad Halal[1], Ahmed Issa Alnahhal[1,2] and Balázs Plesz[1]
[1]Department of Electron Devices
Budapest University of Technology and Economics.
Budapest, Hungary

[2]Department of Biomedical Engineering
University of Palestine
Gaza Strip, Palestine

Abstract

In recent years, tandem solar cell technology (TSCs) has emerged as a great potential to overcome the efficiency limitations of single-junction solar cells by stacking two cells with different absorber materials with different bandgaps to absorb a broader wavelength range from the solar spectrum. Among different materials, Perovskite materials are considered as a promising candidate to be utilized in the top subcell of the tandem cell structure due to their tuneable bandgap, high absorption coefficient, and high carrier mobility. These advantages and the high flexibility of the upper perovskite cell (1.55-2 eV) make it compatible to be paired with the traditional c-Si (1.12 eV) as a tandem device. Optimally tailored matching between the two sub-cells of the tandem device will allow achieving high-performance TSCs. Thus, in this work, 2-terminal monolithic tandem cell-based on $CH_3NH_3PbI_3$ perovskite and c-Si is simulated using SCAPS-1D software. We investigated the thickness adjustment and doping concentration effect of the perovskite active layer with a particular focus on the effect of using different silicon wafer types (n- and p-type). The results showed a significant enhancement on tandem PV cell performance when we raise the doping concentration of the perovskite layer. It was found that a tandem cell constructed with a p-type silicon bottom cell exhibits higher PCE compared to that one constructed from n-type silicon. Overall, under a maximum total defect density of (10^{14} cm^{-3}), the configuration tandem cell of perovskite on Si-based p-type perovskite top cell with n-type bottom absorber layer cell demonstrated a J_{SC} of 17.63 mA/cm^2, V_{OC} of 1.861 V, FF of 73.57%, and a PCE of 24.13% under an optimum top layer thickness of 90.5 nm. While in the case of the p-Si bottom cell, the obtained efficiency is 28.31% with V_{OC} of 1.997 V, J_{SC} of 18.9 mA/cm^2, and FF of 75% under top layer thickness of around 100.7 nm.

Keywords: Tandem Solar cells, Perovskite, Crystalline Silicon, Perovskites Doping, Homojunction.

INTRODUCTION

Energy generation is essential for global expansion and is unquestionably the primary engine of economic development in the developing nations. Therefore, the increasing demand for energy consumption represents one of the most interesting challenges in the upcoming years. The necessity for alternative energy sources and the exploration of renewable energy sources has arisen in the last few decades with the decline in the use of traditional fossil fuel resources due to environmental issues and climate change problems. Among different renewable energy sources, solar cells continue to be one of the significant sources of energy in this respect [1]. Numerous PV systems have been developed to convert solar energy to electrical energy. Photovoltaic devices made of crystalline Si cover nearly 90% of the PV market with a record efficiency of 26.7% [2], the technology comes close to its theoretical maximum efficiency of 29.8% [3]. All other single junction cells (GaAs, perovskite, CIGS, etc.) are also subject to this limitation which means that there is only a little space for further development in the efficiency of single-junction solar cells. Therefore, the single junction devices are not sufficient for producing a high output power due to the fact that only a fraction of the solar energy can be converted by the cell due to high absorption loss and thermalization loss [4].

In recent years, multi-junction or tandem structures technology has emerged with a great potential to overcome this challenge and avail high efficiency that exceeds the Shockley-Queisser limit of single-junction solar cells by combining multiple absorption layers with materials having different bandgap energies. The upper sub-cell layer consists of a material with a wide bandgap constructed over a narrow bandgap material lower cell.

This configuration allows for absorbing a wide range of the solar spectrum, and it is capable of reducing the below band gap loss in addition to diminishing the thermalization loss. Bremner predicted that the conversion efficiency of multigap systems could be greater than 40% [5]. However, although tandem structures are more efficient, manufacturing costs and complexity make them more expensive. Therefore, creating a cost-effective tandem becomes an interesting goal for researchers [6].

Targeting commercial applications, tandem cells based on c-Si bottom cells have been proposed and developed on a low-cost Si substrate [7] for the purpose of producing high-efficiency and low-cost PV modules. However, a major drawback of this technique has been the lack of materials with a high open-circuit voltage (V_{OC}) that are within the requisite bandgap range of 1.55 to 1.9 eV for use in the upper cell of the tandem configuration [8]. The development of methyl-ammonium-lead-halide perovskite over the past years has considerably influenced this issue and opened the path to utilize it as the top cell in Si-based tandem cells, thanks to its features such as high absorption coefficient, high charge carrier mobilities and diffusion lengths. This material exhibits not only a significant efficiency and high open-circuit voltages (V_{OC}) but also low processing cost. Furthermore, perovskite materials have a bandgap of 1.5-2 eV, allowing them to be a good absorbent material in the ultraviolet and visible light ranges and completely transparent in the infrared region. This bandgap can be precisely tuned to greater values by adding Br or Cl, making them able to reach 1.75 eV, which is considered the optimum bandgap for use in the top cell designing of highly efficient crystalline silicon (c-Si)-based tandem solar cells [9].

Perovskite/crystalline silicon tandem cells can be implemented in different architectures according to their fabrication methods and electrical connection [9]. They can either be designed as an electrically separated cell and coupled by optical filters called 4-terminal or can be as a monolithic device called 2-terminal configuration. The monolithic structure or two-terminal configuration contains fewer functional layers resulting in the potential low processing steps and low electrical and optical losses. In this design, perovskite/crystalline silicon tandem cells are considered to be a single unit in which both the top and bottom sub-cells are electrically connected in series through a recombination layer and the total V_{OC} of the tandem is the summation of the two cell voltages. One limitation of this design is the current mismatch between the two sub-cells which will cause charge carrier accumulation at the recombination contact and affect the tandem device functionality. So, it is important to ensure current matching between the upper and lower tandem sub-cells when we are dealing with this tandem design.

Although the PCE of 2-terminal perovskite on c-Si tandem cells can exceed 30% [10], the highest current record is around 29.15% [11]. Therefore, a successful commercial entry is likely to require even greater values of PCE to compete with existing non-perovskite tandem technologies. Many prime parameters have an impact on the PCE improvement of 2-terminal perovskite on c-Si tandem cells and need to be investigated. One of the main parameters in this structure is the requirement of strict current matching between the two sub-cells to reach an optimal tandem efficiency. Other characteristics parameters such as the absorber layer thickness, defect density, and doping concentration need to be examined to understand the influence of these parameters on the performance of 2-terminal perovskite/c-Si tandem cells. Inspecting these parameters experimentally will require enormous resources in terms of time and material consumption. As a result, an appropriate simulation technique is required to assist optimization activities in a faster and more cost-effective manner.

The main goal of this study is to analyse and improve a 2-terminal configuration $MAPbI_3$-on-c-Si tandem devices through numerical simulation studies using the SCAPS-1D simulation tool to better understand the effect of varying different physics parameters characteristics on the performance of the perovskite/c-Si tandem device. Furthermore, our approach for this investigation involves addressing the following points:

- Establishment of the perovskite/c-Si tandem model.
- Validating the simulated results with data published for experimentally fabricated perovskite/c-Si of the same structure.
- Effect of the absorber layers defect density on tandem device performance.
- Effect of absorber layers doping concentration.
- Optimization of absorber layers thickness.
- Investigating the performance of tandem solar cells by inverting the upper cell structure and using opposite dopant type silicon wafer types.

The anticipated outcomes of this study will provide a valuable design guideline for high-performance, low-cost monolithic perovskite/c-Si tandem PVs.

METHODOLOGY

Solar cell devices could be simulated using any numerical software that can solve the basic semiconductor equations. Among different simulation software, SCAPS software has the ability to analyse heterojunction and multijunction solar configuration by varying up to 7 layers. Furthermore, the simulation results are in good agreement with experimental results. This one-dimensional simulation software was established and developed by ELIS, University of Gent, Belgium [12]. It is utilized in this work to numerically

predict the most suitable electronic, electrical and optical properties of the perovskite/c-Si tandem device.

Three basic semiconductor equations, namely, Poisson's (1), electron continuity equation (2), and hole continuity equation (3), are utilized by SCAPS software to compute several electrical and optical properties of the solar cell, such as energy bands, J-V characteristics curve, and spectral response (QE) curve. These curves are used to obtain V_{OC}, J_{SC}, fill factor and the conversion efficiency of the simulated device.

$$\frac{d}{dx}\left(-\epsilon(x)\frac{d\psi}{dx}\right) = q[p(x) - n(x) + N_D^+(x) - N_A^-(x) + p_t(x) - n_t(x)] \quad (1)$$

$$\frac{dp_n}{dt} = G_p - \frac{p_n - p_{n0}}{\tau_p} + p_n\mu_p\frac{d\zeta}{dx} + \mu_p\zeta\frac{dp_n}{dx} + D_p\frac{d^2p_n}{dx^2} \quad (2)$$

$$\frac{dn_p}{dt} = G_n - \frac{n_p - n_{p0}}{\tau_n} + n_p\mu_n\frac{d\zeta}{dx} + \mu_n\zeta\frac{dn_p}{dx} + D_n\frac{d^2n_p}{dx^2} \quad (3)$$

Where ϵ is the permittivity, ψ is the electrostatic potential, N_A^- and N_D^+ are the shallow acceptor and donor concentrations, q is the electron charge, $n_t(x)$ and $p_t(x)$ indicates the concentrations of trapped electrons and holes, G_p and G_n are the generation rate of holes and electrons, ζ is the electric field, μ_p and μ_n indicates the hole and electron mobilities, τ_p and τ_n are the lifetime of holes and electrons, D_p and D_n are the diffusion coefficients for hole and electron, respectively.

The following formula is used to determine the fill factor (FF) of the device:

$$FF = \frac{J_{MP}V_{MP}}{J_{SC}V_{OC}} \quad (4)$$

Here, V_{MP} and J_{MP} are the voltage and current density at the maximum power points. The tandem cell efficiency (η), normalized to input power (P_{in}), is defined as:

$$\eta = \frac{V_{OC}\,J_{SC}\,FF}{P_{in}} \quad (5)$$

The two sub-cells can be described as two diodes connected in series for the 2-terminal monolithic tandem cell. Therefore, the open-circuit voltage (V_{OC}) is the summation of both upper and lower cell voltages, while the short-circuit current density J_{SC} is determined by the minimum current supplied by the two sub-cells.

DEVICE STRUCTURE AND SIMULATION PARAMETERS

We have simulated a monolithic 2-terminal tandem structure according to the experimental design proposed in literature [13]. A conventional p-i-n configuration is used as a top cell. The top cell layers are Spiro-OMeTAD/Perovskite/TiO_2. Here, an intrinsic $MAPbI_3$ is used as a large bandgap absorbent layer of the upper cell sandwiched between p-type Spiro-OMeTAD acting as the hole transport layer (HTL) and n-type TiO_2 as the electron transport layer (ETL). Whereas the bottom cell layers consist of an n-type Si, which represents the lower bandgap absorbent layer, with p^{++} Si as an emitter layer and n^{++} Si as the back surface field layer. These two sub-cells are connected in series through a recombination junction. Fig. 1 illustrates the modelled tandem cell configuration designed in this work.

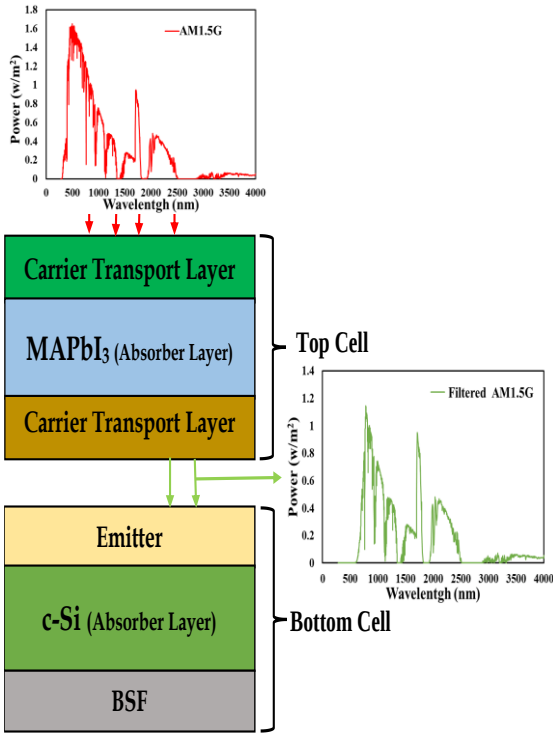

Fig.1. Tandem Cell Device Structure.

Photovoltaic device performance is highly dependent on the parameters such as layers thickness, charge carrier concentration, temperature, shunt and series resistances, and so on. The proposed tandem device is simulated under standard illumination condition of AM 1.5 G and a working temperature of 300 K. The basic physic parameters such as (materials bandgap, electron affinity, Dielectric constant, etc.) that are used for performing this simulation are adopted from the following published literature [14], [15], [16] as it is shown in Table 1. Other parameters such as doping concentration, layers thickness, etc. are adjusted to fit the performance of the simulated device to an experimentally fabricated one of the same structures [13].

It is worth mentioning that SCAPS does not fully support the simulation of multijunction solar cells since the optical coupling of the upper and lower cell is not considered. Therefore, to numerically analyze the tandem device using SCAPS-1D, a filtered spectrum has to be calculated in which the top sub-cell is exposed to the standard solar spectrum while the bottom cell will receive the transmitted spectrum from each layer of the top cell layers. This filtered spectrum is given by:

Parameters	Materials					
	Spiro-OMeTAD	***MAPbI₃***	***TiO₂***	***p⁺Si***	***nSi***	***n⁺Si***
Thickness (µm)	0.030	Variable	0.030	0.1	200	1
Dielectric constant	3	30	9	11.9	11.9	11.9
Electron affinity (eV)	2.45	3.9	4.26	4.05	4.05	4.05
Band gap (eV)	3	1.55	3.2	1.12	1.12	1.12
Effective conduction band density (cm^{-3})	2.2×10^{19}	1×10^{14}	3×10^{13}	2.819×10^{19}	2.819×10^{19}	2.819×10^{19}
Effective valence band density (cm^{-3})	1.8×10^{19}	1.8×10^{20}	1.8×10^{19}	1.04×10^{19}	1.04×10^{19}	1.04×10^{19}
Effective electron (hole) mobility (cm^2/Vs) Mn/Mp	$2\times10^{-4}/2\times10^{-4}$	50/50	20/10	1400/450	1400/450	1400/450
Doping concentration acceptors (cm^{-3})	2×10^{18}	0	0	1×10^{18}	0	0
Doping concentration donators (cm^{-3})	0	0	1×10^{16}	0	Variable	1×10^{18}
Electron thermal velocity (cm/s)	1×10^{7}	1×10^{7}	1×10^{7}	1×10^{7}	1×10^{7}	1×10^{7}
Hole thermal velocity (cm/s)	1×10^{7}	1×10^{7}	1×10^{7}	1×10^{7}	1×10^{7}	1×10^{7}
Bulk defect type	Neutral	Neutral	Neutral	Neutral	Neutral	Neutral
Bulk defect (cm^{-3})	Variable	Variable	Variable	Variable	Variable	Variable
Capture cross section electrons (cm^{-2})	1×10^{-15}	1×10^{-15}	1×10^{-15}	1×10^{-15}	1×10^{-15}	1×10^{-15}
Capture cross section holes (cm^{-2})	1×10^{-15}	1×10^{-15}	1×10^{-15}	1×10^{-15}	1×10^{-15}	1×10^{-15}

Table 1: Input parameters for SCAPS-1D simulation software [14], [15], [16].

$$S(\lambda) = S_0(\lambda).exp\left(\sum_{i=1}^{3} -\left(\alpha_{material_i}(\lambda).d_{material_i}\right)\right) \quad (6)$$

Where $S(\lambda)$ is the transmitted light from the upper cell, $S_0(\lambda)$ is the standard incident spectrum (AM 1.5G) on the upper cell, α is the absorption coefficient, and d represents the thickness of the respective layer. The reflection losses from each interface are ignored. We have assumed a Gaussian defect energy level of 0.6 eV below the conduction band with a characteristic energy of 0.1 eV for both of the two sub-cells [14,16]. The extracted value of shunt resistance in this work is infinity, while the series resistance is set to be 7.5 Ω.cm^2. These values gave the best fitted J-V curve to the experimental one.

RESULTS AND DISCUSSIONS

Validation of existing perovskite/c-Si tandem solar cell

The base tandem solar cell model "Spiro-OMeTAD/ Perovskite/ TiO_2/ p^{++}-Si/ n^+-Si/ n^{++}-Si" was simulated in SCAPS-1D to be validated on an existing perovskite/c-Si tandem device from literature. Fig. 2 shows the J-V curve comparison of the tandem cell structure simulated in SCAPS-1D in comparison with the experimental one adopted from the literature [13]. The simulation results of the designed tandem model reveal a J_{SC} of 11.58 mA/cm^2 and V_{OC} of 1.57 V with an FF and efficiency values of 74% and 13.5%, respectively. These simulation results fit well to the reported work, indicating the built model is suitable for describing the given solar cell structure.

The short-circuit current density J_{SC} of perovskite and c-Si sub-cells are 11.55 mA/cm^2 and 14.7 mA/cm^2, respectively. These J_{SC} values of the two sub-cells also match the reported work in the literature. However, it is clearly noticeable from these results that this reported structure is suffering losses due to the unbalanced current matching between the two sub-cells, and the total short-circuit current density of the tandem cell is limited by the perovskite top cell current. The small short-circuit current density J_{SC} of the perovskite sub-cell is due to the thinner layer that had been used in the tandem structure, while in the case of c-Si, a high level of defect density leads to the limitation of the J_{SC} of this bottom cell. The effects of these parameters on the reported work and the optimization steps for the present work will be discussed in detail in the following sections.

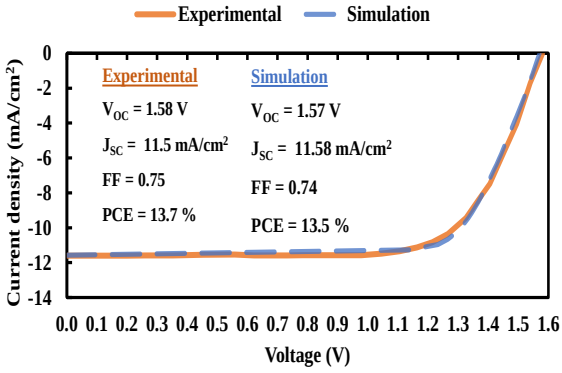

Fig.2. Published experimental curves [13] and simulated J-V curves of the perovskite on Si-based tandem PV cell.

Defect density effect on the tandem solar cell performance.

The performance of solar cells is significantly influenced by the quality of the absorber layers. A high level of defect density in the different absorber layers of tandem configuration will lead to a high recombination rate which in turn will exterminate the charge carriers and degrade device performance. Thus, the defect density value was varied, and the J-V characteristics were determined. The results are shown in Fig. 3.

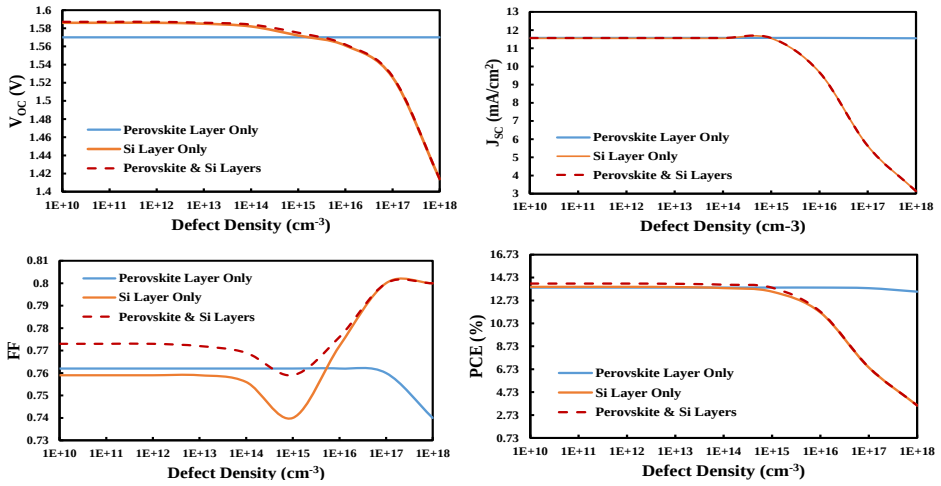

Fig.3. Electrical performance characteristics of perovskite/c-Si tandem cell under the effect of different defect density.

It can be seen clearly in Fig. 3. that this tandem PV device is susceptible to the defects in the Si absorber layer while increasing the defect density in the perovskite absorber layer even to a higher level will not have a significant effect on the performance of the tandem device. This is mainly due to the thicker Si layer used in the bottom cell compared to the thinner perovskite layer of the tandem design. Therefore, to achieve high efficiency of the perovskite/c-Si tandem solar cell, it is essential to fabricate a high-quality crystalline silicon PV cell which will be utilized in the bottom cell of the tandem design. For the optimization process in this paper, the defect density was kept as low as possible and values of 1×10^{14} cm^{-3} and 1×10^{13} cm^{-3} were chosen for the rest of the work as the defect density in the absorbent layers of $MAPbI_3$ and c-Si, respectively.

Doping concentration effect on the tandem solar cell performance.

The doping density in the absorber layer has a prominent influence on PV solar cell performance.

According to the experimental reported work, an n-type Si wafer is used as the base layer of the tandem bottom cell. Therefore, we varied the donor concentration of this layer from 10^{15} to 10^{21} cm^{-3} to examine the effect of increasing the doping concentration on the tandem PV cell's overall performance. In addition to that, we investigated the influence of doping the intrinsic layer of the perovskite absorber layer by increasing the acceptor concentration up to 10^{21} cm^{-3} to form a p-type $MAPbI_3$. Thus, in the upcoming optimization steps, we are going to use a p-p-n configuration in the top sub-cell of the tandem device instead of p-i-n, which was used in the reported work. The term structure A will be used to describe this configuration of the tandem device. However, p-type $MAPbI_3$ was formed in this work instead of n-type $MAPbI_3$ because n-type $MAPbI_3$ is more difficult to realize due to the formation of neutral defects or compensation from intrinsic point defects [17].

According to Fig. 4, raising the doping concentration of the perovskite layer has a significant influence on tandem

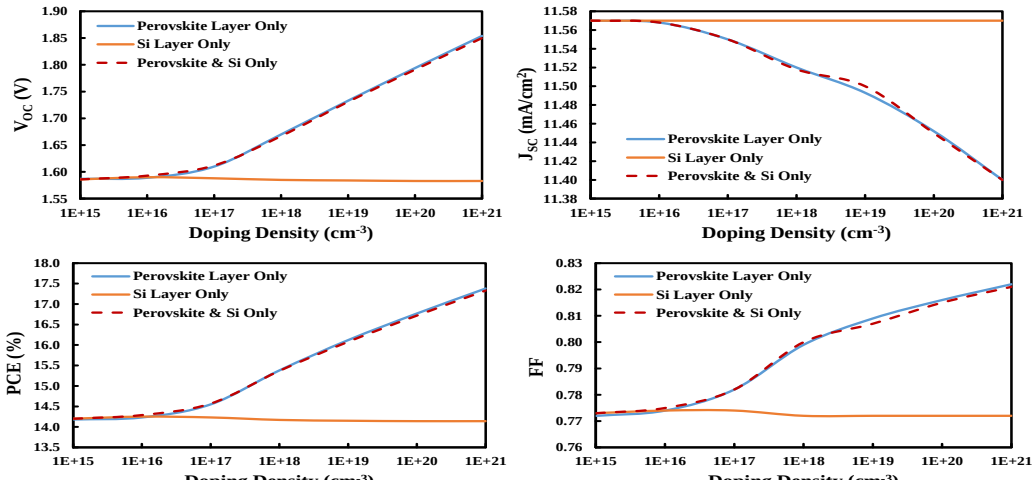

Fig.4. Electrical performance characteristics of perovskite/c-Si tandem cell under the effect of different doping concentration.

PV cell performance enhancement, but excessive doping of the Si layer has a negative impact on tandem device performance. Although there was a slight decrease in short-circuit current, the tandem device efficiency increased dramatically as the perovskite layer doping concentration was increased. This was due to the increase in open-circuit voltage that occurred due to the increase in perovskite layer doping concentration. However, PCE is maximized at $N_A = 1\times10^{21}$ cm^{-3} and $N_d = 1\times10^{17}$ cm^{-3} for $MAPbI_3$ and c-Si, respectively. Therefore, these doping values will be used in the rest of the work in this paper.

Optimization of the thickness of the tandem sub-cells

In 2-terminal monolithic tandem configurations, Adjusting the current between the two sub-cells is extremely important because the current mismatch will cause charge carriers to accumulate at the recombination contact, which affects the recombination behaviour negatively. As previously stated, the fabricated structure referenced from literature lacks a well-balanced current matching between the two sub-cells and thus the total short-circuit current density of the tandem cell is restricted by the perovskite top cell's current. In the previous sections the defect density and doping concentration have been optimized. As a next step the thickness of the absorber layers will be optimized to accomplish a good current matching between the two sub-cells. This is done by increasing the thickness of the simulated perovskite layer to match the same J_{MPP} or J_{SC} values for both sub-cells. To reach the best current matching condition, the top cell thickness is varied from 75 nm to 95 nm. However, the best matching between the two sub-cells short circuit-currents J_{SC} is achieved with 90.5 nm top cell thickness, where the top and bottom cells produce J_{SC} of 17.63 mA/cm^2 and 17.63 mA/cm^2, respectively, as illustrated in Fig. 5.

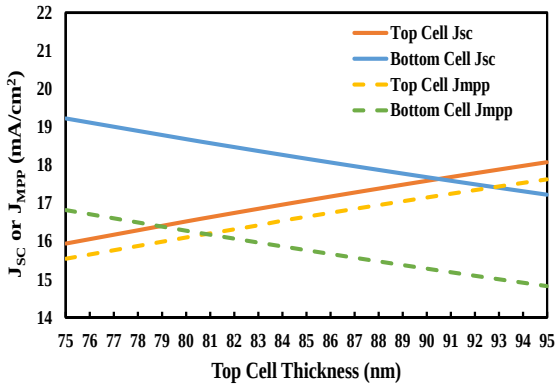

Fig.5. J_{SC} and J_{MPP} comparisons between the top and bottom sub-cells of structure A.

At this match current point and due to the previous optimization processes of defect density and doping concentration, the perovskite/c-Si solar cell efficiency is reached 24.13% from comprising 18.95% perovskite of p-n-n configuration as a top cell and 9.24% c-Si of p-n structure as a bottom cell. The optimized perovskite/c-Si PV device exhibited a fill factor of 73.57%, with J_{SC} and V_{OC} of 17.63 mA/cm^2 and 1.861 V, respectively. The J-V curve is illustrated in Fig. 6.

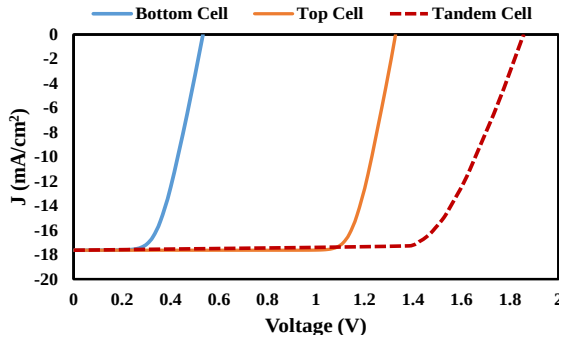

Fig.6. J-V curves of the optimized Structure A.

The effect of the c-Si doping type in the bottom cell of the tandem structure.

We investigated the effect of the doping type of the c-Si bottom cell's base layer on the tandem solar cell performance. We replaced the bottom cell layers of the reported work by considering a p-type c-Si as the base layer together with n^{++} Si as an emitter layer and p^{++} Si as the back surface field layer. The layer stacking order of the perovskite top cell is adjusted to a n-p-p configuration of TiO_2/p-type-perovskite/Spiro-OMeTAD. The term structure B will be used to describe this modified configuration of the tandem device. The optimization steps for defect density and doping density are applied again to the modified structure of the perovskite on the c-Si tandem device. It is found that PCE is maximized at the same previous values of doping concentration and defect density that have been used previously to optimize the reported work. The current matching condition between the two sub-cells is achieved by varying the absorber layer thickness of the perovskite top cell from 90 to105 nm to match the same J_{MPP} or J_{SC} values for both sub-cells. However, the matching point between the two sub-cells short-circuit current J_{SC} is acquired with 100.7 nm of the perovskite absorber layer thickness, where the top and bottom sub-cells produce J_{SC} of 18.9 mA/cm^2 and 18.9 mA/cm^2, respectively as shown in Fig. 7.

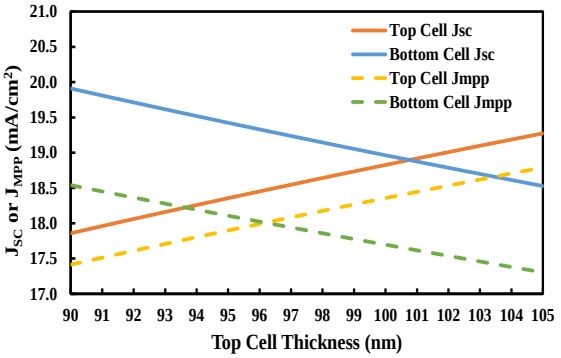

Fig.7. J_{SC} and J_{MPP} comparisons between the top and bottom sub-cells of structure B.

Using an absorber layer of p-type c-Si instead of n-type c-Si led to a significant enhancement in the performance of the tandem device. This modified structure (structure B) exhibits an efficiency of 28.31% compared to the 24.13% of the previous optimized design (structure A) and the 13.7 % of the reported experimental work. The J-V characteristics of the perovskite/c-Si tandem cell are illustrated in Fig. 8. The high output results of this structure can be attributed to the fact that in the p-type c-Si absorber layer, the minority charge carriers are the electrons which have a higher diffusion length and a higher probability of reaching the junction without recombining and hence getting separated than holes. Therefore, it is essential to construct the base layer of the bottom cell of the perovskite/c-Si tandem cell with a p-type semiconductor because it has electrons as minority charge carriers.

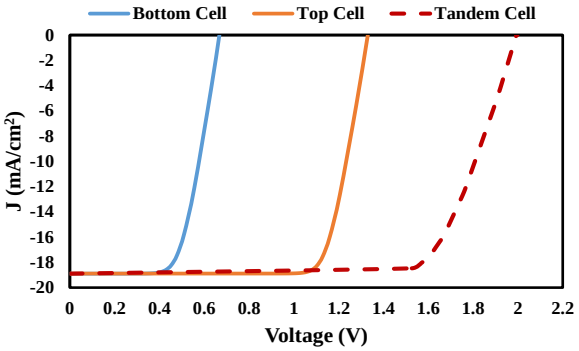

Fig.8. J-V curves of the optimized Structure B.

The electrical performance characteristics of the reported work and the two optimized structures are summarized in Table 2.

Structures / Parameters	Reported Work [13]			Optimized Structure A			Optimized Structure B		
	Top Cell	*Bottom Cell*	*Tandem Cell*	*Top Cell*	*Bottom Cell*	*Tandem Cell*	*Top Cell*	*Bottom Cell*	*Tandem Cell*
J_{SC} (mA/cm^2)	11.5	14.7	11.5	17.63	17.63	17.63	18.9	18.9	18.9
V_{OC} (V)	-	-	1.58	1.328	0.533	1.861	1.33	0.667	1.997
V_{MPP} (V)	-	-	-	1.102	0.358	1.426	1.095	0.472	1.568
J_{MPP} (mA/cm^2)	-	-	-	17.196	15.232	16.92	18.417	17.639	18.055
FF (%)	-	-	75	80.91	58	73.57	80.24	66.12	75
PCE (%)	-	-	13.7	18.95	9.24	24.13	20.16	14.62	28.31

Table 2: Electrical characteristics of the reported work and the two optimized perovskite/c-Si tandem structures.

CONCLUSION

A numerical simulation for perovskite/c-Si monolithic tandem solar cells was performed using SCAPS-1D. After validating our model with experimental results from the literature, our achieved results have enabled us to select the best parameters, such as optimal doping concentration, defect density, and thickness of the perovskite top cell that leading to the highest possible efficiencies. We found that perovskite silicon-based tandem solar cell performance is less sensitive to the defect density of the perovskite absorber layer than the defect density of the c-Si base layer. In addition, utilizing highly doped p-type $MAPbI_3$ instead of the intrinsic perovskite could have a significant effect on the enhancement of the tandem cell output results. At the same time, it is essential to use a moderate doping concentration in the base layer of the c-Si bottom cell. This structure demonstrated an efficiency of 24.13% with a J_{SC} of 17.63 mA/cm^2, V_{OC} of 1.861 V, and FF of 73.57%, under an optimum top absorber layer thickness of 90.5 nm. Moreover, we found that using p-type c-Si instead of n-type c-Si as the base layer of the bottom cell could increase device efficiency further, enabling a PCE of 28.31% with FF of 75% and 18.9 mA/cm^2 and 1.997 V of short-circuit current and open-circuit voltage, respectively, under top layer thickness of around 100.7 nm.

Overall, the presented results in this study demonstrate a beneficial guideline for designing an optimal perovskite on Si tandem solar cells, which can open the path toward the development of high-efficiency and low-cost tandem solar cells in the future.

ACKNOWLEDGEMENTS

The research reported in this paper and carried out at Budapest University of Technology and Economics was partially supported by the Stipendium Hungaricum Scholarship Program of the Hungarian Government and the project number 2020-1.1.2-PIACI-KFI-2021-00242 of the National Research, Development and Innovation Office (NKFIH).

REFERENCES

[1] Kannan, N. and Vakeesan, D.: Solar energy for future world:-A review, Renewable and Sustainable Energy Reviews **62**, 2016, 1092-1105.

[2] Yoshikawa, K., Kawasaki, H., Yoshida, W., Irie, T., Konishi, K., Nakano, K., Uto, T., Adachi, D., Kanematsu, M., Uzu, H. and Yamamoto, K.: Silicon heterojunction solar cell with interdigitated back contacts for a photoconversion efficiency over 26%, Nature energy, **2(5)**, 2017, 1-8.

[3] Swanson, R.M., et al: Approaching the 29% limit efficiency of silicon solar cells, In Conference Record of the Thirty-first IEEE Photovoltaic Specialists Conference (Lake Buena Vista, 2005), 889–894.
[4] Shockley, W. and Queisser, H.J.: Detailed balance limit of efficiency of p-n junction solar cells, Journal of applied physics, **32(3)**, 1961, 510–519.
[5] Bremner, S.P., Levy, M.Y. and Honsberg, C.B.: Analysis of tandem solar cell efficiencies under AM1. 5G spectrum using a rapid flux calculation method, Progress in photovoltaics: Research and Applications, **16(3)**, 2008, 225-233.
[6] Choi, W., Kim, C.Z., Kim, C.S., Heo, W., Joo, T., Ryu, S.Y., Kim, H., Kim, H., Kang, H.K. and Jo, S.: A repeatable epitaxial lift-off process from a single GaAs substrate for low-cost and high-efficiency III-V solar cells, Advanced Energy Materials, **4(16)**, 2014, 1400589.
[7] Mailoa, J.P., Bailie, C.D., Johlin, E.C., Hoke, E.T., Akey, A.J., Nguyen, W.H., McGehee, M.D. and Buonassisi, T.: A 2-terminal perovskite/silicon multijunction solar cell enabled by a silicon tunnel junction, Applied Physics Letters, **106(12)**, 2015, 121105.
[8] Meillaud, F., Shah, A., Droz, C., Vallat-Sauvain, E. and Miazza, C.: Efficiency limits for single-junction and tandem solar cells, Solar energy materials and solar cells, **90(18-19)**, 2006, 2952-2959.
[9] Werner, J., Niesen, B. and Ballif, C.: Marriage of convenience or true love story?–An overview, Advanced Materials Interfaces, **5(1)**, 2018, 1700731.
[10] Filipič, M., Löper, P., Niesen, B., De Wolf, S., Krč, J., Ballif, C. and Topič, M.: CH 3 NH 3 PbI 3 perovskite/silicon tandem solar cells: characterization based optical simulations, Optics express, **23(7)**, 2015, A263-A278.
[11] Al-Ashouri, A., Köhnen, E., Li, B., Magomedov, A., Hempel, H., Caprioglio, P., Márquez, J.A., Morales Vilches, A.B., Kasparavicius, E., Smith, J.A. and Phung, N.: Monolithic perovskite/silicon tandem solar cell with> 29% efficiency by enhanced hole extraction. Science, **370(6522)**, 2020, 1300-1309.
[12] M. Burgelman, K. Decock, A. Niemegeers, J. Verschraegen, and S. Degrave: *Scaps manual*, 2016.
[13] Mailoa, J.P., Bailie, C.D., Johlin, E.C., Hoke, E.T., Akey, A.J., Nguyen, W.H., McGehee, M.D. and Buonassisi, T.: A 2-terminal perovskite/silicon multijunction solar cell enabled by a silicon tunnel junction, Applied Physics Letters, **106(12)**, 2015, 121105.
[14] Minemoto, T. and Murata, M.: Theoretical analysis on effect of band offsets in perovskite solar cells, Solar Energy Materials and Solar Cells, **133**, 2015, 8-14.
[15] Löper, P., Stuckelberger, M., Niesen, B., Werner, J., Filipic, M., Moon, S.J., Yum, J.H., Topič, M., De Wolf, S. and Ballif, C.: Complex refractive index spectra of CH3NH3PbI3 perovskite thin films determined by spectroscopic ellipsometry and spectrophotometry, The journal of physical chemistry letters, **6(1)**, 2015, 66-71.
[16] Kim, K., Gwak, J., Ahn, S.K., Eo, Y.J., Park, J.H., Cho, J.S., Kang, M.G., Song, H.E. and Yun, J.H.: Simulations of chalcopyrite/c-Si tandem cells using SCAPS-1D, Solar Energy, **145**, 2017, 52-58.
[17] Shi, T., Yin, W.J. and Yan, Y.: Predictions for p-type CH3NH3PbI3 perovskites, The Journal of Physical Chemistry C, **118(44)**, 2014, 25350-25354.

Addresses of the authors

Ahmad Halal, 1117 Budapest, Magyar tudósok krt. 2, Budapest, Hungary, ahmadhalalftesah@edu.bme.hu
Ahmed Issa Alnahhal, 1117 Budapest, Magyar tudósok krt. 2, Budapest, Hungary, aalnahhal@edu.bme.hu
Balázs Plesz, 1117 Budapest, Magyar tudósok krt. 2, Budapest, Hungary, plesz.balazs@vik.bme.hu

Heat Pump - PV - Battery Application

E. Harzfeld
Department of Electrical Engineering and Computer Science
Stralsund University of Applied Sciences
Stralsund, Germany

Abstract

The transition of the energy supply from fossil fuels to renewable energies also includes changes in the area of heat supply. Typical boiler systems based on natural gas or heating oil can or must be replaced by heat pumps in the long term. In addition, the electricity demand of the heat pump must be obtained from renewable sources. The presented analyses contain a solution approach for determining optimal Heat Pump - PV Unit - Battery System parameters.

Keywords: Heat Pump, PV Unit and Battery

SUMMARY

The adaptation of a PV System with battery storage to a heat pump system involves some uncertainties with regard to the optimal design. One reason for the existing inconsistencies results from the fact that both consumption and energy feed-in are subject to random or fluctuating processes. The adaptation procedure presented here therefore assumes a balance and uses this to determine the required optimal PV Unit – Battery System. The PV energy that cannot be used by the heat pump is stored in a battery system and used to extend the operating time of the heat pump.

1. INTRODUCTION

Assuming that a demand profile is available as a reference (see Figure 1a) and a feed-in profile of a PV system (see Figure 1b) is available at the same location, both profiles can be directly compared in a first step (see Figure 1c). Furthermore, the surplus and deficit capacities (see Figure 1d) can be determined. For the comparison of the profiles, the data were transformed into a per unit range and transformed back to a reference value of 5kW_el nominal power.

The comparison of heat pump demand and PV feed-in power shows clear differences, with considerable PV feed-in surpluses in summer.

For the power supply of the heat pump, it is now interesting whether and with which installation power a PV system with battery storage can be designed.

1a)

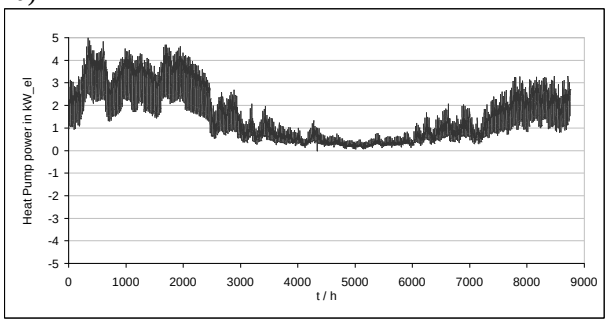

1b)

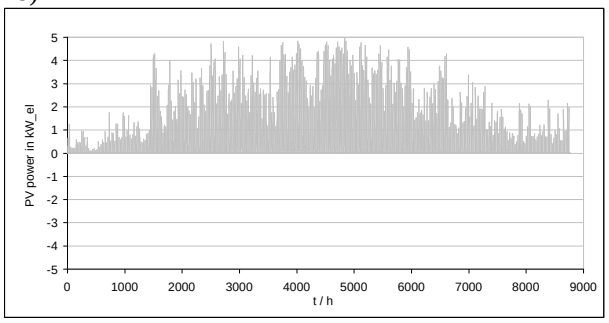

1c)

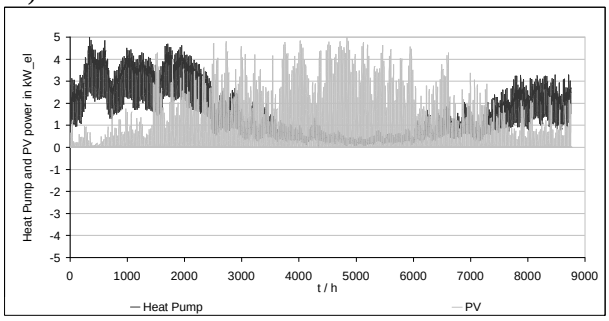

1d)

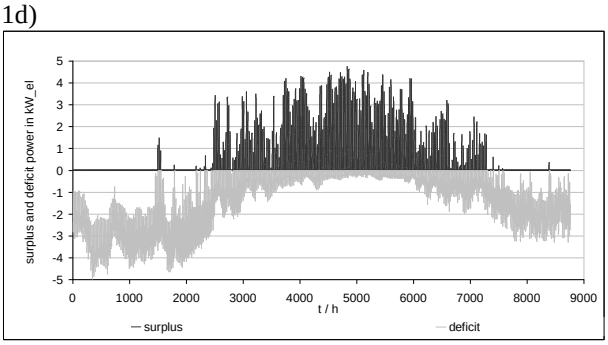

Figure 1. Power profiles
a) Power demand of the heat pump
b) Feed-in power of a PV system
c) Comparison of the power profiles
d) Surplus and deficit feed-in from a PV system for heat pump supply

2. OBJECTIVES AND METHODOLOGY

Based on a given electrical installed load of a heat pump, here assumed 5 kW_el, the optimal PV and battery power is to be determined. From the literature it is known that experienced installation companies advise to design the PV power three times higher than the required electrical heat pump power. However, this does not take into account that additional battery storage can temporarily store surplus energy from the PV system. This temporarily stored energy can be provided in times without PV feed-in of the heat pump. The times considered are the morning hours before sunrise, here about 4 hours, and the evening hours after sunset, here also about 4 hours, in winter time.

If one assumes that the PV system may be covered with snow in the middle of the heating period and the maximum PV installation power has been determined for this peak time of demand, the design could be not optimal. The procedure presented here shows a way to determine the optimal installation capacities for PV and battery storage. In particular, this method takes into account the PV power used by the heat pump and the maximum battery power provided over 2x4 hours.

The iterative optimization process considers the used and unused PV annual energy as well as the annual energy demand of the heat pump and determines the PV and battery installation power from this.

3. RESULTS

The present results, see Table 1, show the determined optimal PV and battery installation power as a function of the annual operating days of the heat pump.

z	1. Day	n. Day	PV_power kW	Bat_power kW	Bat_p	Bat_s	n_Bat	op. Days	PV_u/_HP %	PV_u/_PV %
1	334	31	15,5	2,2	1	19	19	62	15	79
2	304	59	14,6	1,9	1	19	19	120	18	80
3	273	90	7,8	2,5	1	19	19	182	17	77
4	243	120	5,3	2,5	1	19	19	242	17	72
5	212	151	2,7	1,4	1	19	19	304	13	71
6	181	181	1,9	1,0	1	19	19	365	12	68

Table 1. Results
z - sequence number
1. day - first day of the heating period
n. Day - last day of the heating period
PV power - PV installation power optimal
Bat power - battery power optimal
Bat p - batteries connected in parallel
Bat s - serially connected batteries
n Bat - total number of batteries
op. Days - operating time of the heat pump
PV u / HP - used PV feed-in energy to heat pump demand energy per year in %.
PV u / PV - used PV feed-in energy to PV total energy per year in %.

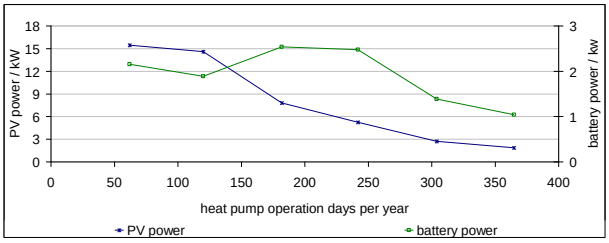

Figure 2. PV and battery power as a function of the heat pump operating time

For a very short heating period of, for example, 62 days results in a PV installation power of 15 kW and a usable battery power of 2 kW over 8 hours, see Table 1. and Figure 2., For longer heating periods, for example, a year-round heat pump use over 365 days, a very low PV installation power of 2 kW and a usable battery power of 1 kW over 8 hours is obtained.

Assuming that a heating period is about 182 days and the installed electrical power of the heat pump is 5 kW, then the optimal PV system power is 7,8 kW and the optimal battery power over 8 hours per day is 2,5 kW, see Table 1 and Figure 2.

REFERENCES

[1] Harzfeld, E.: EXCEL Spreadsheet for determining the PV and battery installation power for a given heat pump system, 2022, not published

Address of the author
Harzfeld, Edgar; Stralsund University of Applied Sciences; Zur Schwedenschanze 15; 18435 Stralsund; Germany; edgar.harzfeld@hochschule-stralsund.de

Teaching electrochemical resources and its implementation during the COVID-19 pandemic

Pavel Hrzina
Department of Electrotechnology
CTU in Prague, Faculty of Electrical Engineering
Prague, Czech Republic

Abstract

Currently, two basic courses focused on electrochemical sources are offered at the CTU in Prague, FEE. One in the bachelor's stage, this is a shared course with the basics of photovoltaics and one in the master's stage, this is a separate course with an hourly allowance of 2 + 2 (2 hours of lectures, and 2 hours of exercises) for 14 weeks. At the time of the greatest restrictions associated with the COVID-19 pandemic, it was necessary to adjust this concept so that students can also carry out practical measurements.

Keywords: teaching electrochemical sources; COVID-19 pandemic

INTRODUCTION

Currently, two basic courses focused on electrochemical sources are offered at the CTU in Prague, FEE. One in the bachelor's stage, this is a shared course with the basics of photovoltaics and one in the master's stage, this is a separate course with an hourly allowance of 2 + 2 (2 hours of lectures, and 2 hours of exercises) for 14 weeks. At the time of the greatest restrictions associated with the COVID-19 pandemic, it was necessary to adjust this concept so that students can also carry out practical measurements.

COURSE CONCEPT

Students of the basic (bachelor's course) are required to have a basic understanding of the principles of energy storage, followed by the technological basics of battery production. The course is logically divided into the basics of basics and components (both PV and batteries), then photovoltaic systems and battery systems are presented, and finally their combinations, as well as economic and environmental aspects of both photovoltaics and operation of electrochemical sources. The course ends with an exam, which tests both the photovoltaic and battery parts.

In the master's course, the acquired skills are deepened, however, completing the bachelor's course is not a prerequisite.

The first part of the course explains electrochemistry as a science and students are introduced to the basics of electrochemical reactions. Next part is an analysis of battery requirements followed by several lectures focused on specific types of batteries (primary, secondary acid, alkaline and lithium). In cooperation with the neighbouring University of Chemistry and Technology, the topics of redox battery systems and fuel cells are presented. Next part is a presentation of the issue of battery protection and operation (BMS design). The next lecture deals with electromobility and storage systems for RES. The course ends again with economic - ecological issues of battery systems.

The teaching also includes laboratory exercises, here we follow a proven lesson scheme. Introductory presentation of the results of the previous measurement to the students, followed by a short discussion of the task and then the measurement itself. Students are divided into 2 groups of a maximum of 5 students. Thus, the teaching of laboratories takes place with a staff of one instructor for 10 students.

DISTANCE LEARNING & IT SUPPORT

The MOODLE system is used to support teaching for long time. MS TEAMS was used preferentially during the COVID pandemic. We evaluate the MOODLE system as a better support for full-time teaching, while MS TEAMS is a support for distance learning.

During the COVID lockdown, the entire semester was implemented remotely. The lectures took place online. The lecturer lectured mostly from the home-office. Students were motivated to attend the lecture, but were provided with a record of study. These were non-public records for which no further use is expected. The exercises then took place in masse (for the whole study group). The syllabus of the exercises was modified with regard to the possibility of conducting experiments directly by students at home.

Students bought or supplemented their home equipment with components at a price of approximately 12 EUR:

- Arduino UNO module
- 2 relays
- basic set of resistors and
- cell holder (type AA).

The assigned tasks first introduced the students to the Arduino system and then the students performed simple measuring tasks.

1) Discharge of the primary cell (AA) with intermittent load and recording to the PC

2) Measurement of internal resistance by the method of two currents

3) Construction of own BMS - short-circuit current limitation, relay switching in case of overvoltage and undervoltage.

The tasks were supplemented by an analysis of the primary cell and several theoretical tasks using LT SPICE (simulation of replacement cell diagrams) and search tasks of individual types of batteries.

In both the online and full-time courses, students are advised to draw on the Linden's Handbook of Batteries [1] in addition to the available Internet resources.

CONCLUSION

The classic form of teaching was adjusted to home exercises which can be provided by students.

Last year, distance learning was evaluated positively by students. The final exam took place by video call with the teacher.

REFERENCES

[1] Thomas B. Reddy. 2011200219951984. Linden's Handbook of Batteries, Fourth Edition. Fourth. McGraw-Hill Education: New York, Chicago, San Francisco, Athens, London, Madrid, Mexico City, Milan, New Delhi, Singapore, Sydney, Toronto. https://www.accessengineeringlibrary.com/content/book/9780071624213

Addresses of the authors

Pavel Hrzina, CTU in Prague, FEE, Dpt. Of Electrotechnology, Technicka 2, 166 27 Prague 6, Czech Republic, hrzinap@fel.cvut.cz

Hydrogen Interactions with Nanostructured Metal Oxide Thin Films Prepared by Reactive Magnetron Sputtering Technique

Nirmal Kumar [a,b], and Stanislav Haviar [a],
[a]Department of Physics and NTIS, University of West Bohemia
[b]Department of Physics, Faculty of Electrical Engineering
Czech Technical University.
Prague, Czech Republic

Abstract

In this paper, we demonstrate the advantages of two advanced sputtering techniques for the preparation of nanostructured thin films of metal oxides. We combined tungsten oxide (WO_3) thin films with other materials to tune the composition, electrical, and structural properties. Thin films of WO_3 were prepared using the DC and HiPIMS technique, which allowed us to tune the phase composition and crystallinity of the oxide by changing the deposition parameters. The second material was then added on top of these films. We prepared nano-islands of copper tungstate ($CuWO_4$) by reactive rf sputtering and Pd particles formed during conventional dc sputtering. The specimens were tested for their conductive response to a hydrogen concentration in synthetic and humid air at various temperatures. The performance of the individual films is presented as well as the details of the synthesis. These nanostructured materials prepared using magnetron sputtering are very suitable for use in miniaturized energy production/storage devices, PEC, PVC, sensing applications etc.

Keywords: Metal Oxides, $CuWO_4$, Magnetron Sputtering, Hydrogen, and HiPIMS.

INTRODUCTION

Nanostructured metal oxides are the most used materials for various applications such as photovoltaic cells, photoelectrochemical cells, water splitting, and other electronic devices due to their tunable bandgap, diverse composition, and high chemical and thermal stability[1], [2].

A variety of methods were used to prepare the metal oxide nanostructured films. Magnetron sputtering is one of the promising preparation methods that provide easy control of the microstructures, structure, and other physical properties.

In this work, we demonstrate magnetron-based techniques which are used to tune the stoichiometry, structural, and electrical properties of sputter (DC) deposited WO_{3-x} films combined with CuO ($CuWO_4$) and Pd/PdO nanoparticles. The electrical properties of as-prepared metal oxide combinations were studied on the surface interaction with H_2 in the synthetic and humid air.

MATERIALS AND METHODS

All the films were deposited by the reactive sputtering technique. Two types of WO_{3-x} films were deposited from a metallic target using reactive dc magnetron sputtering and HiPIMS in the mixture of oxygen and argon gases. The dc sputtering deposited 20 nm WO_{3-x} films were then covered by 5 nm CuO (using rf sputtering deposition) which leads to the formation of $CuWO_4$ nano-islands on the surface of WO_3 due to the higher deposition temperature of CuO film [3]. The three-layered system is prepared by the three-step deposition process where 5 nm WO_3 thin films were deposited on 20 nm CuO films to form $CuWO_4$/CuO. The $CuWO_4$ bilayers were then decorated by 0.8 nm Pd nanostructures.

The HiPIMS deposited WO_{3-x} films were decorated by Pd nanoparticles using rf magnetron sputtering followed by heating up to 350 °C. For more details see Ref. [4].

RESULTS AND DISCUSSION

The SEM micrographs of the combinations of the metal oxides can be seen in Figure 1. The formation of Pd nanoparticles over HiPIMs deposited WO3-x films is shown in Figure 1a. The formation of $CuWO_4$

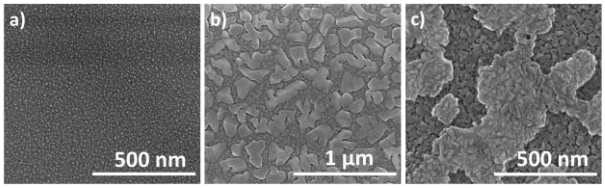

Figure 1 SEM micrographs of a) Pd loaded WO_{3-x} prepared by HiPIMS, b) $CuWO_4/WO_{3-x}$ prepared by rf/dc reactive magnetron sputtering, and c) three layered Pd/$CuWO_4$/CuO system prepared by magnetron spuutering technique

nanoislands over WO_3 and CuO are shown in Fig 1b and Figure 1c. also exhibits the formation of Pd nanoparticles on CuO and PdO nano-islands on $CuWO_4$.
Figure 1
Figure 1c also exhibits the formation of Pd nanoparticles on CuO and PdO nano-islands on $CuWO_4$.
On the basis of the XRD pattern and the SEM analyses, a simple description of the growth process can be formulated. Sputtering of a W target in an Ar and O_2 working gas mixture leads to the deposition of a dense and smooth WO_{3-x} layer. Subsequently, the top-most part of this film reacts with the arriving adatoms during the sputtering of a Cu target in a similar gas mixture leading

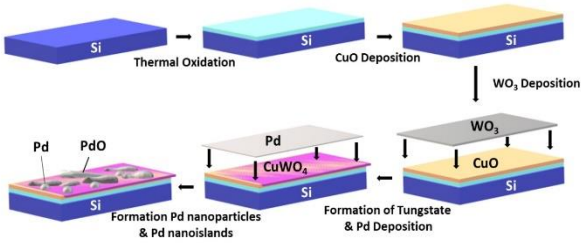

Figure 2 A scheme and description of the deposition process for three-layered system Pd/$CuWO_4$/CuO

to the formation of the $CuWO_4$ islands [3], [5]. The sketch of the process is in Figure 2.

The composition and structure of metal oxides can easily be tuned by varying the HiPIMS deposition parameters as can be seen in Table 1.

Table 1 The stoichiometry and structure of the HiPIMS deposited WO_{3-x} at various voltage pulse lengths. The Sheet resistance is measured at 190 °C

Voltage Pulse Length	Crystalline Phases	Resistance (Ω/sq)	As-Deposited Stoichiometry
500 µs	Monoclinic (triclinic)	3.4 x 10^8	2.76
50 µs	Tetragonal + monoclinic	7.3 x 10^6	3.01
DC	Tetragonal + monoclinic	1.2 x 10^6	2.94
100 µs	Tetragonal + triclinic	1.7 x 10^5	3.07
200 µs	Triclinic (monoclinic)	2.0 x 10^5	2.92
800 µs	Triclinic (monoclinic)	6.3 x 10^2	2.15

The relative response of hydrogen interaction on the corresponding materials is shown in Table 2.
The baseline resistances of as-prepared metal oxides and the resistance in presence of hydrogen (R_{H2}) are measured at higher temperatures (in a range of 200-350 °C) by the four-point probe method. The value of the resistance signaificantly changes with the introduction of the hydrogen.

Table 1 Baseline Resistances of the metal oxides and their combinations in the absence and presence of hydrogen gas.

Specimens	Baseline Resistance	R_{H2}
WO_3 (DC)	1.2 x 10^6	9.7 x 10^5
WO_{3-x} (HiPIMS)	3.4 x 10^5	2.0 x 10^5
Pd/WO_{3-x}	3.4 x 10^8	2.04 x 10^3
$CuWO_4$/WO_{3-x}	1.1 x 10^7	4.5 x 10^6
$CuWO_4$/CuO	5.0 x 10^8	2.0 x 10^8
Pd/$CuWO_4$/CuO	6.0 x 10^{11}	2.6 x 10^{12}
CuO	3.4 x 10^5	8.2 x 10^5

The values of the resistance for the metal oxide combinations are relatively higher than that for the pure metal oxide (WO_3 and CuO). The explanation is based on the formation of the heterojunction at the interface materials. While Pd nanoparticles behaved as the catalyst for the base metal oxide films to improve the variation in resistance even at lower temperatures at a humid environment. The value of the resistance was found to be constant at 0, 30, 60, and 95% of the relative humidity in the synthetic air.
The reaction mechanism for the hydrogen interaction with metal oxide[6], [7] is as follows.
In dry conditions, the surface adsorbed O species react with hydrogen which leads to change (increase or decrease depends on the type of metal oxide semiconductor) in the baseline resistance by changing the depletion layer near the surface (described by green arrows in Figure 3).

$$\frac{1}{2}O_2 + 2e^- \rightarrow O_{ads}^{2-} \quad (1)$$

$$H_{2\,ads} + O_{ads}^{2-} \rightarrow H_2O + 2e^- \quad (2)$$

In humid environment the adsorption of water molecules is described by one of the following mechanisms:

$$H_2O + M + O_O \rightarrow (M^+ - OH^-) + (OH)_O^+ + e^- \quad (3)$$

Or

$$H_2O + 2M + O_O \rightarrow 2(M^+ - OH^-) + V_O^{2+} + 2e^- \quad (4)$$

However, when the Metal oxides are exposed to hydrogen in a humid environment, the water molecules react with adsorbed oxygen species on the surface, leading to an increase in the baseline resistance of the metal oxides. At the same time, hydrogen cannot find the oxygen species to react with and the interchange of electrons, and thus the change in the resistance is reduced (red arrows in Figure 3).
Both involve the formation of OH^- groups on the surface that is bonded to the metal ion M^+. According to the first mechanism, Eq. (3), the other hydrogen from the water molecule forms a rooted hydroxyl group $(OH)_O^+$ with the lattice oxygen O_O.

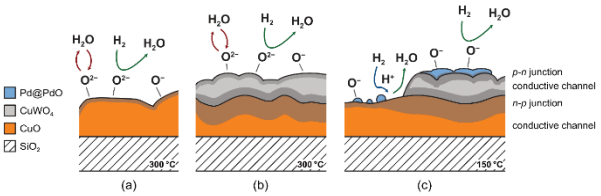

Figure 1 Scheme of synthesized structures with indicated reactions on the surface.

In the other proposed mechanism, Eq. (4), the lattice oxygen forms another adsorbed OH^- bonded to M^+ while leaving an oxygen vacancy $(V)_O^{2+}$.

To overcom the issue of the reduction of the response, the films were decorated with 0.8 nm of Pd. According to Raman spectroscopy, XRD, and other published works on similar systems [8], [9] Pd particles/objects are covered with PdO on their surfaces. Pd and PdO play several important roles in the reaction,:

i) Pd promotes the selectivity towards hydrogen and, at the same time, reduces the response temperature by facilitating the dissociation of H_2 [10] (blue arrow in Fig 3.
ii) PdO favors the adsorption of oxygen over the hydroxyl groups [9].
iii) PdO forms another heterojunction (*p–n)* with the topmost layer of copper tungstate.

See ref. [5] for more details.

CONCLUSION

The synthesis of multilayered thin-film materials using the sputtering technique is demonstrated. The variation in the resistivity of the combined materials is relatively better than the pure material. The structure and composition of the metal oxides are easily controlled by the deposition parameter in the HiPIMS method. resistive response in presence of hydrogen is significantly enhanced just by playing the stoichiometry and structure of the films. Also. by adding Pd particles to the three-layered system the influence of relative humidity was reduced.

These kinds of materials are quite promising for Photovoltaic cells, Solar cells, Gas sensing, Photoelectrochemical cell, energy production, and energy storage devices.

REFERENCES

[1] P. T. Moseley, “Progress in the development of semiconducting metal oxide gas sensors: A review,” *Measurement Science and Technology*, vol. 28, no. 8. Institute of Physics Publishing, Jun. 28, 2017. doi: 10.1088/1361-6501/aa7443.

[2] G. Korotcenkov and B. K. Cho, “Metal oxide composites in conductometric gas sensors: Achievements and challenges,” *Sensors and Actuators, B: Chemical*, vol. 244. Elsevier B.V., pp. 182–210, 2017. doi: 10.1016/j.snb.2016.12.117.

[3] N. Kumar, J. Čapek, and S. Haviar, “Nanostructured CuWO4/WO3-x films prepared by reactive magnetron sputtering for hydrogen sensing,” *International Journal of Hydrogen Energy*, vol. 45, no. 35, pp. 18066–18074, Jul. 2020, doi: 10.1016/j.ijhydene.2020.04.203.

[4] N. Kumar, S. Haviar, J. Rezek, P. Baroch, and P. Zeman, “Tuning stoichiometry and structure of Pd-WO3−x thin films for hydrogen gas sensing by high-power impulse magnetron sputtering,” *Materials*, vol. 13, no. 22, pp. 1–12, Nov. 2020, doi: 10.3390/ma13225101.

[5] N. Kumar, S. Haviar, and P. Zeman, “Three-layer PdO/CuWO4 /CuO system for hydrogen gas sensing with reduced humidity interference,” *Nanomaterials*, vol. 11, no. 12, Dec. 2021, doi: 10.3390/nano11123456.

[6] J. Miao, C. Chen, and J. Y. S. Lin, “Humidity independent hydrogen sulfide sensing response achieved with monolayer film of CuO nanosheets,” *Sensors and Actuators, B: Chemical*, vol. 309, Apr. 2020, doi: 10.1016/j.snb.2020.127785.

[7] B. Urasinska-Wojcik and J. W. Gardner, “H2S Sensing in Dry and Humid H2 Environment with p-Type CuO Thick-Film Gas Sensors,” *IEEE Sensors Journal*, vol. 18, no. 9, pp. 3502–3508, May 2018, doi: 10.1109/JSEN.2018.2811462.

[8] Y. Cao, C. Zhou, Y. Chen, H. Qin, and J. Hu, “Enhanced CO Sensing Performances of PdO/WO3Determined by Heterojunction Structure under Illumination,” *ACS Omega*, vol. 5, no. 44, pp. 28784–28792, Nov. 2020, doi: 10.1021/acsomega.0c04137.

[9] S. Ma, M. Hu, P. Zeng, M. Li, W. Yan, and Y. Qin, “Synthesis and low-temperature gas sensing properties of tungsten oxide nanowires/porous silicon composite,” *Sensors and Actuators, B: Chemical*, vol. 192, pp. 341–349, Mar. 2014, doi: 10.1016/j.snb.2013.10.121.

[10] F. E. Annanouch *et al.*, “p-Type PdO nanoparticles supported on n-type WO3 nanoneedles for hydrogen sensing,” *Thin Solid Films*, vol. 618, pp. 238–245, Nov. 2016, doi: 10.1016/j.tsf.2016.08.053.

Addresses of the authors:

Nirmal Kumar, Department of Physics, Faculty of Electrical Engineering, Czech Technical University, Prague, Czech Republic, kumarnir@fel.cvut.cz
RNDr. Stanislav Haviar, Department of Physics, Faculty of Applied Sciences, University of West Bohemia, Pilsen, Czech Republic, haviar@ntis.zcu.cz

Tunneling oxide based selective contacts for high efficiency solar cells

J.M Serra, I. Costa, G. Gaspar, J.A. Silva and K. Lobato

Instituto Dom Luíz / Faculdade de Ciências da Universidade de Lisboa, Campo Grande, 1749-016 Lisboa, Portugal

*corresponding author: jmserra@fc.ul.pt

Abstract: The conversion efficiency of crystalline silicon solar cells, is limited by recombination losses associated with the contacts. Namely, a contact structure that simultaneously passivates the c-Si surface while selectively extracting only one type of charge carrier (i.e., either electrons or holes) is desired. Such passivating contacts in c-Si solar cells have recently become an important research objective. In this work we studied different selective carrier stacks using tunnelling SiO_2 and TiO_2 layers with variable combinations, along two routes: high temperature route, in which the silicon oxide is obtained by thermal oxidation and a low temperature route where the silicon oxide is obtained by chemical oxidation or by e-beam evaporation. Symmetrical silicon samples with TiO2/SiO2 stacks on each side were prepared and minority carrier lifetimes were measured, to assess the passivation properties of the contacts. SiO2 thickness measured by ellipsometry.

MOTIVATION

Standard contacts have high recombination and limit conversion efficiency

Point metal contacts can reduce this recombination. However this is more complicated to manufacture

Selective contacts allow to achieve both good passivation and carrier selectivity and can be applied on the whole surface

The ultimate goal is to manufacture doping free solar cells

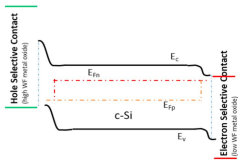

RESULTS

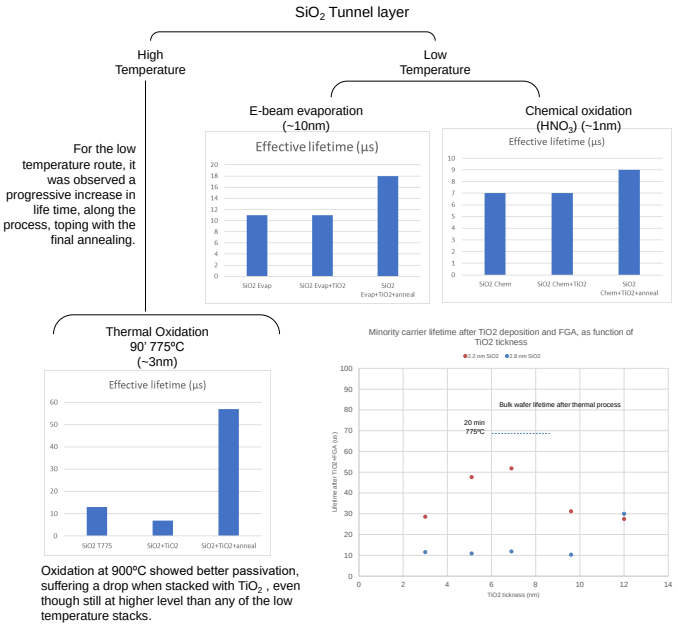

Oxidation at 900ºC showed better passivation, suffering a drop when stacked with TiO_2 , even though still at higher level than any of the low temperature stacks.

Oxidation at 775ºC resulted in the higher increase in lifetime along the process reaching higher lifetimes than the higher temperature approach.

PROCEDEURE

SiO_2 / TiO_2 layer samples

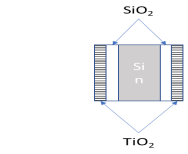

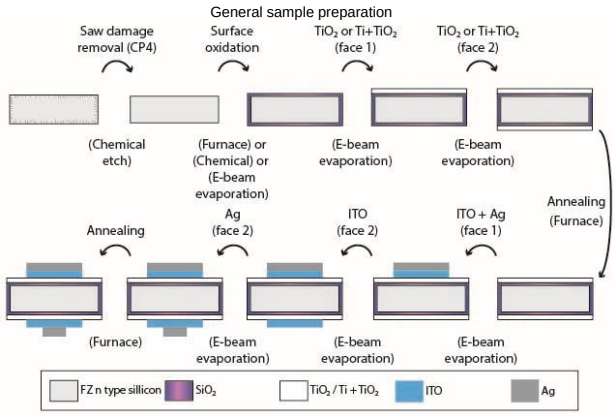

Silicon FZ n-type: 1-5 Ohm.cm, 280 µm thick, double sided polished
Annealing at 350 ºC for 5 min in forming gas

CONCLUSIONS

- The annealing step is critical for the effective selective contact formation.
- The high temperature route can induce lifetime degradation in the bulk of the wafer.
- An optimum TiO2 thickness, to minimize contact recombination, was obtained for the chosen SiO2 layer thickness.

The authors would like to acknowledge the financial support of Fundação para a Ciência e a Tecnologia, I.P./MCTES through (PIDDAC) of projects: **UIDB/50019/2020 – IDL** and **PTDC/CTM-CTM/28860/2017**

Study of PV systems for self-consumption at the UPC based on simulations by using PVSol

S. Silvestre
MNT Group, Electronic Engineering Department, Universitat Politécnica de Catalunya (UPC) BarcelonaTech, C/Jordi Girona 1-3,Campus Nord UPC, 08034 Barcelona, Spain.

Abstract

The aim of this work is to carry out a sustainability study in five campuses of the Universitat Politècnica de Catalunya BarcelonaTech (UPC) around Catalunya, i.e. Campus North and South Campuses in Barcelona city, Campus Baix Llobregat, Campus Manresa and Campus Vilanova i la Geltrú. The amount of consumed energy included in the study for each campus corresponds to monitoring data of previous periods. The study analyses the expected energy production, as well as the self-consumption that can be achieved by using photovoltaic (PV) systems of 25, 50 and 100 kWp and c-Si, Poly or CdTe Technology in order to reduce the environmental impact in each campus. An economic analysis of all the proposed facilities was conducted to examine their financial feasibility.

Keywords: PV Systems, Simulation, Self-consumption.

INTRODUCTION

The photovoltaic (PV) grid parity has been achieved in several countries as Spain, where the Levelized Cost of Energy (LCOE) of the PV technology can be compared with their local retail electricity prices in a competitive way. However, feed-in tariff and/or net metering incentives are still not well defined. This fact is partially due to the bad past renewable energy regulations and to a very sophisticated regulatory framework [1-2].

This study focuses on the analysis, through simulation using PVSol, taking into account the real profiles of consumption, irradiance and temperature in the buildings included in the analysis, of the potential energy production of different photovoltaic systems considering several photovoltaic technologies.

METHODOLOGY

The Universitat Politècnica de Catalunya BarcelonaTech (UPC) is a public Spanish University with more than 30,000 students focused on the fields of engineering, architecture, science and technologies [3].

The UPC schools and faculties are at the service of learning, research and knowledge. The UPC engineering schools are sited in Barcelona and in several nearby towns: Castelldefels, Manresa, Sant Cugat del Vallès, Terrassa, and Vilanova i la Geltrú, as it can be seen in Fig. 1.

Fig.1. Map of UPC Campuses in Catalonia (Spain).

To carry out this study, five UPC campuses were selected: Campus North and South Campus in Barcelona, Baix Llobregat Campus, Campus Manresa and Vilanova i la Geltrú Campus. From each one of them, given that the contracted power is not the same for the entire campus but it depends on how they are divided, the analysis has focused on one or more buildings in particular. As for the North Campus, all the A classrooms buildings where chosen, in the case of the South Campus, the building of the faculty of mathematics was selected, at the Baix Llobregat Campus, the D4C building, on the Manresa Campus the MN123 and at the Vilanova i la Geltrú Campus the VG4 building.

Real consumption profiles were used in the study for the selected buildings of each campus. The data was taken from an internal UPC monitoring platform called SIRENA. The irradiance and temperature profiles were

obtained from the data base included in the PVSol simulation tool for each one of the selected locations, as it can be seen in Fig. 2.

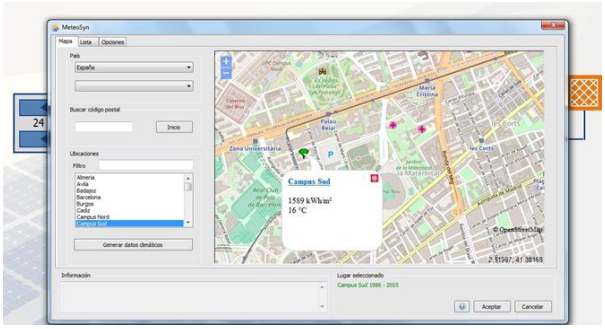

Fig.2. Selection of Irradiance and temperature profiles for South Campus UPC in Barcelona City (Spain).

The selection of PVSol [4] for the simulation of the PV systems is based in the good data base of PV system components included in this tool that allows working with real model parameters of all components included in the system, especially PV modules and inverters.
Moreover, PVSol is used in the simulation practices included in two PV courses at the UPC: Photovoltaic Solar Energy, an elective course of the Master's degree in Energy Engineering at the ETSEIB-UPC [5] and Photovoltaic Systems, an elective course at the Master's degree in Electronic Engineering (MEE) at the ETSETB-UPC [6].
These Master Degrees are aligned with the objectives of the European SET plan and the objectives of KIC InnoEnergy in the field of renewable energies and aim at delivering education for high competency and quality engineering skills in the field. In particular, these courses are focused on technical skills required for engineers in the field of PV applications.
The duration of both courses is one semester: 15 weeks-5 ECTS, and the courses include stand-alone and grid connected applications of PV systems considering both technical and economic criteria to select the most appropriate electrical equipment for a given application and solutions for a smart control and fault detection in the generation systems in order to optimize the energy generation and costs.

The PV modules forming part of the PV arrays included in the simulation study are the following:
c-Si PV module : Suntech Power STP250S-20/wd, CdTe PV module: First Solar FS-390, Poly Silicon PV module: Atersa A-150P.

The inverters selected for all PV systems are inverters Ingecon Sun 25, 50 and 100 kW by Ingeteam SA.
The methodology used in the simulation study is shown in the flowchart included in Fig. 3.

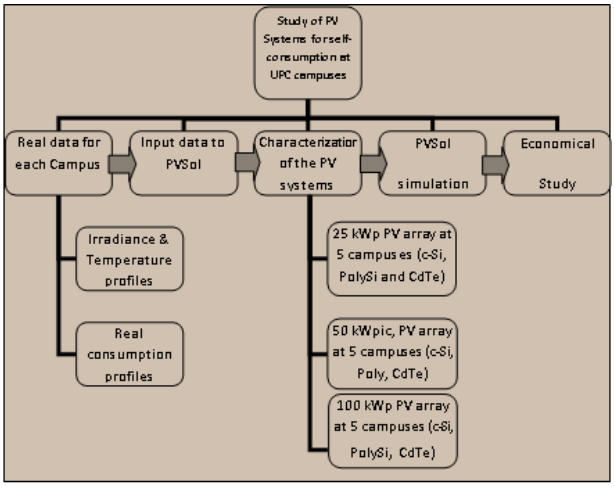

Fig.3. Flowchart of the simulation analysis carried out.

RESULTS

As an example of the results obtained, main parameters obtained in the simulation results for the case of a PV array of 100kWp formed by c-Si PV modules in the five UPC campuses analysed in the study are shown in Table 1.

Fig.4. North Campus UPC in Barcelona and A buildings in red.

Fig.5. Installation of PV system at the roofs of buildings A classrooms.

At the end of this study, the installation of a new solar plant on the north campus of Barcelona has begun as can be seen in Figs. 4 and 5. The PV array is formed by 510 c-Si PV modules of 310 Wp each and a total area of

2,067 m^2 on the roofs of the buildings A of classrooms: A1, A2, A3 and A4.
The PV system includes three Sunny Tripower CORE1 inverters with a nominal power of 50 kW each. The new plant will have an annual output of 225,000 kWh, that is, 50% of the energy consumed by these buildings.

c-Si 100 kWp	Campus Nord	Campus Sud	Campus Baix Llobregat	Campus Manresa	Campus Vilanova i la Geltrú
PV power (kWp)	95	96	94.5	92	93.5
PV surface (m^2)	618.2	624.8	614.9	598.6	608.4
Radiation on the PV array plane (kWh)	1,133,719	1,143,455	1,147,777	1,196,036	1,178,337
Energy produced (AC) (kWh)	140,062	141,706	142,515	146,819	146,209
Energy injected into the grid (kWh)	2,888	0.00	596	38,974	122,091
Load demand (kWh)	624,709	988,331	719,879	271,487	40,032
FV energy directly used (kWh)	137,174	141,706	141,918	107,844	24,118
Energy supplied by the grid (kWh)	487,539	846,629	577,965	163,647	15,918
Performance Ratio (PR)	80.3%	80.5%	80.7%	79.8%	80.6%
Anual Yield (kWh/kWp)	1,474	1,476	1,508	1,596	1,564
CO_2 avoided (kg/year)	86,781	87,005	87,664	100,745	122,978

Table 1. Results obtained for a PV system of 100kWp including c-Si PV modules in all campuses analysed.

REFERENCES

[1] Del Río Pablo: Ten years of renewable electricity policies in Spain: an analysis of successive feed-in tariff reforms, Energy Policy **36**, 2008, 2917–29.
[2] Rosales-Asensio, E., de Simón-Martín, M., Borge-Diez, D., Pérez-Hoyos, A., & Santos, A. C.: An expert judgement approach to determine measures to remove institutional barriers and economic non-market failures that restrict photovoltaic self-consumption deployment in Spain. Solar Energy **180**, 2019, 307-323.
[3] www.upc.edu/ca
[4] PVSol Software, https://www.valentin-software.com/es/productos/pvsol
[5] https://etseib.upc.edu/ca
[6] https://telecos.upc.edu/ca

Addresses of the authors

Santiago Silvestre, C/Jordi Girona 1-3, Mòdul C4 Campus Nord UPC, Barcelona, Spain, Santiago.silvestre@upc.edu

New and Old Types of Storage Batteries for Photovoltaics in Research and in College Curriculum

P. Vanýsek
Department of Electrical and Electronic Technology
Brno University of Technology
Brno, Czech Republic

Abstract

In the photovoltaics teaching curriculum the issue of need of energy storage is not central, but it is unavoidable corollary. Since in many storage applications, it is the electrochemical storage scheme that is employed, fundamental instruction about batteries is needed. From general principles of dissimilar materials and redox reactions one will make transition to various types of electrochemical systems. Knowledge of longevity and modes of failure of batteries became necessary part of complex knowledge needed to grasp the intricacies of energy economy.

Keywords: photovoltaics, education, instruction, batteries, electrochemical energy storage

ENERGY STORAGE AND PHOTOVOLTAICS

Needs to Teach about Energy Storage

For small and short term energy storage from photovoltaics can be a capacitor or a flywheel. For some specific, single-purpose systems, for example water pumping for refrigeration, the storage medium can be water or ice. However, in photovoltaics the most common type of storage by far is chemical storage in the form of battery.

Teaching Electrochemistry

Teaching about electrochemical batteries, either as a convenient energy source or specifically as a pawn in energy storage can take various approaches. With proliferation of technology the present pupils and students paradoxically have less exposure to the "bare" batteries, individual cells that could be explored. While batteries are omnipresent, they are often embedded in devices even without easy means of removal. Gone are the days when hobbyist used the flat 4.5-V battery (3LR12), which was with its metal pads so easy to use in projects.

Fig. 1. Classical 4.5-V dry battery, type 3LR12. The metal tabs were convenient connections for hobbyist projects.

The textbook Cu-Zn Daniell cell [1] is often discussed but hardly ever constructed. What remains is a lemon battery demonstration. Nevertheless, it is possible to introduce new and interesting experiments to the classrooms.

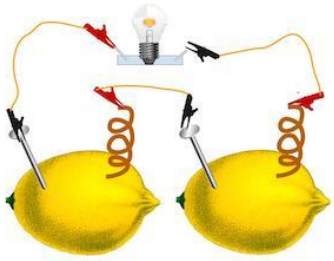

Fig. 2. Schematic drawing of the lemon battery often shown at school science fairs. The electrodes are zinc plated steel nail and copper in the copper conductor. Lemon juice is the electrolyte.

Those who in spite of prior exposure to chemistry and engineering enter the realm of electrochemical power sources research will enter exciting world of material science.

The Primary and Secondary Batteries

The described flat (3LR12) battery, the Daniel cell and even the lemon demonstration project are examples of the called primary batteries, a term used for systems that due to electrochemical reactions produce electrical energy, but once the chemicals are depleted, energy is no longer produced and the batteries cannot be in a simple manner restored to the original state. Therefore, by design these batteries are single use and have to be discarded after one use. While this can be at times convenient, more useful service comes from systems that can be, once discharged, connected to a source of electrical energy and recharged to the original state. These are the secondary batteries, often called rechargeable or storage batteries and in some use also accumulators.

Photovoltaics Can't be Done Overnight

Every student of photovoltaic will at some point come to the realization that a system, which relies on sunshine, will deliver energy only during daylight. For some it may be simply a matter of fact; those involved in complete energy solution will have to deal with the task to store some of the photovoltaic energy generated during daylight for use later on when it is dark. While not the only storage solution, energy storage using electrochemical principles is very convenient and often used.

TYPES OF STORAGE BATTERIES

Lead-acid

This battery was invented already in 1859 by Gaston Planté [2]. It consists of two lead-based electrodes. The negative electrode is metallic lead; the positive electrode is porous mass of lead(IV) oxide. Each individual cell of the battery is filled with sulfuric acid and the cell, when charged, has nominally voltage of about 2.105 V.

The reaction during discharge on the negative electrode is

$$Pb + HSO_4^- \rightarrow PbSO_4 + H^+ + 2\ e^-$$

and on the positive electrode

$$PbO_2 + 3\ H^+ + HSO_4^- + 2\ e^- \rightarrow PbSO_4 + 2\ H_2O.$$

Thus on the negative electrode the metallic lead is oxidized and turns into lead(II) sulfate, while lead(IV) oxide on the positive electrode is reduced and turns also to lead(II) sulfate. While these two reactions are happening, some of the sulfuric acid in the electrolyte is also consumed. Once the oxide in the battery is consumed, the system loses power, but it can be recharged from an outside source of electricity, by inverting the above reactions.

A basic type is so called battery with flooded electrodes - e.g., a car of classical design battery - where the electrolyte is a free liquid between electrodes. Newer design is so called VRLA type (Valve Regulated Lead Acid) which is an encapsulated type with a significant reduction of gas evolution; practically no oxygen evolves and only a very small amount of hydrogen is formed. They can be in the form of AGM (from Absorbent Glass Mat) which has the electrolyte soaked in the glass wool between electrodes and the gel form, where the electrolyte is thickened in the form of a gel.

Nickel-Cadmium and Nickel-Iron

Cadmium was found as impurity in zinc production in 1817. It has similar properties to zinc and mercury, which is the reason why each three of these metals found use in electrochemical cells. Cadmium found its use in energy sector as the negative electrode of a rechargeable nickel-cadmium battery. The cells based on this chemistry were invented in 1899 by Waldemar Jungner [3] [4]. The chemical reactions are as follows:

Reaction on the negative plate made of cadmium

$$Cd + 2\ OH^- \rightarrow Cd(OH)_2 + 2\ e^-$$

Reaction on the positive made of nickel

$$2\ NiO(OH) + 2\ H_2O + 2\ e^- \rightarrow 2\ Ni(OH)_2 + 2\ OH^-$$

Overall reaction

$$2\ NiO(OH) + Cd + 2\ H_2O \rightarrow 2\ Ni(OH)_2 + Cd(OH)_2$$

E^o_{cell}=1.299 V [5], ΔG=-251 kJ mol^{-1}

The electrolyte is usually 21% potassium hydroxide and the average operating voltage is 1.2 V.

The second metal used in this setup is nickel, which has application in another rechargeable battery system, the nickel-iron secondary battery.

The nickel iron (Ni-Fe) battery is a storage battery quite tolerant and more so than a lead-acid battery to overcharge, deep discharge and short circuit and thus it has been popular in backup situations and in on-site industrial electric vehicles and forklifts. Just as the nickel-cadmium, the nickel-iron battery was invented in 1899 by W. Jungner [3], but the nickel-iron design was improved in 1901 by Thomas Edison. The battery uses alkaline electrolyte, sodium or potassium hydroxide. Open circuit voltage of the cell is 1.4 V, and drops during discharge to 1.2 V.

Reaction on the negative plate is

$$Fe + 2\ OH^- \rightarrow Fe(OH)_2 + 2\ e^-$$

Reaction on the positive made of nickel

$$2\ NiO(OH) + 2\ H_2O + 2\ e^- \rightarrow 2\ Ni(OH)_2 + 2\ OH^-$$

(same as in the Ni-Cd cell)

Overall reaction is

$$2\ NiO(OH) + Fe + 2\ H_2O \rightarrow 2\ Ni(OH)_2 + Fe(OH)_2$$

E^o_{cell}=1.2 V, ΔG= -232 kJ mol^{-1}

Nickel-plated or nickel based items are quite common, including some coins, though they are known in some individuals cause nickel allergy (e.g., in jewelry). Even though nickel is less problematic than cadmium, it is still considered toxic and is a category 3 carcinogen (in European Union classification, i.e., "Substances which cause concern for humans, owing to possible carcinogenic effects but in respect of which the available information is not adequate for making a satisfactory assessment") so one category less severe than cadmium. Because of the nickel-cadmium combination of rechargeable batteries, nickel ends up to be suppressed as a material for electrochemical sources as well. Nickel finds its use in the Ni-Fe rechargeable batteries, which have low charge/discharge efficiency but are operational up to – 40 ºC and excel in longevity from 30 up to perhaps 50 years [1]. Iron is not environmental hazard in these applications.

While Jungner invented the nickel-cadmium battery already in 1899 as a wet cell [3] sealed cells became very popular towards the later part of the twentieth century as portable electronics became more and more available. The Ni-Cd batteries are able to deliver high currents and thus they became very popular as a power for remote controlled models. The advantage was also that the batteries can operate at higher temperatures and they can also operate well below 0 ºC. The low temperature is somewhat an advantage over presently used (standard) lithium cells, which lose both capacity and ability to be charged by high currents unless electrolytes with particularly low viscosity at low temperature are employed.

Cadmium is, however, environmental pollutant, a category 2 carcinogen (in European Union classification, i.e. "Substances which should be regarded as if they are carcinogenic to humans.") and its use in batteries became in Europe heavily curtailed. The 2006 Battery Directive [6] restricted severely the use of cadmium batteries to be used only in emergency lighting, emergency doors and alarms systems, in medical equipment and in cordless power tools. In 2006 battery operated power tools were widespread and the Ni-Cd batteries were still the only viable alternative, so there were included in the exception. However, as lithium batteries became more available, the Battery Directive was amended and in 2013 the use of Ni-Cd in power tools was also banned. It should be also noted that through effort of individual countries the efficiency of recycling Ni-Cd systems (regardless of the 2013 ban in power tools) has increased significantly (Fig. 5).

Lithium

Lithium ion batteries are ubiquitous today, used in cell phones, laptops, and many other devices. Efficient battery development is also a key in allowing move away from fossil fuels, as the batteries enable storage of energy generated from solar, wind and other renewable sources.

The importance of the lithium cells and the world-wide impact of these devices were significantly acknowledged by the 2019 Nobel Prize in Chemistry that has been awarded to three electrochemists for the development of a rechargeable battery based on lithium. Stanley Whittingham developed the first functional lithium battery in the early 1970s, but it was possibly too explosive to be commercially acceptable. John B. Goodenough was responsible for developing far more powerful batteries. Akira Yoshino later eliminated pure lithium from the battery, using lithium ions only to shuttle between the cathode and anode, producing the first commercially viable lithium ion battery in 1985. This is safer than pure lithium and made the battery workable for real-world applications. While lithium batteries are undoubtedly most prominently on people's minds today, other chemistry schemes are finding their application as well.

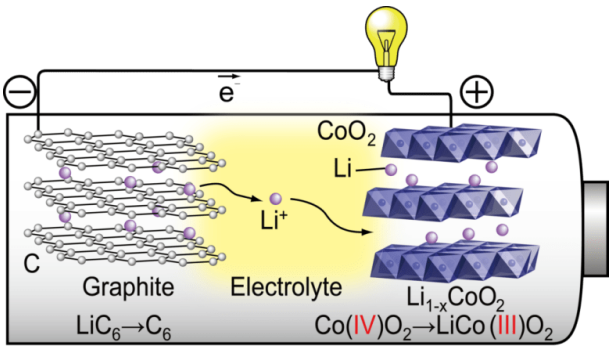

Fig. 3. A diagram of the modern type of lithium-ion based rechargeable battery.

Lithium-ion battery of the modern design is not based on reduction or oxidation processes. Instead, lithium cation is driven during charging and then during discharging between two materials that can efficiently incorporate and then release the ions. So the charging/discharging is moving the ions back and forth, a scheme sometimes referred to as "rocking chair." The negative electrode is a form of graphite, the positive electrode is, in the simplest form, cobalt(IV) oxide, that can incorporate lithium ion, rendering in the step cobalt formally trivalent [7].

Flow-Through Cells (RedOx)

The expression "redox" is derived from joining two words, reduction and oxidation, implying simultaneous occurrence of both of these processes, oxidation, loss of electrons and reduction, gain of electrons. From the general electrochemical point of view, where the overall

charge balance is thermodynamically required, any electrochemical system will be a "redox" system. However, in the vernacular of electrochemical power sources, the *redox flow battery* was adopted for a particular concept of electrochemical energy storage.

Fig. 4. An actual commercial vanadium flow cell. The left and right upper containers in the transport cages hold the respective vanadium solutions. The middle is the armature of the electrochemical cell. The containers and the cell are placed over the blue reservoirs intended to capture any spill in case of an accident. For sizing an Estwing 22, a 13" geological hammer, is leaning against the middle retention reservoir.

The expression "redox" is derived from joining two words, reduction and oxidation, implying simultaneous occurrence of both of these processes, oxidation, loss of electrons and reduction, gain of electrons. From the general electrochemical point of view, where the overall charge balance is thermodynamically required, any electrochemical system will be a "redox" system. However, in the vernacular of electrochemical power sources, the redox flow battery was adopted for a particular concept of electrochemical energy storage.

A redox flow battery (often abbreviated RFB) describes a power source that uses for energy generation two separate solutions, one in an oxidized form, the other in a reduced form. During release of energy the solutions react on electrodes, the first is reduced and the other is oxidized and in the outside circuit between the two electrodes flows electric current. During the process of charging the function of oxidation and reduction is reversed and the system is charged from an external energy source.

The principle of the flow redox cells is the same as the principle of any galvanic cell. Oxidation and reduction, occurring simultaneously, but in separate half-cells, cause the flow of an electric current, carried by ion flow in the electrolyte of the electrochemical cell and by electrons in the external electric circuit. This electric current is then the source of energy carried by conductors to wherever it is needed. Compounds that undergo oxidation or reduction are sources of chemical energy. When these substances are reacted and spent, the electrochemical cell is discharged. For rechargeable (secondary) cells, the discharge process can be reversed and the cell again recharged via an external power source. Reactive substances pass into their original form during charging. However, the redox flow cells differ from the conventional electrochemical cells by the fact that the reacting material is not part of the construction of the cell, but it is supplied from external storage tanks in a form of electrolytes which, during cycling, pass from the charged to the discharged state. The total energy capacity of the system is proportional to the amount of electrolytes in the external reservoirs, while the total output power is dependent on the electrode arrangement (the surface of the electrode system). In a sense, the behavior of the flow cell, when delivering energy, is identical to the fuel cell operating principle. However, the fuel cell is not expected to reverse the current flow and recharge the system again. The diagram of the redox flow cell, showing its principle, is given in Fig. 5.

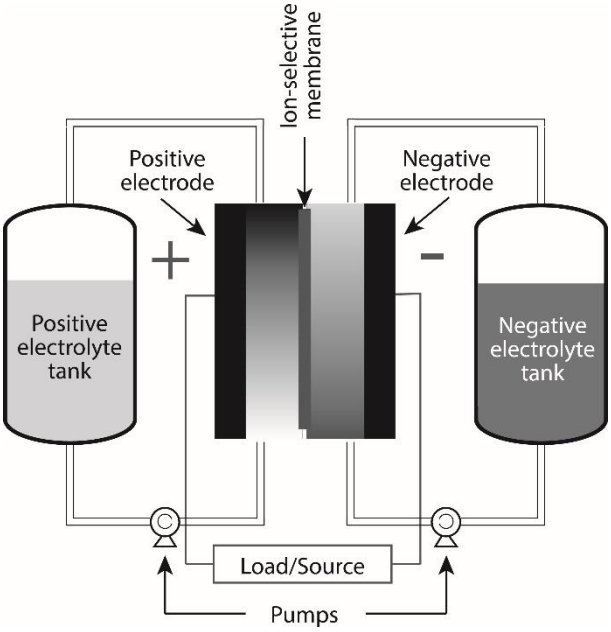

Fig. 5: Diagram of the principle of a redox flow-through cell.

ACKNOWLEDGEMENTS

This work was supported by the specific research program of the Brno University of Technology No. FEKT-S-20-6206.

REFERENCES

[1] Linden, D. and Reddy, T. B., *Handbook of Batteries*, p., McGraw-Hill (2002).

[2] Planté, G., *Recherches sur l'électricité de 1859 à 1879*, p., Rev. La lumière électrique, Paris (1883).

[3] Jungner, E. W., *Satt att framstalla positiva elektroder for ackumulatorere, afsenom pa detta satt framstalda elektroder*, K.P.-O. Registreringsverket, Editor. 1899: Sweden.

[4] Desmond, K., *Innovators in Battery Technology: Profiles of 95 Influential Electrochemists*, p. *114-118*, McFarland & Company (2016).

[5] Falk, S. U. and Salkind, A. J., *Alkaline Storage Batteries*, p. *533*, John Wiley and Sons, Inc., New York (1969).

[6] *Directive 2006/66/EC of the European Parliament and of the Council of 6 September 2006 on batteries and accumulators and waste batteries and accumulators and repealing Directive 91/157/EEC (Text with EEA relevance) OJ L 266, 26.9.2006, p. 1–14.*

[7] Goodenough, J. B. and Park, K.-S., *J. Am. Chem. Soc.*, **135**, 1167 (2013).

Address of the author

P. Vanýsek, Brno University of Technology, Department of Electrical and Electronic Technology, Technická 3058/10, 616 00, Brno, Czech Republic, vanysek@vut.cz

Environmental Modelling Tools for Simulating of the Photovoltaic Power Plants Operation

J. Vaněk, P. Maule and F. Šmatlo
Department of electrotechnology
Brno University of Technology
Brno, Czech Republic

Abstract

This paper describes the creation of a 3D model of the PV system environment directly in the PVSOL software tool and compares it with a second 3D model created in the PIX4D photogrammetric software. The main advantage of both 3D models is the accuracy of the shading simulation. Any shadow on the PV module reduces the output power, so it is important to have an accurate model of any object that could shade the PV modules. This paper also describes the PV system design in the PVSOL design software.

Keywords: A line of keywords should be a 1 cm below the last of abstracts.

GENERAL INFORMATION

When designing a photovoltaic system, it is important to evaluate several aspects. These aspects include the geographical location, specific system location and orientation, system size, and shading effects. Because the shading greatly affects the output power of the photovoltaic modules, great care should be taken to avoid this effect. For this reason, it is advisable to precisely determine the degree of shading of the photovoltaic modules and adjust the system to ensure the highest efficiency and yield of the system. The PVSOL design software allows you to create 3D models of buildings on which photovoltaic modules can be installed. Creating larger and more complex 3D models in PVSOL is very laborious and time consuming. That is why the photometric software PIX4D was used in this work, which enables to create a real 3D model of larger building complexes and their surroundings and thus increase the accuracy of the screening and also to determine the influence of larger surroundings on the screening of photovoltaic modules.

CREATING 3D MODELS¨

PVSOL

PVSOL software allows you to create 3D building models by pulling an object from the map. Use this tool to eject a 3D object from an aerial photo of a building. The tool is sufficient to determine the degree of shading of panels and is often used for most buildings. It is very suitable for determining the degree of shielding of objects placed on the roof (chimney, satellite, sunroof). With this tool it is also possible to create distant large objects eg factory chimney. A problem may arise if a building with a photovoltaic system is surrounded by a large number of buildings that cast shadow on the photovoltaic modules. These objects can be created, but implementation would be very time consuming.

Fig. 1: 3D model created in PVSOL (part of town)

Fig. 2: Detail 3D model created in PVSOL (building)

PIX4D

Photometric software PIX4D is used for digitizing photographs taken from drones. However, any 3D model can be created using this software. Unlike PVSOL, where one photo and knowledge of all building dimensions is used to create 3D models, PIX4D needs a large number of photos to create a real 3D model. 103 photos from different angles were used for the 3D model (Fig. 3). However, the advantage is that to determine the exact scale of the model, it is necessary to know only one exact dimension of the building, eg the length of the wall. For this work, photos taken in Google Earth were used. By combining the photographs, a 3D model of the part of the city of Brno, in which the building with the proposed photovoltaic system is located, was created.

Fig. 3: 3D model created in PIX4D (part of town)

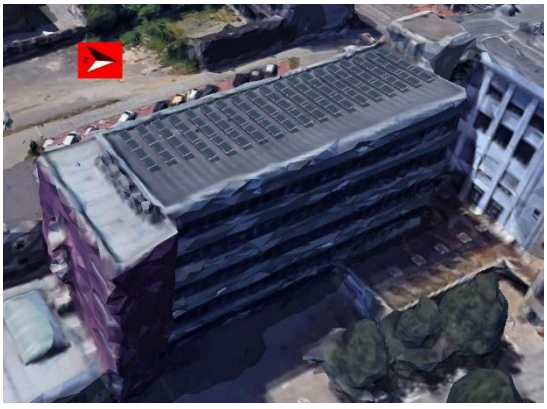

Fig. 4: Detail of3D model created in PIX4D (building)

PHOTOVOLTAIC SYSTEM DESIGN

After creating a 3D model, the design of the photovoltaic system is very individual. In the PVSOL software it is possible to select the type of the modules, their placement and fixing to the roof. Regarding the selection of the inverter for the designed system, PVSOL allows for automatic configuration and selection of the inverter based on the selected panels, their distribution into strings and performance. The cable connection is generated automatically and can be modified. The big advantage of PVSOL is that every photovoltaic component (inverters, modules, batteries) available on the market is cataloged and has a model with exact parameters in PVSOL. [3]

SHADING SIMULATION

The PVSOL software allows simulation of average annual shading. An important input parameter for the simulation is the geographical location of the object with a photovoltaic system. Shading simulation calculates the average annual shading of each module in the system. The result of the simulation is shown as a percentage and using a color scale. Comparing the shading simulations of the two 3D models, we can see that the models are very similar (Fig. 5, 6). Both 3D models also have very similar specific annual yields. Yield differs by 4.52 kWh / kWp, or 0.44%. Another important output value of the simulation is to reduce the yield by shading. At this value, the models differ by about 0.5% / year or 9.8% of the total yield of the photovoltaic system.

Fig. 5: Shading simulation of PVSOL model

Fig. 6: Shading simulation of PIX4D model

ECONOMIC SIMULATION RESULTS

The total energy produced by the PV generator is 28 282 kWh/year. Almost all of the energy produced is consumed directly in the building (99.5%). Only 137 kWh/year will flow into the distribution network. Although almost all energy produced is consumed directly, the degree of self-sufficiency is only 15.2%.

The investment costs for the PV plant were estimated at CZK 2 064 271.62. Half of this is the cost of system components. The other half is the cost of installation and all design. The aid amounts to 65% of the investment costs. The amount of support was estimated between the amount of support for medium and large enterprises according to the subsidy program that the proposed PV

system could use. Furthermore, the annual cost was estimated at CZK 25 791. This amount is used to cover the maintenance of the PV plant.

After the installation of the PV plant, the amount of energy savings is approximately CZK 133 000. If we deduct maintenance costs, we get annual savings of about 110 000 CZK. With the same savings each year, the payback is just 6.6 years. This means that in nearly 7 years the PV system will save the same amount as the initial investment with a subsidy.

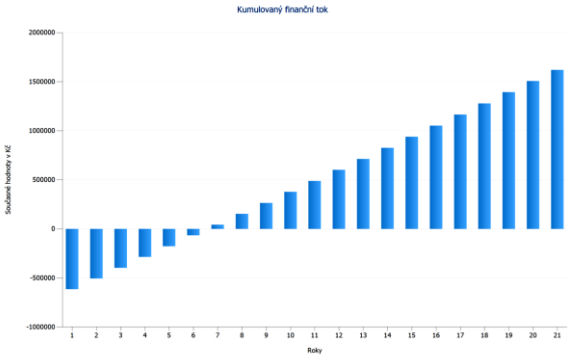

Fig. 7: Economic simulation of designed PV system

Table I: Financial analysis

Total investment costs	CZK 2 064 271.62
Total return on capital	15.38%
Amortization period	6.6 Years
Own production costs of electricity	2.27 CZK / kWh

CONCLUSION

Shading is an important influence on the output of the photovoltaic system. By determining the exact screening rate, the system yield can be determined sufficiently accurately. The main aim of this work is to describe the creation of 3D models in PVSOL and PIX4D, accuracy of shielding simulations and their comparison. Comparing the results of the shielding simulation it was found that both models are very similar. The model created in PIX4D has a greater degree of shading. This was probably due to inequalities in the 3D model. Due to small variations in simulation results, this model can be described as sufficiently accurate. In terms of the time required to create 3D models, it depends on the complexity of the objects that can obscure the photovoltaic modules. If it is an environment with minimal shading of surrounding objects (arrays, separate objects) it is preferable to use the 3D editor PVSOL. On the other hand, for built-up environments (cities, company premises) it is better to use the photogrammetric software PIX4D.

ACKNOWLEDGEMENTS

This work was supported by the specific graduate research of the Brno University of Technology No. FEKT-S-20-6206.

REFERENCES

[1] [1] Valentine Software [online]. [cit. 2019-03-14]. Dostupné z: https://www.valentin-software.com/en/products/photovoltaics/57/pvsol-premium

[2] [2] PIX4D [online]. [cit. 2019-03-14]. Dostupné z: https://www.pix4d.com/

[3] [3] HASELHUHN, Ralf a Petr MAULE. Fotovoltaické systémy: energetická příručka pro elektrikáře, techniky, instalatéry, projektanty, architekty, inženýry, energetiky, manažery, stavitele, studenty, učitele, ostatní odborné a profesní soukromé nebo veřejné instituce a zájemce o fotovoltaický obor a energetickou nezávislost. Plzeň: Česká fotovoltaická asociace, 2017. ISBN 978-80-906281-5-1.

Addresses of the authors

Jiří. Vaněk, Department of electrotechnology, Brno University of Technology, Technická 10, 612 00 Brno, Czech Republic tel.: +420 54 11 61 22, mail: Jiri.Vanek@vut.czvanek

Petr Maule, Department of electrotechnology, Brno University of Technology, Technická 10, 612 00 Brno, Czech Republic
Filip Šmatlo, Department of electrotechnology, Brno University of Technology, Technická 10, 612 00 Brno, Czech Republic

AUTHOR INDEX

Proceedings of the
10th International Workshop on Teaching in Photovoltaics
IWTPV'22

Editor: Vítězslav Benda and Ladislava Černá

Proceedings

Published by Czech Technical University in Prague
Processed by Faculty of Electrical Engineering in cooperation with IET Czech Republic Network
Contact address: Technická 2, 166 27 Praha 6
Phone: +420 224 352 163

Number of pages: 104 Edition: 1st electronic edition
ISBN 978-80-01-07013-0 (print)
ISBN 978-80-01-07014-7 (on-line)